GEOLOGICAL SURVEY OF DENMARK AND GREENLAND BULLETIN 23 • 2011

Review of Survey activities 2010

Edited by
Ole Bennike, Adam A. Garde and W. Stuart Watt

GEOLOGICAL SURVEY OF DENMARK AND GREENLAND
MINISTRY OF CLIMATE AND ENERGY

Geological Survey of Denmark and Greenland Bulletin 23

Keywords
Geological Survey of Denmark and Greenland, survey organisations, current research, Denmark, Greenland.

Cover photographs from left to right
1. Small-scale miner with gold concentrate. Photograph: Peter W.U. Appel.
2. Work at the microscope. Photograph: Peter K. Warna-Moors.
3. Many Survey employees are engaged in laboratory work. Photograph: Peter K. Warna-Moors.
4. Development of geological models is becoming increasingly important. Photograph: Peter K. Warna-Moors.

Frontispiece: facing page
In 2010 the Survey carried out extensive mapping projects in the North Sea. The crane is carrying a tow-fish with (1) a side-scan sonar for mapping the seabed and (2) a chirp sonar for mapping the layers below the seabed. Photograph: Ole Bennike.

Printers: Rosendahls · Schultz Grafisk A/S, Albertslund, Denmark
Manuscripts received: 21 December 2010 – 6 May 2011
Final versions approved: January–May 2011, Fig. 2, page 10 updated 30.08.2011.
Printed: 15 July 2011

ISSN 1603-9769 (Review of Survey activities)
ISSN 1604-8156 (Geological Survey of Denmark and Greenland Bulletin)
ISBN 978-87-7871-313-1

Citation of the name of this series
It is recommended that the name of this series is cited in full, viz. *Geological Survey of Denmark and Greenland Bulletin*.
If abbreviation of this volume is necessary, the following form is suggested: *Geol. Surv. Den. Green. Bull.* 23, 84 pp.

Available from
Geological Survey of Denmark and Greenland (GEUS)
Øster Voldgade 10, DK-1350 Copenhagen K, Denmark
Phone: +45 38 14 20 00, fax: +45 38 14 20 50, e-mail: geus@geus.dk
And at *www.geus.dk/publications/bull*

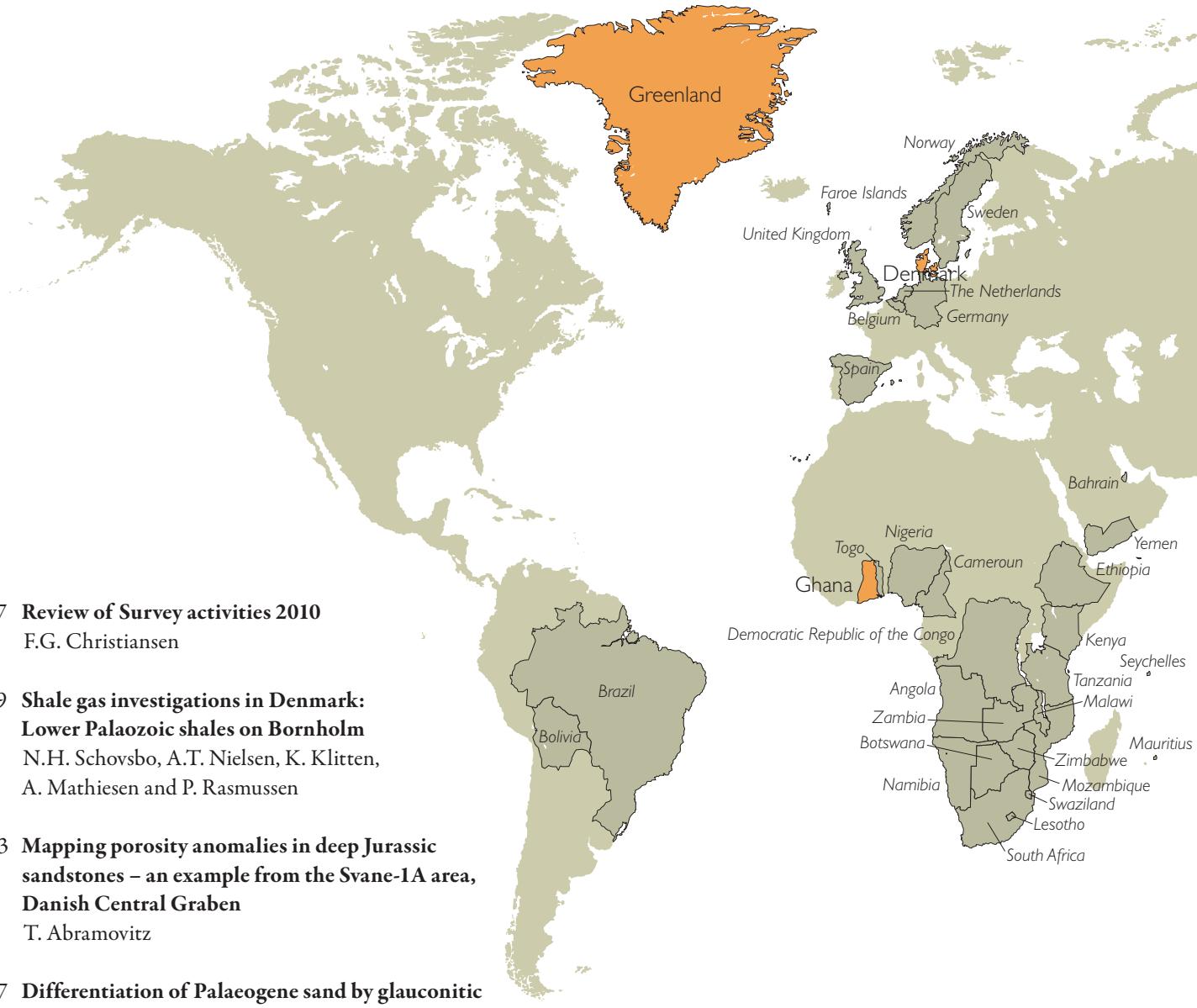

GEUS working areas 2010.
Orange areas are covered in this volume.

For further information on other working areas please refer to our website: *www.geus.dk/international*

Review of Survey activities 2010

Flemming G. Christiansen

Deputy Director

2010 was a good and stable year for the Geological Survey of Denmark and Greenland (GEUS) with focus on research, often in international collaboration. Despite the continued effects of the international financial crisis, which has had serious implications for many of our national and international partners, GEUS has had a period with many new projects and successful completion of many projects. This is also reflected in the present eighth annual issue of Review of Survey activities which describes selected projects that GEUS and its partners carry out in Denmark, Greenland and internationally. Together with the previous seven published issues, it provides a good overview of the Survey's range of research and advisory activities. It contains a total of 19 four-page papers: 12 on Denmark, six on Greenland, and one project in Ghana.

Energy policy is again high on the political agenda in Denmark. The Government presented a new Energy 2050 Strategy with strong emphasis on the reduction of CO_2 emission. The strategy depends on a stable supply of and income from oil and gas in the North Sea during a long transition period before most of Denmark's energy supply becomes CO_2 neutral, competitive and stable. GEUS' research lies within a variety of different aspects of energy as well as of climate development, climate monitoring and adaptation to climate changes.

Three papers concentrate on various aspects of petroleum geology in Denmark. One of them provides an overview of a core-drilling project in Lower Palaeozoic shales on Bornholm as an unconventional shale gas resource analogue. Another paper describes mapping of very deep Jurassic targets in the Svane-1 area in the North Sea, and a third paper gives a geochemical fingerprinting of Palaeogene reservoir sands from the Siri Canyon in the North Sea and discusses the implications from being able to distinguish between *in situ* and mobilised sand.

GEUS works on many other aspects of the geology of Denmark, such as groundwater, climate and the environment including issues where geology is important to society. Seven papers ranging from applied geology to more basic research are found in this volume. Decisions on disposal of Danish low- and intermediate-level radioactive waste have to be taken in the coming years, and a number of key geological parameters are used for the final selection of a permanent depository. The work has resulted in the selection of 22 areas, of which six are preferred.

The Miocene succession in Jylland contains several large groundwater bodies, and a 3D model is important for future planning; this is described in another paper. With a continued need for raw materials to large infrastructure projects, systematic mapping and understanding of available marine resources are important. The results from a project in the North Sea carried out for the Danish Nature Agency are presented in one paper. Two papers describe basic research on a new Pleistocene interglacial sequence from Sjælland and on postglacial relative shore-level changes in Lillebælt. Another paper presents results of the detection of terrain changes using satellite data with south-western Jylland as a case. One paper discusses how sensitive the groundwater quality in Denmark is to the use of road salt in winter. The Danish contribution to the Nuclear-Test-Ban Treaty is also described, demonstrating how useful the data from the monitoring systems are for understanding earthquakes.

In 2010, there was a high level of field activities in Greenland. In addition to major projects in southern West Greenland, South-East Greenland and North-East Greenland there were many smaller activities in other areas. The work in southern West Greenland continued, and results are described in a paper on the Tartoq Group, a possible very old slab of oceanic crust. Field work and shallow core drilling in North-East Greenland continued in 2010. In this issue results on previously almost unknown Palaeogene sand are presented, including new critical information on age and depositional environment. Structural data from the Sødalen area in southern East Greenland are presented in a paper that concentrates on unravelling the strike-slip tectonics in Palaeogene time. One paper adds additional evidence from magnetic data contra-

dicting the existence of a major structural feature (the Wegener Fault) in the Kennedy Channel between North Greenland and Ellesmere Island in Canada.

Studies of the ice sheet and glaciers in Greenland have attracted international interest over many years due to the possible implications of a rising sea level. GEUS is involved in many glaciological and meteorological projects and monitoring programmes. One paper gives a presentation on the large-scale Programme for Monitoring of the Greenland Ice Sheet (PROMICE) with description of the weather station network and preliminary temperature data.

Easy access to comprehensive and updated information and data is a very important part of the work GEUS carries out in Denmark and Greenland. This is the topic of two papers, one on free, online Danish geological data where the Jupiter database currently includes information from more than 260 000 shallow wells. The other paper gives a description of DODEX (Geoscience Documents and Data for Exploration in Greenland), which is an interactive web application, which gives the public and mining companies easy access to all non-confidential reports relevant to mineral exploration.

Internationally GEUS works in many different countries with many project types. The last paper in this issue is about work in Ghana where GEUS has been active for many years with capacity building and geological and geophysical projects. The paper gives an overview of quality control of airborne geophysical data.

Shale gas investigations in Denmark: Lower Palaeozoic shales on Bornholm

Niels Hemmingsen Schovsbo, Arne Thorshøj Nielsen, Kurt Klitten, Anders Mathiesen and Per Rasmussen

The Cambrian to Lower Silurian succession in Denmark is mostly composed of organic-rich black shales that were deposited in an epicontinental sea during a period of high global sea level (Haq & Schutter 2008). The mid-Cambrian to early Ordovician Alum Shale was intensively studied in the 1980s for its source-rock properties (e.g. Buchardt *et al.* 1986). Recent attention has focused on its potential as an unconventional shale gas source (Energistyrelsen 2010). On southern Bornholm, many wells have been drilled through the Lower Palaeozoic succession because of its importance for groundwater exploitation. In western Denmark, only the deep exploration wells Slagelse-1 and Terne-1 have penetrated the Alum Shale, and knowledge of the unit west of Bornholm is thus very limited (Fig. 1).

The project 'Shale Gas in Europe (GASH)' was launched in 2009 to address the European shale gas potential (Horsfield *et al.* 2008) and is organised by the German Research Centre of Geosciences and sponsored by oil and energy companies. It deals with basic research of key aspects of gas shale from regional to reservoir scales, and focuses on four 'natural laboratories', namely the Lower Palaeozoic Alum Shale, the Carboniferous (Namurian) shales, the Lower Jurassic Posedonia Shale and as a reference the North American Barnet Shale. As part of GASH, a European black shale database is under construction in order to facilitate exploration and exploitation of gas shales in Europe. The Geological Survey of Denmark and Greenland (GEUS) has taken part in both the gas shale research and in the national data compilation for the European shale database.

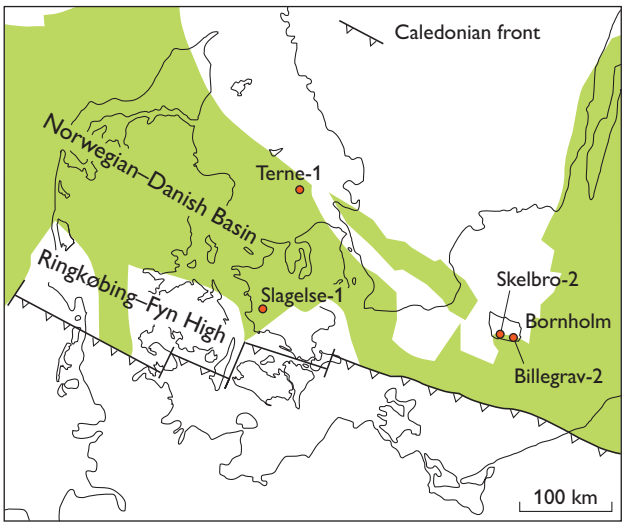

Fig. 1. Map of Denmark showing the distribution of Lower Palaeozoic strata (modified from Buchardt *et al.* 1997) and the location of the Slagelse-1 and Terne-1 exploration wells, and the Skelbro-2 (DGU 246.817) and Billegrav-2 (DGU 248.61) wells.

This paper presents the results of drilling on Bornholm in August 2010 by GEUS with the aim of obtaining fresh core material relevant to shale gas studies within the GASH project (the Skelbro-2 core) and providing new stratigraphic and geochemical information on the Lower Palaeozoic (the Billegrav-2 core). In particular, logging of the Silurian was needed to improve the log-stratigraphical template of Pedersen & Klitten (1990) which will enable the correlation of geophysical logs from non-cored water wells.

Drilling and logging project on Bornholm

The southern part of Bornholm is characterised by a mosaic of fault blocks (Graversen 2010). Outcrops, old core data and logs from water wells were used to find the best drilling locations for the two new wells. Both wells were fully cored and subsequently subjected to an extensive logging programme by GEUS in order to characterise the lithology as well as the water composition and the flow capacity of the fracture systems (Fig. 2). Spectral gamma and density scanning of the cores was subsequently carried out at GEUS.

Skelbro-2 well

The Skelbro-2 well was drilled 275 m east of Skelbro-1 (DGU 246.749; Pedersen 1989). The mid-Ordovician Komstad Limestone is 4 m thick at this locality. The top of the Alum Shale was encountered at 8.5 m below surface, and a total of 33.5 m of Alum Shale was drilled. The well was terminated at 42.9 m in the Lower Cambrian Rispebjerg Member (Læså Formation). The cored succession is virtually identical to the one described by Pedersen (1989) from the Skelbro-1 core.

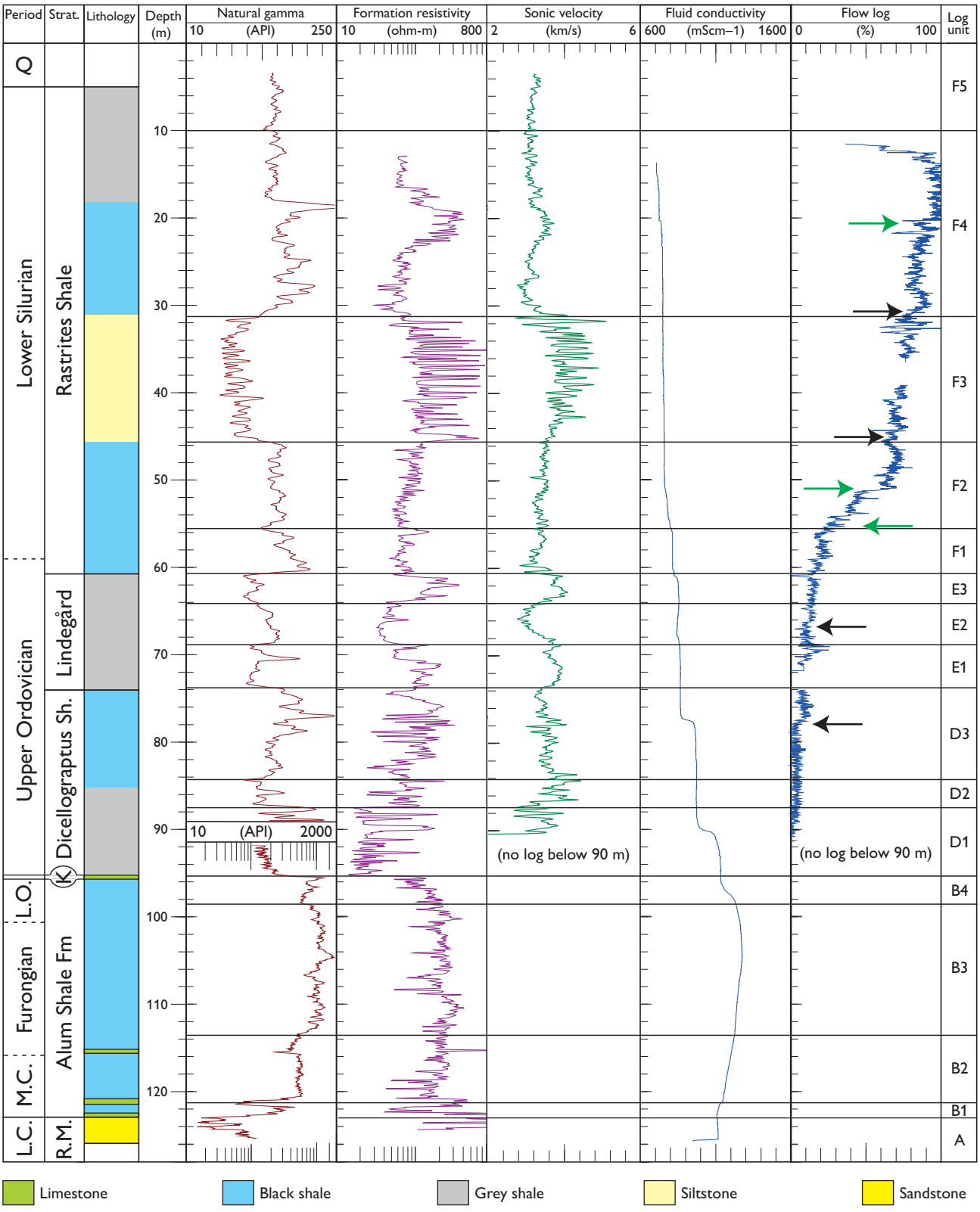

Fig. 2. Stratigraphy, lithology, natural gamma ray, formation resistivity, sonic velocity, fluid conductivity and flow logs for Billegrav-2. Log units **A–F** according to Pedersen & Klitten (1990). Dashed lines: uncertain biostratigraphical boundaries. Green arrows: major inflow zones; black arrows: minor inflow zones. **Q**: Quaternary. **K**: Komstad Limestone. **L.O.**: Lower Ordovician. **L.C.**: Lower Cambrian. **M.C.**: Middle Cambrian. **R.M.**: Rispebjerg Member. **API**: American Petroleum Institute (a standard unit for gamma-ray measurements). Note change in scale for natural gamma at 90 m.

Billegrav-2 well

The Billegrav-2 well was drilled close to locality 14b of Bjerreskov (1975) and 800 m south of the Billegrav-1 well (DGU 247.560; Pedersen 1989). The Silurian Rastrites Shale was cored from 4.5 m below surface down to 60.5 m. The Rastrites Shale comprises light to dark mudstone except for a distinct grey mud- to siltstone unit containing carbonate-cemented sandy beds at a depth between 31.2 and 46.0 m (Fig. 2). The Upper Ordovician includes the Lindegård Formation (previously referred to as the Tretaspis Shale or Tommarp and Jerrestad Mudstones), comprising grey mud- and siltstone and the dark organic-rich Dicellograptus Shale (Fig. 2). The base of the Dicellograptus Shale is located at a depth of 95 m. In its lowermost part the shale contains numerous bentonite beds including a 1 m thick K-bentonite bed that represents an important regional marker bed (Bergström & Nilsson 1974).

The Komstad Limestone is 0.1 m thick and only represented by its basal conglomerate. A thin bentonite rests directly on the Komstad Limestone conglomerate; there is no conglomerate at the base of the overlying Dicellograptus Shale. The Alum Shale Formation is 27 m thick and includes the Middle Cambrian Andrarum and Exsulans Limestone beds that are important regional marker beds (Nielsen & Schovsbo 2006). The base of the Alum Shale was reached at a depth of 122 m, and the well was terminated at 125.9 m in the Rispebjerg Member (Fig. 2).

Log-stratigraphy of the Billegrav-2 well

Correlation of water wells based on gamma variation has served as an effective mean of correlation between wells (Pedersen & Klitten 1990). All gamma-ray, log-defined units identified in nearby water wells can also be recognised in the Billegrav-2 well (Fig. 2). The resistivity and sonic logs provide important additional information (Fig. 2). In the Rastrites Shale, the resistivity is particularly powerful in resolving the lithological variation, since the carbonate-cemented sandy beds in the middle part (the F3 unit) stand out as high-resistivity beds (Fig. 2).

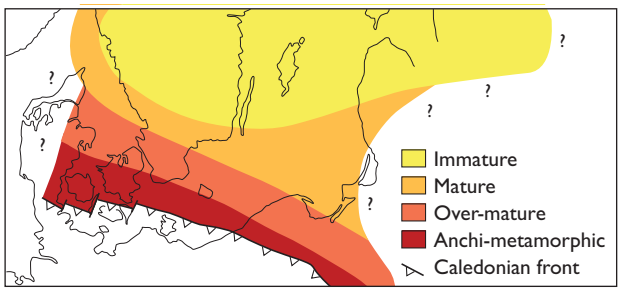

Fig. 3. Maturity of the Lower Palaeozoic sequence based on reflectance of vitrinite-like particles. The thermal maturity increases towards the Caledonian front, reflecting deep burial in Late Silurian to Early Devonian time. Modified from Buchardt *et al.* (1997).

Water-flow zones in the Billegrav-2 well

The flow log from this well clearly indicates that the water flow is related to three major and three minor influx zones (Fig. 2). The majority of the water flow takes place in the lowermost part of the Rastrites Shale at around a depth of 56–50 m. Relatively high water influx is also seen in the Rastrites Shale at about a depth of 20 and 30 m, whereas there is very little water flow from log unit F3 (Fig. 2). Water influx is seen in the Dicellograptus Shale at 77 and 90 m as well as in the uppermost part of the Alum Shale at 96 m. No flow is observed deeper in the well. Interestingly, the conductivity data suggest that the pore water in the Alum Shale has a much higher conductivity than in the shales above, suggesting that it is stagnant. This indicates that the Alum Shale acts as a hydraulic barrier between the silt- and sandstone aquifers below and the shale aquifers above this unit.

Potential shale gas units onshore Denmark

Shale gas units of potential economic interest have to be (1) matured to at least the gas generative stage, (2) organic rich (total organic carbon (TOC) >2 wt%), (3) volumetrically important (thickness >20 m and regionally distributed) and (4) preferentially located away from structurally complex areas. The Lower Palaeozoic succession on Bornholm contains up to 10 wt% TOC in the Alum Shale, up to 5 wt% in the Dicellograptus shale and up to 2 wt% in the Rastrites Shale (Buchardt *et al.* 1986). Also Mesozoic organic-rich units occur in Denmark, but those onshore are all thermally immature to marginally mature (Petersen *et al.* 2008) and thus have no potential for shale gas.

Thermal maturity and burial of the Lower Palaeozoic succession

The thermal maturity of Lower Palaeozoic shales in Denmark is only known from a few wells that all have vitrinite reflectance values >2.5%, indicative of a post-mature rank with regard to oil generation (Fig. 3). The shales are thus theoretically favourable for shale gas. The high maturity reflects deep burial and a high geothermal gradient in Late Silurian – Early Devonian time (Buchardt *et al.* 1997).

The present burial depth of the Lower Palaeozoic can be evaluated from the pre-Zechstein depth map (Fig. 4) that represents the deepest level that can be mapped with some con-

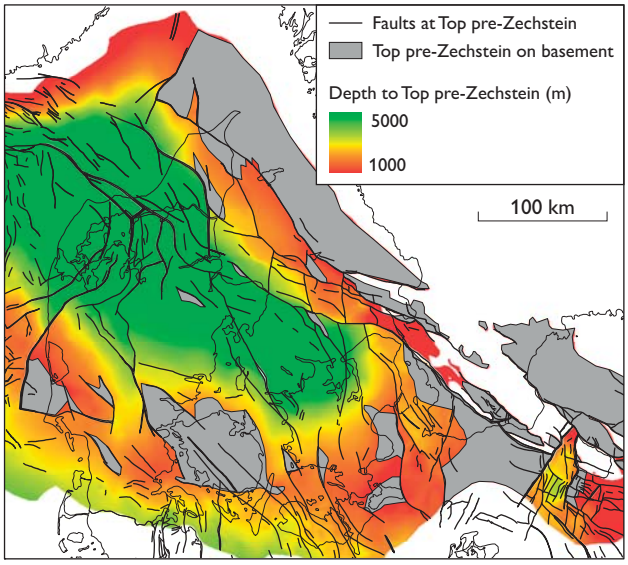

Fig. 4. Depth to the Top pre-Zechstein surface. Note the depocentre in the Norwegian–Danish Basin (>5000 m) and the shallow Ringkøbing–Fyn High (<1000 m). Areas where the Top pre-Zechstein surface coincides with basement are shown in grey. Modified from Vejbæk (1997).

fidence on a regional basis (Vejbæk 1997). Lower Palaeozoic shales are buried to very deep levels in the central parts of the Norwegian–Danish Basin and are probably not within reach of shale gas exploration. Lower Palaeozoic shales buried to moderate depths of 2–4 km occur in a broad belt around the margin of the Norwegian–Danish Basin. Shale gas investigations have focused on this region (Energistyrelsen 2010).

Conclusions

Shale gas research and exploration in Denmark is currently focused on Palaeozoic shales. The prospective units are poorly known in Denmark outside Bornholm. The play involves deeply buried, post-mature shale in which many basic rock properties are still unknown. Key questions that remain to be addressed include the gas storage capacity of the shales, their mineralogy and how they respond to fracturing. The hydrogeology of water wells on Bornholm may provide a test case to assist in unravelling how fracture systems and flow are distributed in the Lower Palaeozoic shales.

Acknowledgements

The GASH project financed the Skelbro-2 drilling. Funding for the Billegrav-2 drilling was provided by GEUS, the Natural History Museum of Denmark, the University of Southern Denmark and Bornholm's Regionskommune. Peter and Kristian Turner from Faxe Kalk A/S assisted with the drilling. The land owners Andres Ipsen, Jørn Erik Koefoed and Jesper Koefoed kindly permitted us to drill on their properties.

References

Bergström, S.M. & Nilsson, R. 1974: Age and correlation of the Middle Ordovician bentonites on Bornholm. Bulletin of the Geological Society of Denmark **23**, 27–48.

Bjerreskov, M. 1975: Llandoverian and Wenlockian graptolites from Bornholm. Fossils and Strata **8**, 1–94.

Buchardt, B., Clausen, J. & Thomsen, E. 1986: Carbon isotope composition of Lower Palaeozoic kerogen: effects of maturation. Organic geochemistry **10**, 127–134.

Buchardt, B., Nielsen, A.T. & Schovsbo, N.H. 1997: Alun Skiferen i Skandinavien. Geologisk Tidsskrift **3**, 1–30.

Energistyrelsen 2010: Denmark's oil and gas production 2009, 156 pp. Copenhagen: The Danish Energy Agency.

Graversen, O. 2010: Structural analysis of superposed fault systems of the Bornholm horst block, Tornquist Zone, Denmark. Bulletin of the Geological Society of Denmark **57**, 25–49.

Haq, B.U. & Schutter, S.R. 2008: A chronology of Paleozoic sea-level changes. Science **322**, 64–68.

Horsfield, B., Schulz H.-M. & GASH Team 2008: GASH: a shale gas initiative for Europe. EGU general assembly. Geophysical Research Abstracts **10**, EGU 2008-A-01508.

Nielsen, A.T. & Schovsbo, N.H. 2006: Cambrian to basal Ordovician lithostratigraphy in southern Scandinavia. Bulletin of the Geological Society of Denmark **53**, 47–92.

Pedersen, G.K. 1989: The sedimentology of Lower Palaeozoic black shales from the shallow wells Skelbro 1 and Billegrav 1, Bornholm, Denmark. Bulletin of the Geological Society of Denmark **37**, 151–173.

Pedersen, G.K. & Klitten, K. 1990: Anvendelse af gamma-logs ved korrelation af marine skifre i vandforsyningsboringer på Bornholm. Danmarks Geologisk Forening Årskrift **1987–89**, 21–35.

Petersen, H.I., Nielsen, L.H., Bojesen-Koefoed, J.A., Mathiesen, A., Kristensen, L. & Dalhoff, F. 2008: Evaluation of the quality, thermal maturity and distribution of potential source rocks in the Danish part of the Norwegian–Danish Basin. Geological Survey of Denmark and Greenland Bulletin **16**, 66 pp.

Vejbæk, O.V. 1997: Dybe strukturer i danske sedimentære bassiner. Geologisk Tidsskrift **4**, 31 pp.

Authors' addresses

N.H.S., K.K., A.M. & P.R., *Geological Survey of Denmark and Greenland, Øster Voldgade 10, DK-1350 Copenhagen K, Denmark*. E-mail: *nsc@geus.dk*

A.T.N., *Natural History Museum of Denmark, Øster Voldgade 5–7, DK-1350 Copenhagen K, Denmark*.

Mapping porosity anomalies in deep Jurassic sandstones – an example from the Svane-1A area, Danish Central Graben

Tanni Abramovitz

Hydrocarbon-bearing Upper Jurassic sandstone reservoirs at depths of more than 5000 m may form a future exploration target in the Danish Central Graben (Fig. 1). The Upper Jurassic sandstone play in the Danish sector has historically been less successful than in the neighbouring Norwegian and British sectors of the North Sea. This is mainly due to poor reservoir quality of the sandstones. However, the discovery in 2001 of an oil accumulation at a depth of more than 5000 m in the Svane-1 well has triggered renewed interest in the Upper Jurassic High Temperature – High Pressure (HTHP) sandstone play in Danish waters. The Jurassic plays comprise sandstone reservoirs deposited in a variety of environments, ranging from fluvial to deep marine.

This paper presents a study of a minor area around the Svane-1A well in the Tail End Graben (Fig. 1). The objective was to map acoustic impedance variations and hence to identify porosity anomalies associated with Jurassic sandstone units.

Interpretation in a tectonic setting such as the Jurassic HTHP petroleum system in the Danish part of the Central Graben is hampered by low seismic vertical resolution. However, by combining regional seismic mapping with inversion results and petrophysical log analysis, such obstacles can be tackled by mapping acoustic impedance variations. Application of seismic inversion techniques for porosity prediction in sandstone is a standard geophysical tool (Dolberg *et al.* 2000). Petrophysical analysis of well-log data from the upper part of the Jurassic sandstones encountered in the Svane-1A well shows a relationship between acoustic impedance (AI) and total porosity (PHIT), see later. This log-derived AI-PHIT relationship can be applied to transform acoustic impedance variation into porosity variation, when the acoustic impedance is predicted from seismic inversion of a 2D profile, and can be used to locate porosity anomalies associated with sandstone intervals in the area around the Svane-1A well.

Setting

The Danish Central Graben is part of the Jurassic North Sea rift complex and consists of a system of NNW–SSE-trending half-grabens bounded by the Coffee Soil Fault and the Mid North Sea High (Fig. 1; Japsen *et al.* 2003; Møller & Rasmussen 2003). Rifting took place from the Middle Jurassic and persisted into the Early Cretaceous. The syn-rift sedimentary fill is dominated by mudstone with subordinate layers of sandstone. In some stratigraphic intervals, the mudstone is rich in organic matter (Petersen *et al.* 2010).

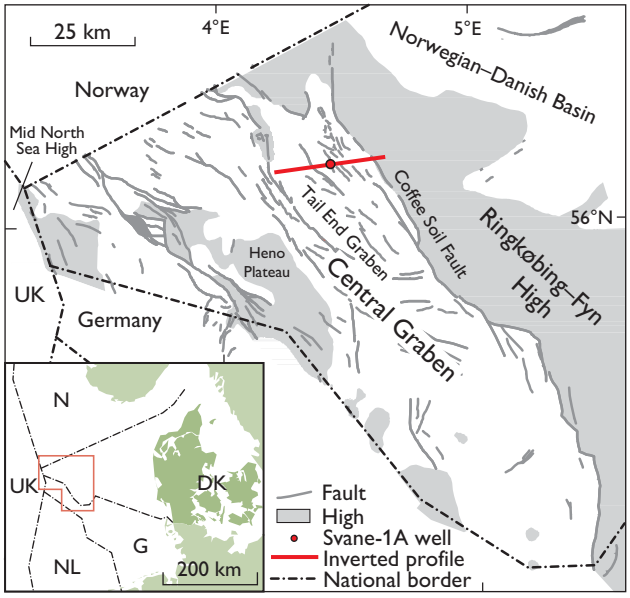

Fig. 1. Map of the Danish Central Graben showing the location of the Svane-1A well and the 2D seismic profile that was inverted for acoustic impedance.

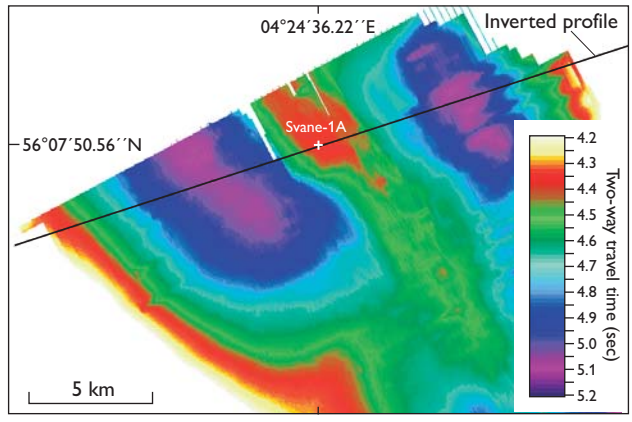

Fig. 2. Two-way travel time structure map of the intra-Kimmeridgian marker horizon corresponding to the top of the drilled Svane-1A sandstones.

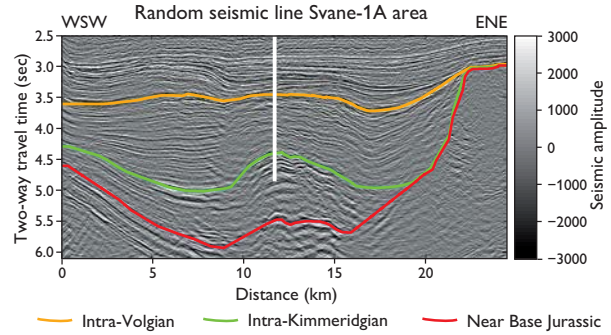

Fig. 3. The input for the seismic inversion is a 2D seismic profile extracted from the 3D PAM_99 survey with three interpreted intra-Jurassic marker horizons: intra-Volgian, intra-Kimmeridgian and Near Base Jurassic. The Svane-1A well location is indicated by the white line. Note the alternating high and low amplitude layers below the intra-Kimmeridgian marker horizon.

The Svane-1A area

The Svane-1A well is located on a 4-way-dip closure structure at an intra-Kimmeridgian level in the northern part of the Tail End Graben (Fig. 2). It is one of the deepest wells ever drilled in Denmark (total depth 5952 m). The structure map of an intra-Kimmeridgian marker horizon corresponding to the top of the Svane-1A sandstones shows that the well is located on a NNW–SSE-oriented structural high along the basin axis bounded by two depocentres (Fig. 2).

Upper Jurassic sandstone with dry gas was encountered at 5311 m. Unfortunately, no cores or sidewall cores were collected due to unstable borehole walls. At depths over 5400 m, the sandstone layers in Svane-1A are characterised by porosities of 15–24% and low permeabilities. The Svane-1A well is situated in a HTHP environment with overpressures of 8630 psi at a depth of 5350 m, which may imply that the pore pressure is close to the fracture pressure according to Johannessen *et al.* (2010).

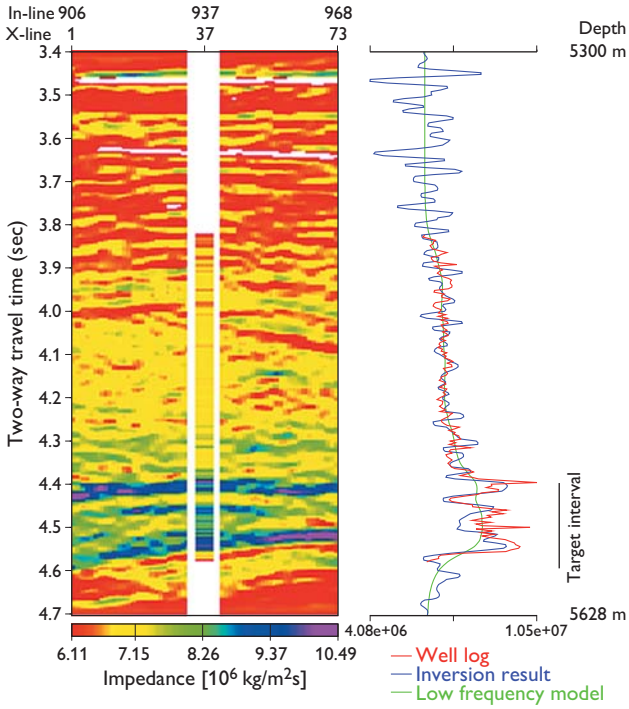

Fig. 4. Quality control of the absolute acoustic impedance inversion result. **A**: Section of the inversion result with the acoustic impedance log inserted at the well location. **B**: Comparison between the acoustic impedance trace estimated at the well location (blue), the low frequency model at the well location (green) and the acoustic impedance well log (red).

Seismic inversion for acoustic impedance

Seismic inversion is the process of transforming seismic reflection data into quantitative rock properties such as acoustic impedance (AI) using reflection seismic data constrained by borehole data in order to describe a possible reservoir. Acoustic impedance is the product of the rock density and the compressional P-wave velocity, which are both commonly measured in boreholes as the bulk density and the sonic velocity. A log-derived AI-PHIT relationship based on the petrophysical well log is used to transform the inversion-derived AI into total porosity (PHIT). Seismic inversion for acoustic impedance was carried out using the 2D ISIS seismic inversion software. The inversion algorithm is a deterministic approach based on a simulated annealing algorithm (Maver & Rasmussen 1995; Rasmussen & Maver 1996).

Both seismic and well-log data were used for the inversion. The input data consist of a 2D seismic profile (Fig. 3) and raw log data (sonic and density) as well as the time-depth data from the Svane-1A well.

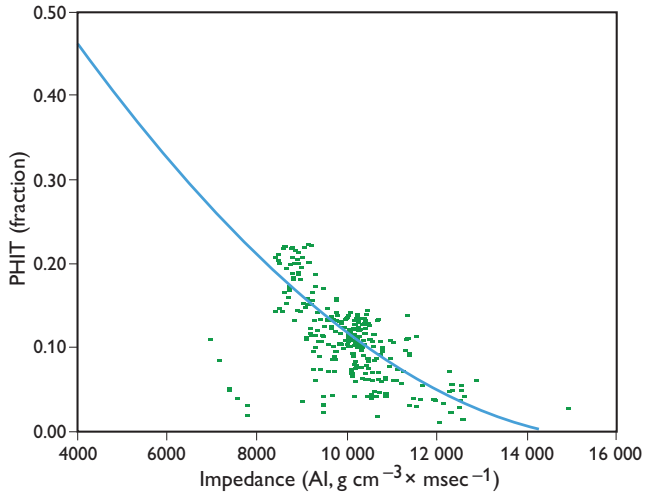

Fig. 5. Cross plot of the log-derived acoustic impedance (AI) versus the log-derived total porosity (PHIT), based on the Svane-1A sonic and density log data from 5300–5627.93 m.

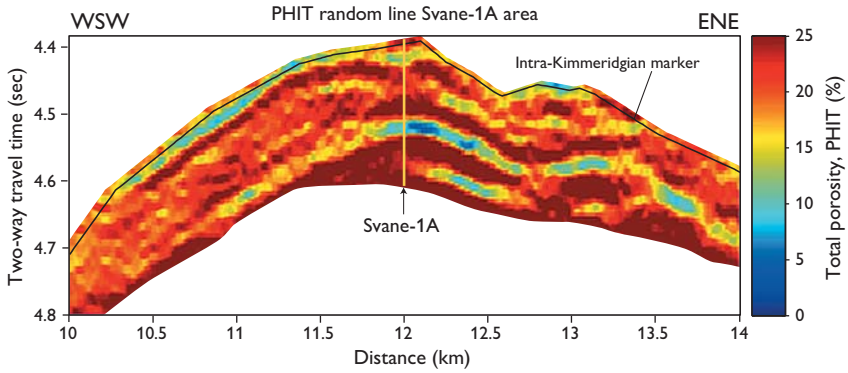

Fig. 6. Close-up of the 2D total porosity (PHIT) variation around the Svane-1A well, showing the PHIT variation below the intra-Kimmeridgian marker horizon along part of the inverted 2D seismic profile between faults A and C (Figs 7, 8). The high porosity (>25%) between 4.55 and 4.6 sec TWT at the well location is an artefact due to underestimation of the absolute acoustic impedance in the inversion (see text and Fig. 4). The shape of the PHIT profile is governed by the limited depth interval 5300–5628 m, for which the applied AI-PHIT transform is defined, corresponding to a time window of 200 msec below the intra-Kimmeridgian marker horizon.

In order to ensure a well-to-seismic tie, the available time-depth data were used to create a reflectivity series with the same sampling rate (4 msec) as the input seismic data and to convert the log data from a depth to a two-way travel time (TWT). The acoustic impedance was calculated by multiplying the calibrated density log and the velocity log derived from the calibrated sonic log. The reflectivity series was computed by differentiating the acoustic impedance series. After the log calibration, the Svane-1A wavelet was estimated by deriving the convolution operator between the reflectivity log and the seismic trace at the well location using a least squares wavelet estimation method. The length of the wavelet was estimated over the Jurassic target interval to 4.2–4.58 sec TWT.

In general, seismic data have limited frequency bandwidth at the low and high ends. The (missing) low frequencies contain the critical information concerning the absolute values of impedance. In order to invert for absolute acoustic impedance, a low frequency model is needed to introduce the sub-seismic frequencies into the seismic inversion result. The 2D low frequency model is constructed by laterally extrapolating the final calibrated impedance log from the Svane-1A well between three interpreted horizons extracted from the 3D seismic PAM_99 survey to guide and yield the absolute level of acoustic impedances along the seismic 2D profile.

Evaluation of the absolute acoustic impedance inversion result is shown with the acoustic impedance log inserted at the well location (Fig. 4). An excellent fit is seen between the inverted log trace (blue), the low frequency model log trace (green) and the well log trace (red) at the top (4.4 sec TWT) and bottom (4.45 sec TWT) of the target sandstone interval. However, it is important to notice that the inversion result (blue line) underestimates the absolute acoustic impedance in the deeper parts of the sandstone interval. This will lead to an overestimation of the porosity in this interval.

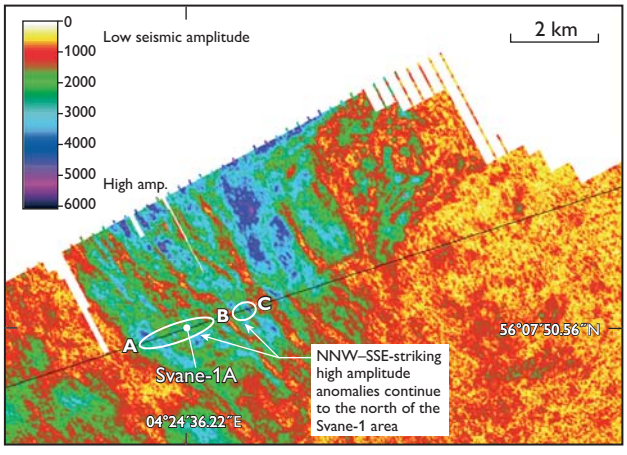

Fig. 7. Seismic amplitude extract from a 65 msec time window below the intra-Kimmeridgian marker horizon. NNW–SSE-trending high amplitude anomalies (blue colours) continue to the north of the Svane-1A well. **A**, **B** and **C** mark the location of faults (see Fig. 8).

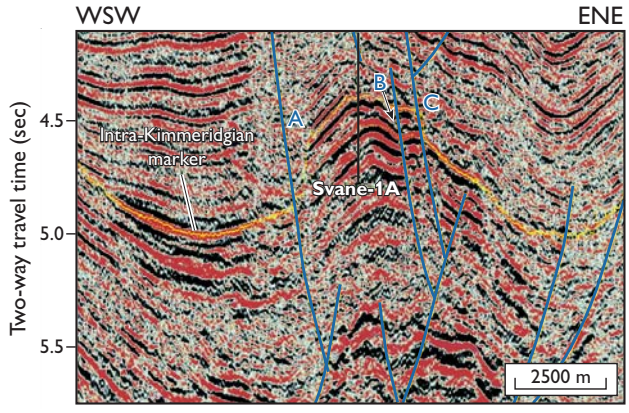

Fig. 8. Close-up of the 2D seismic section across the Svane-1A well (black). Notice the high amplitude reflections below the intra-Kimmeridgian marker horizon (yellow) between faults **A**, **B** and **C** (blue).

Calculating porosity from acoustic impedance

Cross-plotting the log-derived acoustic impedance (AI) and the log-derived total porosity (PHIT) using the Svane-1A sonic and density log data from the depth interval 5300–5628 m results in an AI-PHIT transform obtained from a second-order polynomial regression line (Fig. 5):

$$PHIT = 0.8176 - 1 \times 10^{-4}AI + 3 \times 10^{-9}AI^2$$

where porosity is given in fraction and AI in g cm^{-3} × $msec^{-1}$.

The AI-PHIT transform, which is valid for the limited depth interval 5300–5628 m corresponding to a time window of 200 msec below the intra-Kimmeridgian marker horizon, can be applied to convert the 2D acoustic impedance inversion result into a 2D total porosity (PHIT) profile in this time window (Fig. 6). This 2D PHIT profile is a close-up of the central part of the inverted seismic profile at the 4-dip closure. The PHIT profile shows the lateral distribution of porosity anomalies below the intra-Kimmeridgian marker horizon around the well location.

Alternating high (15–25%) and low porosity (5–15%) layers are seen below the intra-Kimmeridgian marker horizon. In the time window 4.47–4.51 sec TWT, the modelled porosities are up to 5% too high as a consequence of underestimation of the absolute acoustic impedance in the deeper parts. The derived total porosity values show good agreement with the observed Svane-1A well porosities (up to 20–22% in the upper sandstone units), and indicate the presence of high porosity intervals off-structure down along the flanks of the structural high.

Porosity prediction tool

The existence of Upper Jurassic sandstones with high porosities (15–25%) has been demonstrated in the Svane-1A well and interpreted from the inversion result. Thus an important question concerns the lateral extension and distribution of these sand-rich layers, and the challenge is to predict the location of yet undrilled high-porosity sandstone layers away from the well. For this purpose, a seismic amplitude extraction map for a narrow time window of 65 msec below the intra-Kimmeridgian marker horizon was created to illustrate the lateral distribution of porosity anomalies in the vicinity of the Svane-1 well (Figs 7, 8).

The seismic amplitude extraction map indicates that high amplitudes associated with the high porosity sandstone unit are concentrated along NNW–SSE-trending anomalies that extend to the north of the Svane-1A area (Fig. 7). A close-up of the seismic data shows a correlation between fault planes (Fig. 8 A–C) and low amplitude features on the amplitude extraction map (Fig. 7). The amplitude extraction map also implies high lateral variability in the distribution of porosity anomalies corresponding to lateral variations in reservoir quality over the area. A possible new target area for further exploration could thus be located further to the north along the Svane structure where high amplitudes prevail. The application of seismic inversion data based on well-log data, seismic data and a thorough geological model can significantly increase the possibility for finding new targets.

References

Dolberg, D.M., Helgesen, J., Hanssen, T.H., Magnus, I., Saigal, G. & Pedersen, B.K. 2000: Porosity prediction from seismic inversion, Lavrans Field, Halten Terrace, Norway. The Leading Edge **19**, 392–399.

Japsen, P., Britze, P. & Andersen, C. 2003: Upper Jurassic – Lower Cretaceous of the Danish Central Graben: structural framework and nomenclature. In: Ineson, J.R. & Surlyk, F. (eds): The Jurassic of Denmark and Greenland. Geological Survey of Denmark and Greenland Bulletin **1**, 233–246.

Johannessen, P.N., Dybkjær, K., Andersen, C., Kristensen, L., Hovikoski, J. & Vosgerau, H. 2010: Upper Jurassic reservoir sandstones in the Danish Central Graben: new insights in distribution and depositional environments. In: Vining, B.A. & Pickering, S.C. (eds): Petroleum geology: from mature basins to new frontiers. Proceedings of the 7th Petroleum Geology Conference, 127–143. London: Geological Society. Doi: 10.1144/0070127.

Maver, K.G. & Rasmussen, K.B. 1995: Seismic inversion for reservoir delineation and description. Society of Petroleum Engineers paper, 10 pp. Doi: 10.2118/29798-MS.

Møller, J.J. & Rasmussen, E.S. 2003: Middle Jurassic – Early Cretaceous rifting of the Danish Central Graben. In: Ineson, J.R. & Surlyk, F. (eds): The Jurassic of Denmark and Greenland. Geological Survey of Denmark and Greenland Bulletin **1**, 247–264.

Petersen, H.I., Nytoft, H.P., Vosgerau, H., Andersen, C., Bojesen-Koefoed, J.A. & Mathiesen, A. 2010: Source rock quality and maturity and oil types in the NW Danish Central Graben: implications for petroleum prospectivity evaluation in an Upper Jurassic sandstone play area. In: Vining, B.A. & Pickering, S.C. (eds): Petroleum geology: from mature basins to new frontiers. Proceedings of the 7th Petroleum Geology Conference, 95–111. London: Geological Society. Doi: 10.1144/0070095.

Rasmussen, K.B. & Maver, K.G. 1996: Direct inversion for porosity of post stack seismic data. Society of Petroleum Engineers paper, 12 pp. Doi: 10.2118/35509-MS.

Authors' address

Geological Survey of Denmark and Greenland, Øster Voldgade 10, DK-1350 Copenhagen K, Denmark. E-mail: *tab@geus.dk*

Differentiation of Palaeogene sand by glauconitic and geochemical fingerprinting, Siri Canyon, Danish North Sea

Mette Olivarius, Christian Knudsen and Johan B. Svendsen

The submarine Siri Canyon is NE–SW-oriented and located in the Danish North Sea (Fig. 1). It contains a number of oil reservoirs with glauconite-rich sand. The reservoirs of interest in the Nini oil field are the Late Paleocene Tyr Member of the Lista Formation and the Kolga Member of the Sele Formation (Schiøler *et al.* 2007), presumably of Early Eocene age. These members have previously been known as the Ty and Hermod members (Hamberg *et al.* 2005; Poulsen *et al.* 2007). The sand shows signs of injection, both in cores and in seismic data. The aim of this work is to chemically characterise and fingerprint the sand in order to reveal the origin of the sand found in three horizontal wells, which could have been injected from one or both of the Tyr and Kolga members. Core samples were collected from two vertical wells of known stratigraphy to make a basis of comparison, whereas samples of the cuttings were collected from the three horizontal wells with ages primarily corresponding to the Kolga Member. The purpose was moreover to evaluate whether cuttings samples can be used for fingerprinting as an alternative to core samples.

The interest in discriminating between the ages of the injected sand is the fact that the reservoir properties (porosity and permeability) are largely controlled by the original composition of the sand. Consequently, results from this study could affect the property modelling of the field.

Sand from the Tyr and Kolga members is dominated by quartz and glauconite and contains fairly well-preserved K-feldspar, plagioclase and mica. The content of feldspar and mica is quite constant, and the feldspar and quartz grains are equally rounded. K-feldspar is more common and better preserved than plagioclase, and K-feldspar overgrowth is often found on plagioclase grains. Barite and siderite are important authigenic phases in several intervals, but the presence of barite may be due to the use of drilling mud, potentially contaminating the sand samples with both barium and strontium. Most of the sand is fairly loose, but parts of the Tyr Member are cemented by quartz and calcite as it was located below the oil-water contact, whereas cementation was largely inhibited by oil in most of the Kolga Member.

Methods

Geochemical analyses were performed using a number of methods including inductively coupled plasma mass spectrometry (ICP-MS). The advantages of this method compared with X-ray fluorescence (XRF) are that the former measures a wider range of trace elements including rare-earth elements (REE), and that the detection limits are lower than those of XRF, which allows more accurate interpretation of elements found in low concentrations. Core material has previously been analysed by Friis *et al.* (2007) using XRF.

The modal composition of the sand as well as the chemical composition of the individual mineral grains have been analysed using computer-controlled scanning electron microscopy (CCSEM), where each grain is classified as a specific mineral on the basis of its chemical composition (Keulen *et al.* 2008). This method was applied in order to discern whether the samples could be differentiated based on their glauconite composition and to test if injected sand could be identified by its glauconite composition. The >45 μm fraction of the sand was used for the analyses. Oil was extracted by toluene, and detergent applied to remove the oily drilling mud and disintegrate the slightly lithified sand.

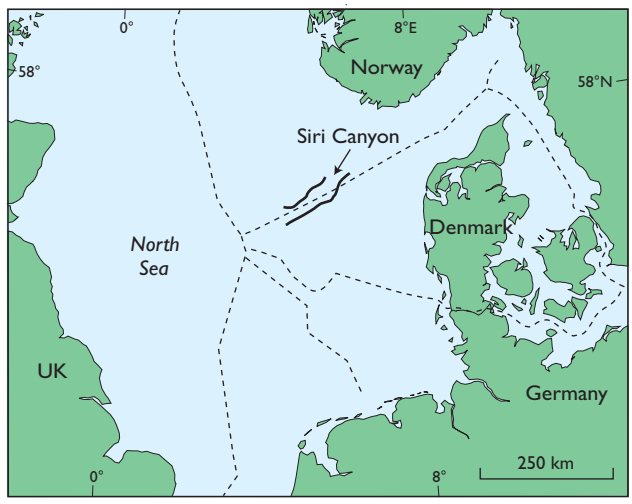

Fig. 1. Map of the North Sea region showing the location of the NE–SW-oriented Siri Canyon with the Tyr and Kolga members under investigation in the Nini oil field. Dashed lines: national borders.

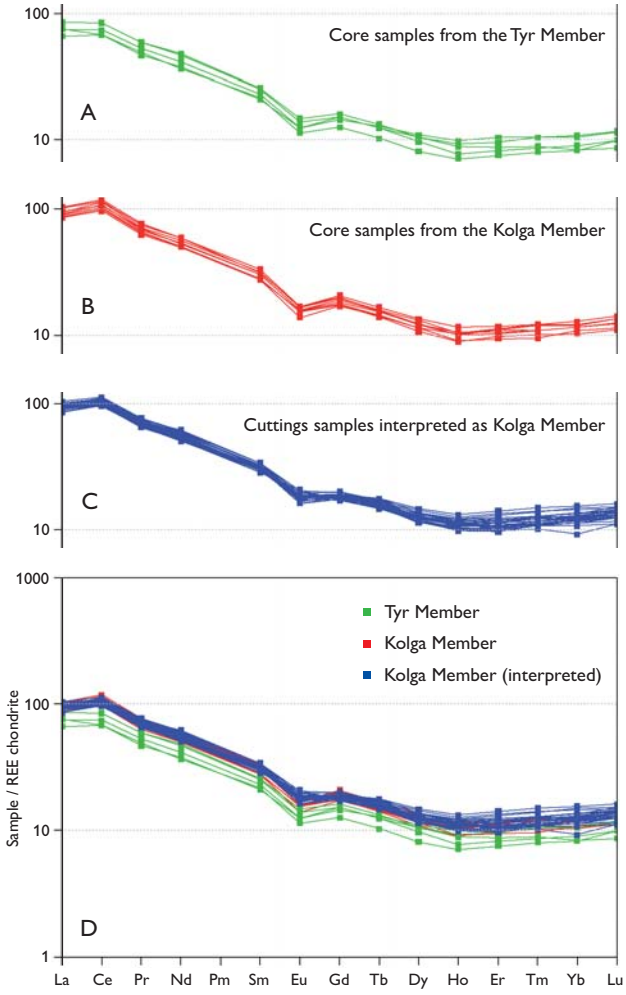

Fig. 2. REE spectra measured by ICP-MS and normalised to the chondrite composition of Boynton (1984). **A**: The Tyr Member has lower REE concentrations than the Kolga Member. **B**: The Kolga Member is characterised by a small positive cerium anomaly. **C**: REE spectra from cuttings samples from intervals without infiltration by drilling mud or clayey deposits and with normal resistivity. **D**: Composite diagram with REE spectra from A, B and C indicating that the known and interpreted intervals of the Kolga Member are idential and that they are different from those of the Tyr Member.

Bulk geochemical analyses were carried out at AcmeLabs, Vancouver, on 14 core samples and 73 cuttings samples. Major and several minor elements were determined by inductively coupled plasma emission spectrometry (ICP-ES) on fused glass discs, whereas trace elements, including REE, were identified by ICP-MS also on fused glass discs.

The modal content of minerals in 10 core samples and 16 samples of the cuttings mounted in epoxy were determined at GEUS by CCSEM on a Philips XL40SEM (Keulen *et al.* 2008). Approximately 1200 grains were analysed per sample. The method integrates backscattered electron micrographs with energy dispersive X-ray spectrometry (EDX) to measure the element composition of each grain. The major element weight percentages (wt%) were measured as oxides. The analysis is performed by sweeping over the entire grain, and hence the chemical analysis represents an average of the whole grain and not a point. This is important because the glauconite grains are inhomogeneous. Grain size and shape parameters were also measured at the cut surface in the polished section. The fragile nature of the glauconite grains made crushing of the more consolidated parts of the sand inexpedient, so a new application of the CCSEM method was developed with measurement of chemical composition in points defined by a grid. This was done in five additional core samples.

Geochemistry

Chondrite-normalised REE spectra of the Tyr and Kolga members are quite similar (Fig. 2), except for a positive cerium anomaly in the Kolga Member. The REE concentrations are moreover higher in the Kolga Member. The REE spectra of the cuttings samples fit very well with the Kolga Member (Fig. 2D). However, the wells from which the cuttings were sampled have some intervals with high resistivity, and these are generally characterised by a lower content of cerium and an enlarged negative europium anomaly.

The lower content of trace elements in the Tyr Member than in the Kolga Member makes the sand distinguishable by a number of factors. For example, Th and Ce in the Tyr Member are below 6 ppm and 70 ppm, respectively, whereas the concentration is higher in the Kolga Member. All samples of the cuttings except four are, on this basis, interpreted as Kolga Member. The four outliers are diluted by either calcite cementation or organic matter, which is seen as high values of calcium and loss on ignition (LOI), respectively.

Glauconite composition

The glauconite grains show a wide range in chemical composition, which is reflected in green to brown colours. Green grains are usually rounded and well preserved, whereas brown grains show some structural and chemical resemblance to clay minerals. The roundness of the grains could either be caused by their formation process or by subsequent physical abrasion (Odin & Matter 1981). The best preserved grains are usually those with the highest iron content. Zonation seen in many glauconite grains with light centres and dark rims is apparently related to outward decreasing magnesium content.

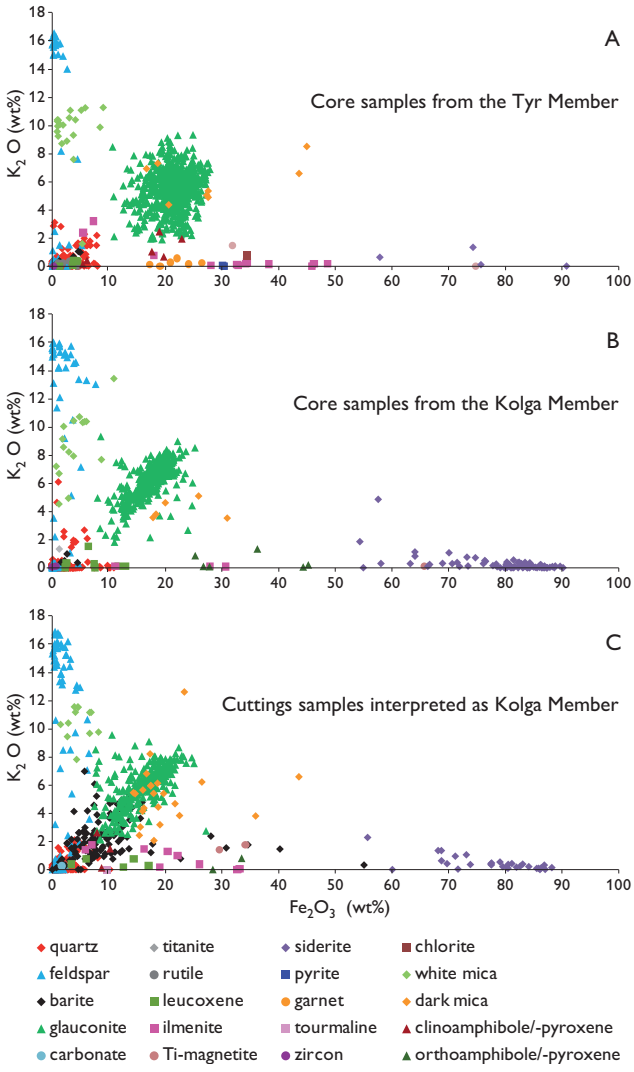

Fig. 3. Fe-K composition of the minerals expressed as Fe_2O_3 versus K_2O measured by CCSEM. **A**: The Tyr Member shows a broad glauconite composition without a linear trend. **B**: The Kolga Member is characterised by a narrow glauconite composition. **C**: The sand from the cuttings samples has a glauconite composition that closely resembles that of the Kolga Member.

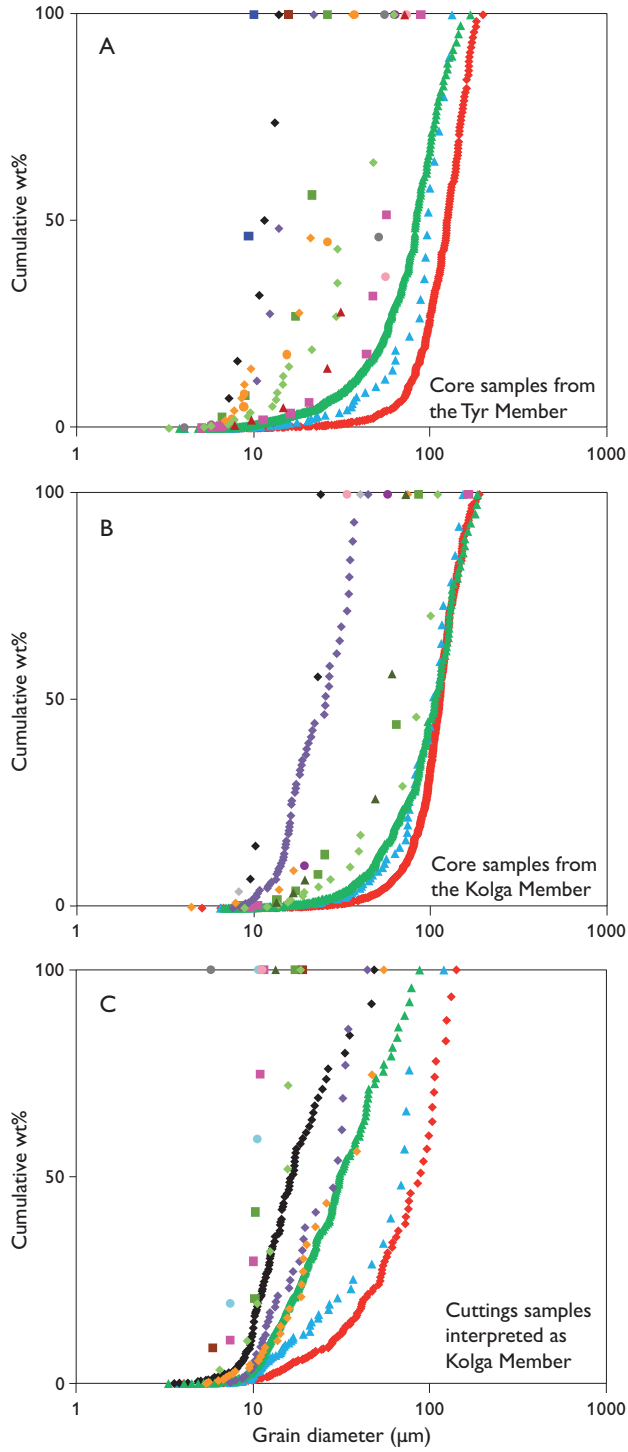

Fig. 4. Grain-size distribution curves for the minerals measured by CCSEM. **A**: The grain-size distribution of the Tyr Member has only been measured in one sample, where the glauconite shows a smaller grain size than quartz. **B**: Quartz and glauconite grains in the Kolga Member are of medium size. **C**: The cuttings samples have undergone severe crushing and hence the origin of the sand is difficult to determine from the grain-size distribution alone. For legend see Fig. 3.

Compositional variation is recorded in the glauconite in every sample. However, this variation range is different in the Tyr and Kolga members. The glauconite in core samples from the Tyr Member is characterised by a broad scatter and high iron content (Fig. 3A), which is distinctly different from the glauconite of the Kolga Member. The Kolga Member shows positive correlation between iron and potassium (Fig. 3B), which represents a substitution series with aluminium. The Kolga Member is moreover distinguishable by a high siderite content compared to the Tyr Member. All the cuttings samples of unknown stratigraphy are interpreted as Kolga Mem-

ber on the basis of mineralogy, as their glauconite compositions and siderite contents fit well with this sand (Fig. 3C).

A large amount of barite is found in many of the cuttings samples, but at least some of it comes from the drilling mud. Five of the six samples from the cored Tyr Member have been measured in single points instead of whole grains because of the extensive cementation, so the results are not entirely reliable. However, the measured glauconite compositions fit well with the broad scatter measured in the un-cemented sample.

Grain curves

The quartz of both the Tyr and Kolga members is well-sorted, and the variation in grain-size distributions is small (Fig. 4). The heavy minerals are finer grained than the light minerals, showing that hydraulic sorting has occurred. The average grain size of the glauconite and quartz grains is almost equal in the Kolga Member, but the sorting of glauconite is poorer than quartz due to a broad, fine-grained tail, which may be caused by crushing of the fragile glauconite grains. The glauconite in the Kolga Member is coarser grained than in the Tyr Member. However, the grain size of the Tyr Member has only been measured in one sample because of the cementation in the other samples. Siderite is silt-sized, and the almost straight grain curves in most samples show that the siderite is authigenic (Weibel *et al.* 2010).

Cores and cuttings are dominated by quartz grains of about the same size (Fig. 4), but the cuttings also contain a fine-grained tail (Fig. 4C) which may have been generated by crushing during the drilling process. The glauconite grains are especially susceptible to crushing because of their fragile nature, and this explains why glauconite from cuttings samples is more fine grained than from core samples.

Concluding remarks

The samples of the cuttings collected from the horizontal wells are interpreted as Kolga Member on the basis of trace element concentrations, REE spectra, glauconite compositions and siderite contents. This implies that remobilisation is restricted to intra-strata processes, rather than between strata. Modelling of the injected part of the field is therefore likely to be comparable to that of the *in situ* parts, as the original composition of the sand is the same.

ICP-MS and CCSEM have proved useful in characterising sand types, and from these observations it was possible to identify the origin of the intrusive sand bodies. Especially the REE spectra measured by ICP-MS and the glauconite compositions measured by CCSEM have enhanced the understanding of the sediments.

Acknowledgements

This study was conducted in cooperation with the partnership of Licence 4/95 in the Danish North Sea, operated by DONG Energy. The partnership is thanked for permission to publish the results.

References

Boynton, W.V. 1984: Geochemistry of the rare earth elements: meteorite studies. In: Henderson, P. (ed.): Rare earth element geochemistry, 63–114. Amsterdam: Elsevier.

Friis, H., Poulsen, M.L.K., Svendsen, J.B. & Hamberg, L. 2007: Discrimination of density flow deposits using elemental geochemistry – implications for subtle provenance differentiation in a narrow submarine canyon, Palaeogene, Danish North Sea. Marine and Petroleum Geology **24**, 221–235.

Hamberg, L., Dam, G., Wilhelmson, C. & Ottesen, T.G. 2005: Paleocene deep-marine sandstone plays in the Siri Canyon offshore Denmark, southern Norway. In: Doré, A.G. & Vining, B.A. (eds): Petroleum geology: North-West Europe and global perspectives, 1185–1198. Proceedings of the 6th Petroleum Geology Conference. London: Geological Society.

Keulen, N., Frei, D., Bernstein, S., Hutchison, M.T., Knudsen, C. & Jensen, L. 2008: Fully automated analysis of grain chemistry, size and morphology by CCSEM: examples from cement production and diamond exploration. Geological Survey of Denmark and Greenland Bulletin **15**, 93–96.

Odin, G.S. & Matter, A. 1981: De glauconiarum origine. Sedimentology **28**, 611–641.

Poulsen, M.L.K., Friis, H., Svendsen, J.B., Jensen, C.B. & Bruhn, R. 2007: The application of bulk rock geochemistry to reveal heavy mineral sorting and flow units in thick, massive gravity flow deposits, Siri Canyon Palaeocene sandstones, Danish North Sea. Developments in Sedimentology **58**, 1099–1121.

Schiøler, P. *et al.* 2007: Lithostratigraphy of the Palaeogene – Lower Neogene succession of the Danish North Sea. Geological Survey of Denmark and Greenland Bulletin **12**, 77 pp.

Weibel, R., Friis, H., Kazerouni, A.M., Svendsen, J.B., Stokkendal, J. & Poulsen, M.L.K. 2010: Development of early diagenetic silica and quartz morphologies – examples from the Siri Canyon, Danish North Sea. Sedimentary Geology **228**, 151–170.

Authors' addresses

M.O. & C.K., *Geological Survey of Denmark and Greenland, Øster Voldgade 10, DK-1350 Copenhagen K, Denmark.* E-mail: *mol@geus.dk*

J.B.S., *DONG Energy, Exploration and Production, Agern Allé 24–26, DK-2970 Hørsholm, Denmark.*

Geological characterisation of potential disposal areas for radioactive waste from Risø, Denmark

Peter Gravesen, Merete Binderup, Bertel Nilsson and Stig A. Schack Pedersen

Low- and intermediate-level radioactive waste from the Danish nuclear research facility, Risø, includes construction materials from the reactors, different types of contaminated material from the research projects and radioactive waste from hospitals, industry and research institutes. This material must be stored in a permanent disposal site in Denmark for at least 300 years (Indenrigs- og Sundhedsministeriet 2007). The Ministry of Health and Prevention presented the background and a decision plan for the Danish Parliament in January 2009 (Ministry of Health and Prevention 2009) and all political parties agreed to the plan.

In the beginning of 2011 three studies were presented to the parliament (http://www.im.dk/Aktuelt/Nyheder/Forebyggelse/2011/Maj/Slutdepot.aspx): (1) A pre-feasibility study for the final disposal of radioactive waste,

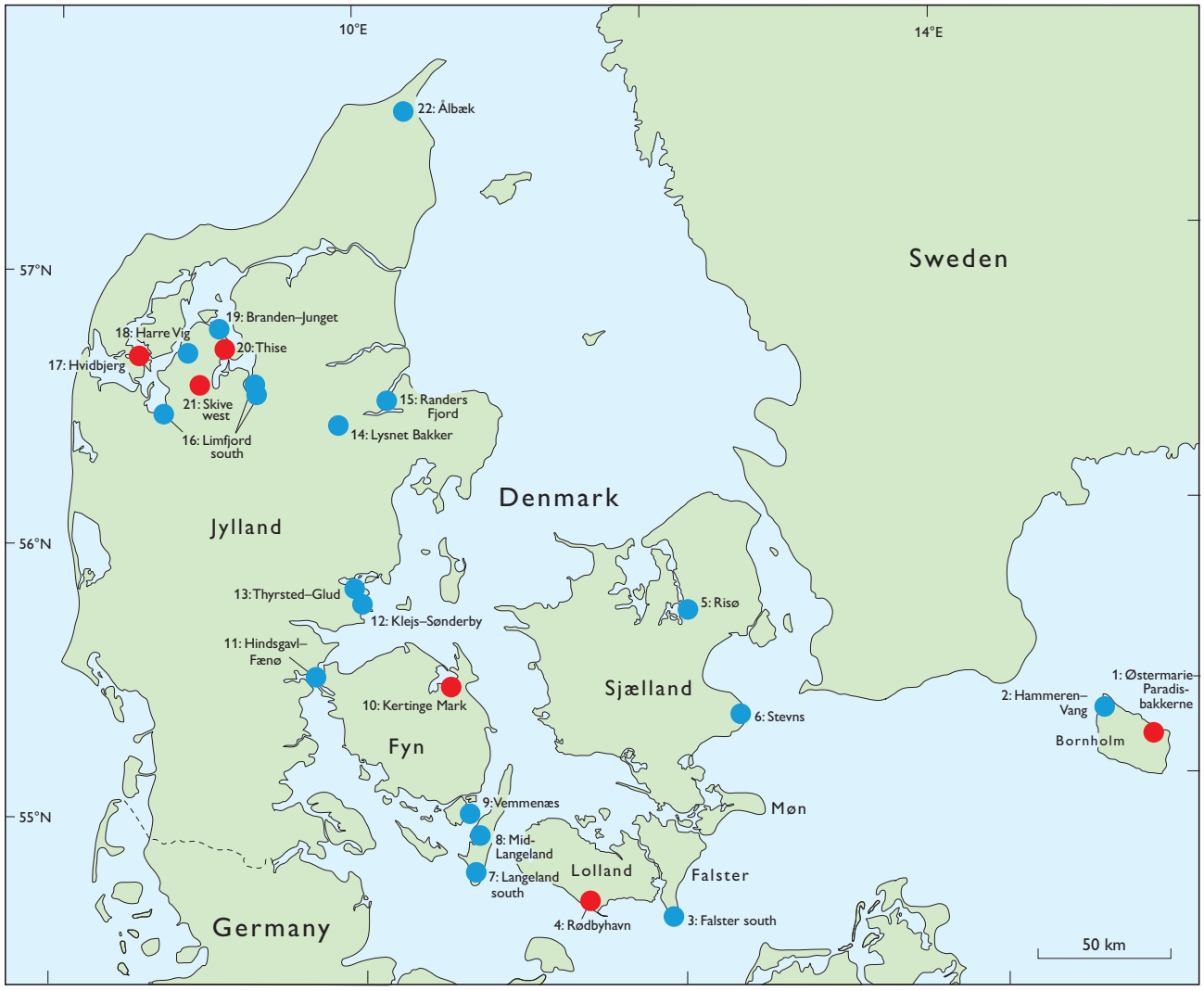

Fig. 1. Map of Denmark showing the location of the 22 selected areas. Red: the six best areas. Blue: the 16 remaining areas.

(2) a study on radiation doses from the transport of radioactive waste to a future repository and (3) a study on identifying potential disposal areas. The latter study was conducted by the Geological Survey of Denmark and Greenland (GEUS) and the aim was to locate a sediment or rock body with low permeability down to 100–300 m below the ground surface. The ultimate goal is long-term protection of people and environment by isolating the radioactive waste in a final depository. This goal can be reached by identifying a significant volume of sediments or rocks characterised by a low flow regime and high absorption potential. GEUS was given the task to locate approximately 20 potential disposal areas.

Geological setting and data requirements

In Denmark, many types of fine-grained sediments and crystalline rocks occur from the ground surface down to a depth of 300 m. Descriptions of these sediments and rocks are based on existing information and include four main types: (1) granite and gneiss on Bornholm, (2) chalk and limestone, (3) fine-grained Palaeogene and Neogene clay and (4) Quaternary clayey till and clay. In Europe, the most studied geological formations for disposal of radioactive waste are clay (Belgium, France, Germany and Switzerland), crystalline rocks (Sweden, Finland and Switzerland) and salt (Germany). Salt diapirs and salt pillows as well as deep-seated basement rocks are not included in the current study.

Several types of existing data were compiled for the preliminary selection of the approximately 20 potential areas as outlined by Indenrigs- og Sundhedsministeriet (2007). The recommendations follow the guidelines of the International Atomic Energy Agency (IAEA 1994, 1999, 2005). The study provides an overview of the distribution of various deposits and tectonic features in Denmark. Tectonic features, the distribution of layers of low permeability and the distribution of fractured sediments and rocks are important for the assessment and selection of areas suitable for disposal of radioactive waste (Gravesen *et al.* 2010).

Data collection and compilation

The deposits are described from the ground surface down to a depth of at least 100 m. The description of each area comprises: (1) geological conditions such as general geology, surface geology and profiles, sediment and rock characteristics, tectonic features and structures, seismic activity, geological and structural models, ground stability; (2) hydrogeological conditions such as groundwater characteristics, vulnerable drinking-water supply areas, geo- and hydrochemical conditions; (3) ground-surface conditions: terrain and topography, surface processes, climate and climate changes, restrictions and limitations in connection with protection of nature areas; (4) summary of area conditions with final remarks and literature.

The area descriptions address the following important issues (IAEA 1994, 1999, 2005): (1) The final disposal site should be situated in an area with homogeneous geological conditions. It should be demonstrated that these conditions are found with a high degree of probability at the selected site. As the geological conditions in many parts of Denmark are heterogeneous on both local and regional scales, the goal was to find a sufficiently large area with continuous and homogeneous sediment or rock bodies without fractures or preferential flow paths. (2) The geological deposits shall contribute to isolate the radioactive waste. This is most effective if the disposal site is underlain or surrounded by low permeability layers such as clay, silt or crystalline rock. (3) Restriction of pore water flow from the disposal site is favoured by deposits of low permeability. (4) The disposal site must be placed at the greatest possible distance from the nearest groundwater aquifer. (5) The disposal site must be located outside areas of special drinking-water interests. (6) The surrounding groundwater aquifer must be able to contribute to dilution of any radioactive material that might leak from the disposed material. (7) The surrounding sediments, rocks and ground water aquifer material must have a high potential for absorption of any leaking radioactive components. (8) Geological processes at the terrain surface should not have any influence on the quality of the disposal site.

Criteria and methods for selection

The potential disposal areas fit the criteria set up by Gravesen *et al.* (2010, 2011) to various degrees. Due to the heterogeneous geological conditions in Denmark it is not possible to fulfil all the criteria within one area. Therefore, it is necessary to assess the criteria and to compare the areas.

Criteria – The geological and hydrogeological criteria have been central for the selection of the areas. The type of disposal site had not been decided when the study started and the following criteria were considered the most important: (1) The deposits from the ground surface and downwards should be as homogeneous and of as low permeability as possible. This means that highly permeable deposits such as sand and gravel should be of limited extent. (2) The deposits of low permeability that enclose the waste should comprise thick layers of large horizontal extent.

Other criteria were also important for the selection: (1) Areas of special drinking-water interests have been totally avoided. Areas of drinking water interests comprise a large part of Denmark and it was impossible to totally exclude these areas. (2) We tried to avoid groundwater bodies of good status. (3) EU nature protection areas (NATURA 2000) were completely avoided; other nature and heritage protection areas were avoided if possible. (4) Large cities and suburbs of larger cities were also avoided.

Methods for selection – The methods used were as follows: (1) The geological conditions in Denmark have been evaluated based on existing data and information (e.g. Pedersen 1989, Håkansson & Pedersen 1992). It was decided which types of sediments and rocks should be included in the work. The sediments and rocks fulfilling most of the demands are: Crystalline rocks (granite and gneiss), some types of limestone, fine-grained pre-Quaternary clay and fine-grained Quaternary clay. If possible, layers of clayey tills should cover these deposits. (2) The next step was to identify and avoid the areas of special drinking-water interests, NATURA 2000 areas and large cities; these areas were not treated further. (3) The remaining areas were analysed according to the criteria of thick deposits of low permeability with large horizontal extent from the ground surface and downwards.

Possible future climate changes were also considered during the selection process. The current prognoses from the Intergovernmental Panel on Climate Change cover *c.* 100 years. The waste facility must exist for at least 300 years; predictions of climate changes for the latter part of this period are highly uncertain. The sea level is expected to rise 0.5–1.0 m, but it may rise more.

Survey results

Our survey resulted in the selection of 22 areas throughout Denmark (Fig. 1). The compilation and scientific evaluation of the data resulted in several new findings concerning the Danish geology. Data from a large number of boreholes have been compiled from areas that normally attract little interest from geologists and water-resource managers. In addition, the selected areas are of no or little interest for local drinking-water exploitation, nature protection or archaeology.

The selected areas are larger than required for the final depository. Therefore the final site can be located according to other limitations or parameters within the selected area.

From 22 to six areas – It is suggested that the work of the next phase be concentrated on six areas, chosen from among the 22 areas. The 22 areas were chosen so that they fulfil the criteria or most of the criteria. They are all qualified areas, according to an evaluation based on existing data and knowledge, but the amount of information and knowledge varies from area to area. The six areas are assessed as being slightly better than the remaining 16 areas, which are reserve areas that can be included if the six areas cannot be used for some reason

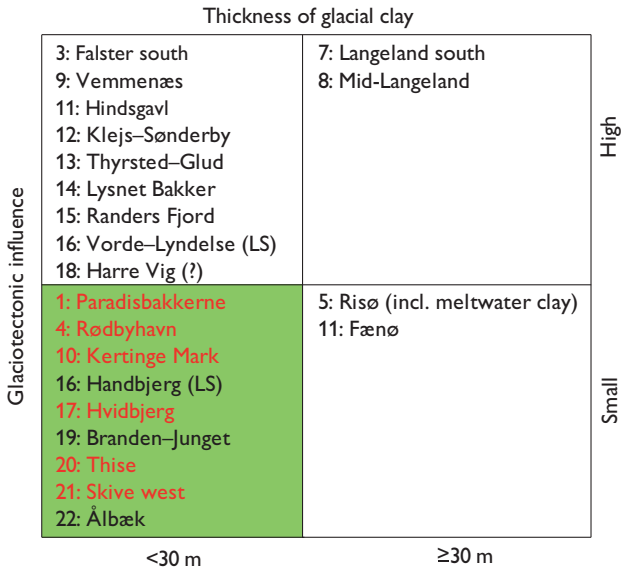

Fig. 2. Diagram showing the thickness of glacial clay (mainly clayey till) versus the importance of glaciotectonic influence. The green box show the best localities and the red localities are the selected ones. **LS**: Limfjord south.

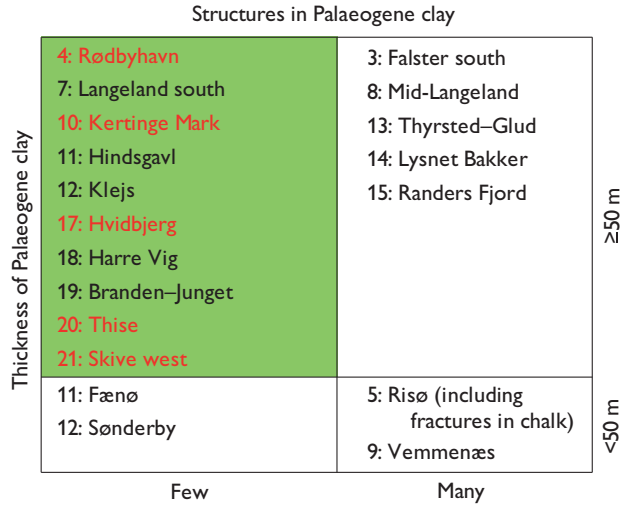

Fig. 3. Diagram showing the structures in Palaeogene clay versus the thickness of Palaeogene clay. The green box show the best localities and the red localities are the selected ones with Palaeogene clay, the sixth locality is in crystalline rock (Østermarie–Paradisbakkerne). The localities Hammeren-Vang and Stevns are not shown in the diagrams, because they have no Palaeogene clay or they have not been influenced by glaciotectonics.

that 'overrides' the geological criteria. The overriding factors could be grounded in infrastructure and regional planning as well as protests from citizens. Results from future detailed field and laboratory studies may also lead to the rejection of some areas, which were considered suitable according to existing knowledge.

The six areas are Østermarie–Paradisbakkerne in Bornholm's Regionskommune, Rødbyhavn in Lolland Kommune, Kertinge Mark in Kerteminde Kommune, Hvidbjerg in Struer Kommune, Thise in Skive Kommune and Skive west also in Skive Kommune (Fig. 1).

The geological criteria used to select the six potential areas were: (1) The areas have clay or crystalline rocks of low permeability from the ground surface to at least 100 m depth with only few subsurface structures. (2) Clayey till dominates the upper part, but this covering layer of clayey till is relatively thin (less than 30 m) in most of the area, and layers of low permeability are rapidly reached. This meets the requirements for a medium deep repository (30–100 m), where the depository should be surrounded by layers of low permeability. (3) Glaciotectonic influence has little significance (down to 30 m) but this is often difficult to assess for a large area, because glaciotectonic features can only be demonstrated from outcrop or borehole data. (4) In the selected areas, only areas of no, limited or some drinking-water interests are found. (5) In the areas, there are no significant occurrences of groundwater bodies with good status. (6) The terrain is mostly flat and of little relief, and the landscape is considered stable and without risk of landslides.

The different properties of the 22 areas were compared. Areas with glacial till less than 30 m thick and Palaeogene clay over 50 m thick were considered the best areas (Figs 2, 3). Also areas with only minor glaciotectonic influence and areas with only few tectonic structures in the Palaeogene clay were ranked as best. Areas with glaciotectonic deformations such as fractures, faults and folds (Klint & Gravesen 1999) are often characterised by sand and gravel occurring between finer grained layers. With respect to tectonic structures in the Palaeogene clay, it should be noted that some areas are poorly covered by data.

As far as possible, the selected areas are located in regions with limited or no drinking-water interests. However, some of the selected areas are located partly or wholly in areas of drinking- water interests.

Six of the areas are located in areas with Quaternary clay, basement rock or chalk/limestone and do not include Palaeogene clay. These areas have relatively thin top layers of clayey till (less than 20 m). Fractures and tectonic structures may occur. Based on our analysis of the properties we conclude that the six named areas are better suited for radioactive waste disposal than the other 16 areas.

Final remarks

Our survey resulted in the selection of 22 areas throughout Denmark. Six of these areas are preferred on geological and hydrogeological criteria. Eventually, the six areas will be reduced to one, two or three areas that appear promising in which further detailed field work will be carried out. The field investigations include analysis of the geological, hydrogeological, hydrochemical and geomechanical conditions. Finally, one site will be chosen for the final waste disposal.

Acknowledgement

Financial support was provided by the Parliament of Denmark.

References

Gravesen, P., Nilsson, B., Pedersen, S.A.S. & Binderup, M. 2010: Low- and intermediate radioactive waste from Risø, Denmark. Location studies for potential disposal areas. Report no. 1. Data, maps, models and methods used for selection of potential areas. Danmarks og Grønlands Geologiske Undersøgelse Rapport **2010/122**, 47 pp.

Gravesen, P., Nilsson, B., Pedersen, S.A.S. & Binderup 2011: Low- and intermediate radioactive waste from Risø, Denmark. Location studies for potential disposal areas. Report no. 11. Områdebeskrivelser – Description of areas. Dansk og engelsk resume. Danmarks og Grønlands Geologiske Undersøgelse Rapport **2011/51**, 64 pp.

Håkansson, E. & Pedersen, S.A.S. 1992: Geologisk kort over den danske undergrund. 1:500 000. Copenhagen: Varv. (Map sheet).

IAEA 1994: Siting of near surface disposal facilities. Safety guides. Safety Series **111-G-3.1**, 37 pp.

IAEA 1999: Near surface disposal of radioactive waste. Requirements. Safety Standards Series **WS-R-1**, 29 pp.

IAEA 2005: Borehole facilities for the disposal of radioactive waste. Specific safety guide. Safety Standards Series **SSG-1**, 102 pp.

Indenrigs- og Sundhedsministeriet 2007: Beslutningsgrundlag for et dansk slutdepot for lav- og mellemaktivt affald, 47 pp. Unpublished report, Indenrigs- og Sundhedsministriet, Copenhagen, Denmark.

Klint, K.E.S. & Gravesen, P. 1999: Fractures and biopores in Weichselian clayey till aquitards at Flakkebjerg, Denmark. Nordic Hydrology **30**, 267–284.

Ministry of Health and Prevention 2009: Redegørele om beslutningsgrundlag for et dansk slutdepot for lav- og mellemaktivt affald, 13 pp. Report, Ministry of Health and Prevention, Copenhagen, Denmark.

Pedersen, S.A.S. (ed.) 1989: Jordartskort over Danmark 1:200 000. Four map sheets: Nordjylland; Midtjylland; Sydjylland; Fyn, Sjælland, øer og Bornholm. Copenhagen: Danmarks Geologiske Undersøgelse.

Authors' address

Geological Survey of Denmark and Greenland, Øster Voldgade 10, DK-1350 Copenhagen K, Denmark. E-mail: *pg@geus.dk*

A digital, spatial, geological model of the Miocene in Jylland, Denmark

Margrethe Kristensen, Thomas Vangkilde-Pedersen and Erik Skovbjerg Rasmussen

A major hydrogeological programme has been carried out to map the Miocene succession in central and southern Jylland (Fig. 1). The Miocene deposits comprise several aquifers with potential drinking water resources and have been investigated by drilling and acquisition of seismic data integrated with sedimentology and biostratigraphy. Scharling *et al.* (2009) described a 3D hydrogeological model that covers part of the onshore Danish Miocene deposits. The model was based on a sequence-stratigraphic approach and led to a better understanding of the geological architecture of the aquifers than traditional lithofacies models. Hence it was decided to establish a digital, spatial, geological model covering the entire onshore Miocene succession (Kristensen *et al.* 2010).

Geology

The onset of the Miocene is characterised by inversion tectonics causing a change in the depositional regime from full marine, clayey sediments to shallow-water, sand-rich, delta deposits (Rasmussen *et al.* 2010). During the Early – early Middle Miocene, regressions and transgressions were strongly controlled by eustatic sea-level changes, resulting in three phases of shoreline progradation into the basin that covers present-day Denmark. The three phases are represented by the sand-rich Billund, Bastrup and Odderup Formations, intercalated with the clayey and silty marine Vejle Fjord, Klintinghoved and Arnum Formations (Fig. 2). During the late Middle Miocene to the Late Miocene, the marine clay of the Hodde, Ørnhøj and Gram Formations were deposited and towards the end of the Miocene a new progradation resulted in deposition of the sandy Marbæk Formation.

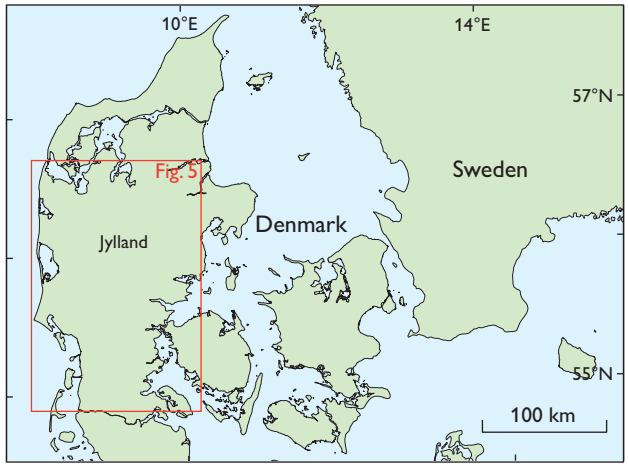

Fig. 1. Map of Denmark showing the study area in central and southern Jylland (rectangle).

Sequence stratigraphic framework

The Miocene digital, spatial, geological model is based on the sequence-stratigraphic framework of Rasmussen (2004) and Rasmussen & Dybkjær (2005) and the lithostratigraphy of Rasmussen *et al.* (2010). These studies are based on new borehole data, high-resolution seismic profiles (Vangkilde-Pedersen *et al.* 2006) and high-resolution biostratigraphy (Dybkjær & Piasecki 2010). In sequence stratigraphy a geological succession is divided into a succession of different lithofacies (a sequence) bounded by key-surfaces and commonly stacked in a cyclic manner. Each sequence represents

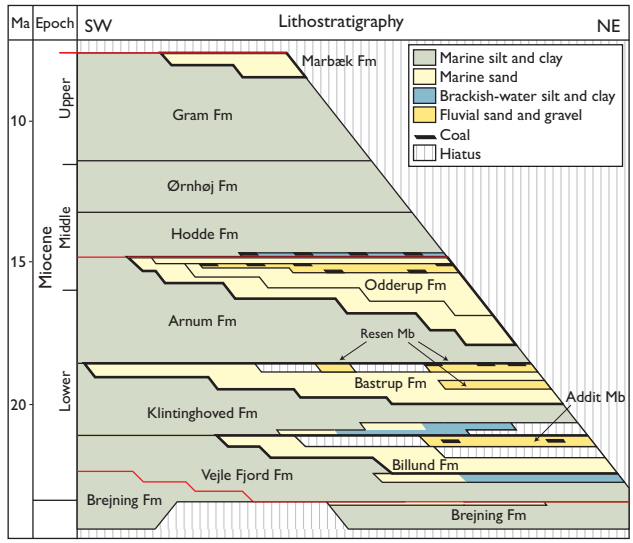

Fig. 2. Lithostratigraphic scheme of the Miocene of onshore Denmark showing the distribution of the formations from south-west to north-east Jylland. Marine deposits dominate in the south-western part of Jylland. Delta or fluvial sand deposits are mainly found in the central parts of Jylland, where they form large potential groundwater reservoirs (Rasmussen *et al.* 2010).

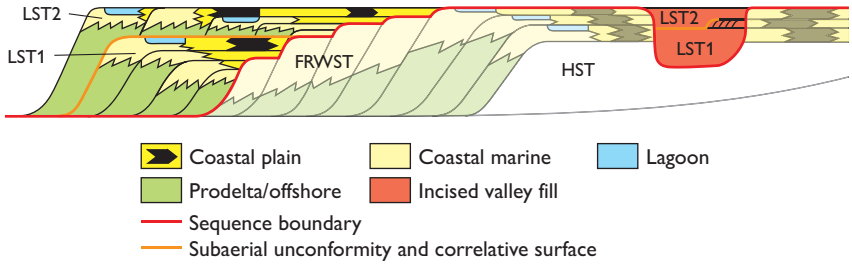

Fig. 3. A conceptual model for the development of the Miocene deposits in Jylland. **HST**: Highstand systems tract, **FRWST**: Forced regressive wedge systems tract. **LST2**: lowstand systems tract unit 2. **LST1**: lowstand systems tract unit 1.

a cycle in relative sea level and can be subdivided into four systems tracts that link contemporaneous deposits together. (1) During the early stage of sea-level rise the *lowstand systems tract* is formed when the sediment supply from the hinterland is greater than the sea-level rise. The shoreline progrades into the basin and sands and clays are deposited in association with delta progradation. Incised valleys are filled up by fluvial deposits, which are usually dominated by coarse-grained sediments. (2) The *transgressive systems tract* is formed when the base-level rise outpaces the sediment supply from the hinterland, causing the shoreline to move landwards. This landward movement of the shoreline results in predominant clay and silt deposition on the former delta platform and in the basin. However, sand is still deposited along the shoreline, commonly on the shoreface and in inlets of barrier complexes, as bars in tidally influenced estuaries and in incised valleys associated with fluvial systems. (3) During the late stage of sea-level rise the *highstand systems tract* is formed. The sediment supply from the hinterland outpaces the sea-level rise and the shoreline again progrades into the basin. The highstand systems tract commonly shows fine- to coarser-grained deposits laid down on the slope of delta complexes or as shoreface sands alternating with lagoonal clays. (4) The *forced regressive wedge systems tract* is formed in the marine part during falling sea level and is hence characterised by progradation of the shoreline. During falling sea level, incision commences on the highstand delta complex. The deposits are typically dominated by well-sorted, relatively coarse-grained sediments. Common deposits include different types of off-lapping shallow marine shoreface and delta deposits and deep-sea submarine fans.

In the Miocene succession of Denmark some of the best aquifers are associated with lowstand systems tracts (Fig. 3). The sand that constitutes the aquifers was partly deposited in incised valleys and partly as prograding deltas in the basinal area. The incised valleys are dominated by fluvial deposits, namely the Addit Member of the Billund Formation and the Resen Member of the Bastrup Formation (Fig. 2). Both generations show a two-fold subdivision of the valley fill that coincides with delta progradation into the basin. This pattern is, however, interrupted by minor flooding where a thin sequence of marine sand, clay and coal was deposited. An example of two such successive delta deposits from the lowstand systems tract of the Bastrup Formation is shown in Fig. 4.

The glacio-eustatic sea-level changes in the Miocene resulted in an asymmetric pattern of slow regressions and rapid transgressions, which explains why transgressive sand or clay was rarely deposited.

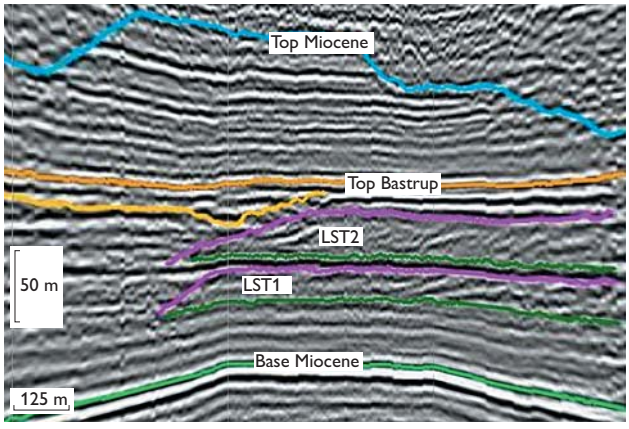

Fig. 4. Seismic profile showing two successive delta complex deposits of the lowstand systems tract of the Bastrup Formation. **LST1**: lowstand systems tract unit 1. **LST2**: lowstand systems tract unit 2. For location see Fig. 5B.

Modelling of the Miocene succession

The backbone of the Miocene digital, spatial, geological model is nine correlation panels (five W–E- and four S–N-oriented), which constitute a conceptual geological model of the Danish Miocene (Rasmussen *et al.* 2010). The conceptual model is based on sedimentological investigations of samples from 150 boreholes (*c.* 100–400 m deep), detailed biostratigraphical studies of samples from 50 boreholes and studies of 25 outcrops tied together with a dataset of *c.* 1200 km high-resolution seismic profiles.

With the conceptual model as the starting point, a 3D geological model has been established using the software package GeoScene 3D (www.i-gis.dk). The GeoScene 3D software gives the user direct access to carry out interpretation moving through the subsurface and better understand 3D structures. Borehole data, geophysical logs and seismic

data have been imported to the modelling software and interpretation performed both on 2D profiles and in the 3D environment. The set-up is constructed as a layer model, but emphasis has been on distinguishing between different generations of delta lobes as the shoreline prograded into the basin during deposition of the Billund, Bastrup and Odderup Formations. Thus the model comprises 75 layers and lithological units, which have been named according to the formation and depositional environment. The top of each lithological unit is interpreted using interpretation points. The interpretation is based on data from: stratigraphically described boreholes, high-resolution seismic profiles or boreholes from the national borehole database. Free digital points have also been added to indicate the outline of deltalobes. The interpretation includes an evaluation of the quality of the points. The Top Miocene, Top Bastrup, Top Billund and Base Miocene surfaces are interpreted in almost the entire model area. Unlike these surfaces, the propagation of each generation of delta lobes, is limited and follows the position of the coastline, at the time of deposition.

On the basis of high-resolution seismic profiles and detailed lithological descriptions of borehole samples, the extension of each delta lobe has been interpreted. In Fig. 5 the maximum extension of 10 generations of delta lobes of the Bastrup Formation and 11 generations of delta lobes of the Billund Formation is shown together with the coverage of high-resolution seismic profiles and boreholes used in the sequence-stratigraphic interpretation.

To support the model, detailed interpretation of the seismic profiles shown in Fig. 5 has been conducted with focus on mapping the extent of sand-rich bodies. All previous interpretations of the Top Miocene, Top Billund, Top Ba-strup and Base Miocene have been checked, and if necessary, revised, according to the present level of knowledge. Top and bottom of sand-rich bodies in the form of delta or fluvial deposits have been interpreted on all seismic lines in order to assist the modelling work in GeoScene 3D. Internal, parallel, clinoform, reflection patterns with dips of 5–10° have been interpreted as a direct indicator of fine- to coarse-grained sand, whereas sigmoidal clinoform internal reflection patterns typically indicate alternating layers of clay and sand (Rasmussen *et al.* 2007: Bassetti *et al.* 2008; Hansen & Rasmussen 2008). Incised valleys and fluvial channels expressed by concave-up erosion surfaces are typically filled with coarse- to fine-grained sand and coarse-grained sand and gravel, respectively (Rasmussen *et al.* 2007). In places where the seismic data do not directly indicate sandy deposits, the profiles have nevertheless been used to extrapolate available borehole information in the best possible way.

Gamma-ray logs have been a valuable supplement to the geological descriptions of borehole samples. Most of the boreholes were drilled using the airlift drilling technique which may result in poor recovery of coarse silt and fine sand (Ditlefsen *et al.* 2008). Therefore, gamma-ray logs have been useful both for checking and correcting the lithological logs and as an indicator of depositional environment. Sand-rich delta units are generally coarsening upwards and are seen on the logs as upward-decreasing gamma-ray values. Fluvial channel deposits are characterised by fining-upward trends and are seen as upward-increasing gamma-ray values (Fig. 6).

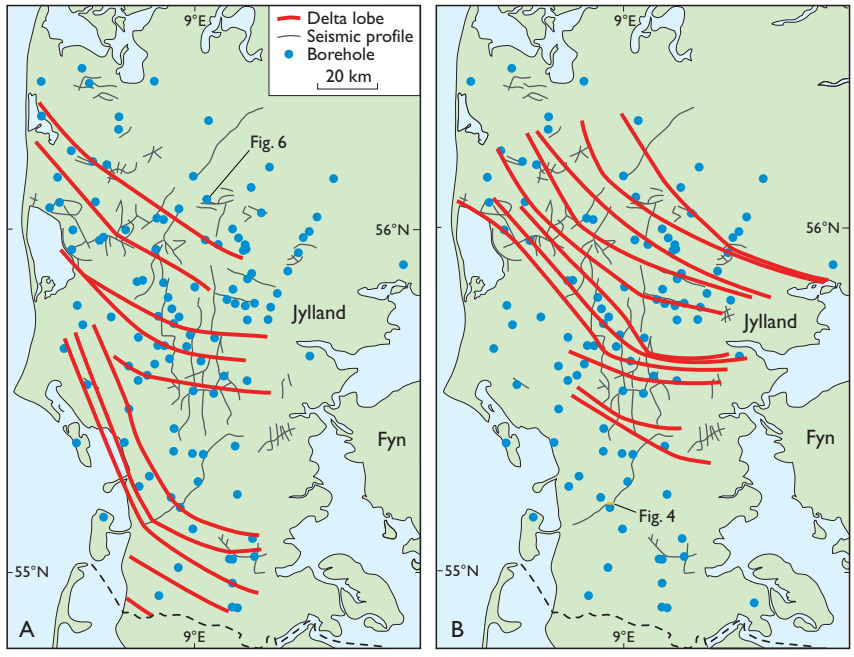

Fig. 5. Map of southern and central Jylland showing the maximum extent of individual generations of delta lobes of **A**: Billund Formation and **B**: Bastrup Formation. The interpretation is based on high-resolution seismic profiles and data from boreholes.

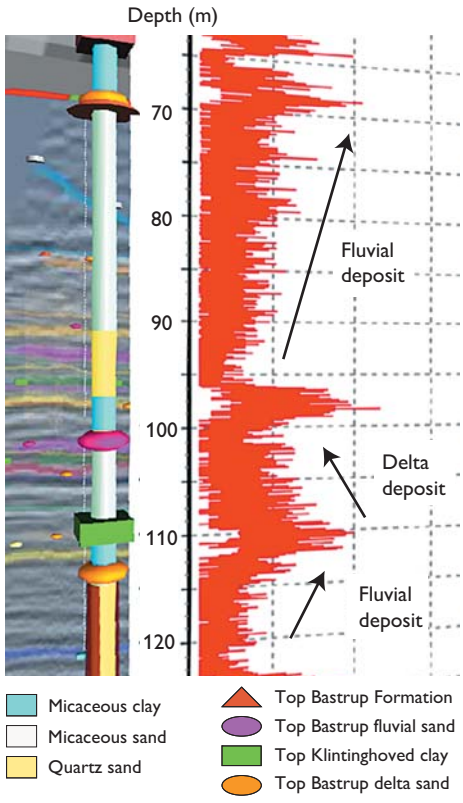

Fig. 6. Example of interpretation of depositional environment from gamma-ray log patterns. Upward-increasing gamma-ray values are interpreted as a fining-upward fluvial deposit and upward-decreasing gamma-ray values are interpreted as an upward-coarsening delta complex. For location see Fig. 5A.

Future work and perspectives

The Miocene 3D model reflects the basin development and the depositional processes as well as the palaeogeographical development during the Miocene in Denmark. The spatial, geological model is intended to serve as a geological database of lithological and stratigrafical information and can be seen as a visual archive of the geological knowledge of the Miocene in the model area. As such, it will serve as the foundation for different types of application-oriented models. The Miocene 3D model is already used in the Danish Nature Agency as a framework for at least 11 modelling projects. The model will be updated on an annual basis in the coming years as new boreholes, seismic profiles and other data become available, or following new interpretations.

Acknowledgements

The Nature Agency Centres in Ribe, Ringkøbing and Aarhus are thanked for financial support.

References

Bassetti, M.A., Berne, S., Jouet, G., Taviani, M., Dennielou, B., Flores, J.A., Gaillot, A., Gelfort, R., Lafuerza, S. & Sultan, N. 2008: The 100-ka and rapid sea level changes recorded by prograding shelf sand bodies in the Gulf of Lions (western Mediterranean Sea). Geochemistry Geophysics Geosystems **9**, Q11R05, 27 pp.

Ditlefsen, C., Sørensen, J., Pallesen, T.M., Pedersen, D., Nielsen, O.B., Christiansen, C., Hansen, B. & Gravesen, P. 2008: Jordprøver fra grundvandsboringer, vejledning i udtagning, beskrivelse og geologisk tolkning i felten, 108 pp. Geo-vejledning 1. København: De Nationale Geologiske Undersøgelser for Danmark og Grønland.

Dybkjær, K. & Piasecki, S. 2010: Neogene dinocyst zonation for the eastern North Sea Basin, Denmark. Review of Palaeobotany and Palynology **161**, 1–29.

Hansen, J.P.V. & Rasmussen, E.S. 2008: Structural, sedimentologic, and sea-level controls on sand distribution in a steep-clinoform asymmetric wave-influenced delta: Miocene Billund sand, eastern Danish North Sea and Jylland. Journal of Sedimentary Research **78**, 130–146.

Kristensen, M., Vangkilde-Pedersen, T. & Rasmussen, E.S. 2010: Miocæn 3D. Den rumlige geologiske model. Danmarks og Grønlands Geologiske Undersøgelse Rapport **2010/91**, 46 pp.

Rasmussen, E.S. 2004: Stratigraphy and depositional evolution of the uppermost Oligocene – Miocene succession in western Denmark. Bulletin of the Geological Society of Denmark **51**, 89–109.

Rasmussen, E.S. & Dybkjær, K. 2005: Sequence stratigraphy of the Upper Oligocene – Lower Miocene of eastern Jylland, Denmark: role of structural relief and variable sediment supply in controlling sequence development. Sedimentology **52**, 25–63.

Rasmussen, E.S., Vangkilde-Pedersen, T. & Scharling, P.B. 2007: Prediction of reservoir sand in Miocene deltaic deposits in Denmark based on high-resolution seismic data. Geological Survey of Denmark and Greenland Bulletin **13**, 17–20.

Rasmussen, E.S., Dybkjær, K. & Piasecki, S. 2010: Lithostratigraphy of the Upper Oligocene – Miocene succession of Denmark. Geological Survey of Denmark and Greenland Bulletin **22**, 92 pp.

Scharling, P.B., Rasmussen, E.S., Sonnenborg, T.O., Engesgaard, P. & Hinsby, K. 2009: Three-dimensional regional-scale hydrostratigraphic modeling based on sequence stratigraphic methods: a case study of the Miocene succession in Denmark. Hydrogeology Journal **17**, 1913–1933.

Vangkilde-Pedersen, T., Dahl, J.F. & Ringgaard, J. 2006: Five years of experience with landstreamer vibroseis and comparison with conventional seismic data acquisition. Proceedings of the 19th Annual SAGEEP Symposium on the Application of Geophysics to Engineering and Environmental Problems, Seattle, USA, 1086–1093.

Authors' address

Geological Survey of Denmark and Greenland, Lyseng Allé 1, DK-8270 Højbjerg, Denmark. E-mail: *mkr@geus.dk*

A new Middle Pleistocene interglacial sequence from Måløv, Sjælland, Denmark

Ole Bennike, Esben Lindgård, Henrik Jønsson Granat, Richard C. Preece and Finn Viehberg

Interglacial deposits in Denmark have traditionally been referred to the Cromerian complex (Hareskovian), Holsteinian or Eemian stages. However, based on studies of sediment cores from the deep sea many more than three Quaternary interglacials have been documented, and in other parts of north-western Europe it is becoming increasingly clear that the on-shore Quaternary sequences are much more complex than previously believed. Interglacial deposits are characterised by plant and animal remains indicating longer periods with climatic conditions similar to or warmer than today, whereas interstadial deposits were formed during shorter time spans and usually contain remains of relatively cold-adapted, arctic or sub-arctic species. Interglacial and interstadial deposits can be dated more or less precisely, and thus provide information about the relative age of glacial deposits.

In 2010 the Geological Survey of Denmark and Greenland (GEUS) described samples from a 75 m deep borehole at 55°45.37′N, 12°19.63′E (elevation 20.7 m a.s.l.), at the address Bakketoften 50 in Måløv on north-eastern Sjælland (Fig. 1). Coring was conducted for Ballerup municipality (kommune) using the reverse circulation technique ('omvendt skylning med lufthævning') by the well-drilling company Thomas Brøker, and samples were collected every 2 m and sent to GEUS. A few shells of freshwater gastropods were noted, and since pre-Holocene shell-bearing deposits are rare on Sjælland, we decided to analyse the macrofossil content. We initially assumed that the sediments were deposited in a lake during a Weichselian interstadial, because an interstadial deposit was reported from Måløv by Frederiksen & Rosbirk (1999). However, we question this dating since Frederiksen and Rosbirk did not provide any data that could confirm an interstadial age or a lacustrine environment. This article gives details of macrofossil analyses of five samples from the borehole, which allow for more definite conclusions about the depositional environment of the site and its possible age.

Lithostratigraphy

The drilling penetrated 52 m of Quaternary sediments, 16 m of Danian limestone and 7 m of Cretaceous chalk (Fig. 2). It stopped at a depth of 75 m below the ground surface. The Quaternary sediments are dominated by glacial till and meltwater deposits. However, a unit of clay with a few shells of freshwater gastropods was found between 34 and 44 m. The clay unit is underlain and overlain by clayey till.

Material and methods

Five sediment samples were available for analysis of macrofossils, each weighing around 1 kg. The samples were soaked in a NaOH solution at room temperature for two weeks and wet sieved on 0.4, 0.2 and 0.1 mm sieves. The residue left on the sieves was analysed using a dissecting microscope. The plant and animal remains studied are much larger than for example pollen grains or diatom frustules, and we call them macrofossils, even though for example ostracods are traditionally considered microfossils by palaeontologists.

Palaeoecology

The results of the macrofossil analyses are presented in Table 1. One of the samples did not contain any macrofossils, one contained only a few moss remains, one contained

Fig. 1. Map of Denmark showing the location of Måløv and other localities on Sjælland with non-marine interglacial deposits discussed in the text.

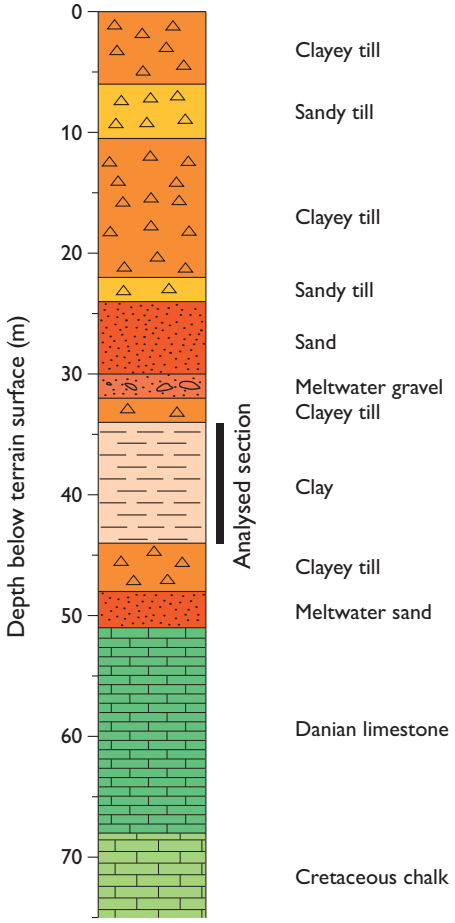

Fig. 2. Lithological log of core DGU 200.5351 from Måløv.

Table 1. Macrofossils in five samples from interglacial deposits near Måløv

Sample no.	38775	38776	38777	38778	38779
Depth (m)	34–36	36–38	38–40	40–42	42–44
Mosses					
Bryum sp.	–	–	–	r	c
Polytrichum s.l. sp.	1	–	–	–	–
Sphagnum sp.	2	3	–	–	–
Vascular plants					
Nymphaeaceae indet.	1	–	–	–	–
Potentilla sp.	–	1	–	–	–
Rumex maritimus	–	4	–	–	–
Stratiotes aloides	2	–	–	–	1
Typha sp.	2	–	–	–	–
Juncus sp.	1	–	–	–	–
Ostracods					
Cyprideis torosa	4	–	–	–	–
Scottia tumida	r	1	–	–	–
Darwinula stevensonia	1	–	–	–	–
Molluscs					
Borysthenia naticina	9	3	–	–	–
Sphaerium cf. *solidum*	1	–	–	–	–
Sphaerium cf. *corneum*	r	–	–	–	–
Sphaerium sp.	–	r	–	–	–
Pisidium supinum	2	–	–	–	–
Pisidium moitessierianum	2	–	–	–	–
Bivalvia indet.	–	r	–	–	–
Bryozoans					
Plumatella repens	2	1	–	–	3
Fredericella indica	–	–	–	–	2
Cristatella mucedo	–	1	–	–	–

r: rare, c: common.

frequent moss remains and a few other macrofossils. The two most shallow samples were somewhat richer in macrofossils, but their concentration and diversity are low.

The macrofossils are dominated by freshwater organisms, but at least one brackish-water species, the ostracod *Cyprideis torosa*, is also present. It occurred with articulated carapaces, suggesting that reworking is unlikely. The carapaces and shells of *C. torosa* are noded (forma *torosa*), a feature indicating a salinity <7‰ (Meisch 2000; Frenzel *et al.* 2010). Shells of freshwater gastropods are also present. Some are fragmented, but this damage may have occurred during coring. The presence of both brackish-water and freshwater organisms implies low salinity conditions that would allow such a co-occurrence. A similar situation is found in many places today, for example at river mouths, in estuaries and in the Gulf of Bothnia. The lack of head capsules of Chironomidae, as well as carapaces and head shields of Cladocera, may also imply weakly brackish waters. Interglacial lake deposits usually contain hundreds of head capsules of non-biting midge larvae (chironomids) per millilitre sediment, and thousands of cladoceran remains per millilitre. Although it is risky to use negative evidence, we suggest that the absence of chironomid and cladoceran remains is due to brackish-water conditions. On the other hand, the lack of these remains could perhaps also be attributed to poor preservation, but the other macrofossils are well preserved, and this possibility is considered unlikely. No rivers are found on Sjælland today, and it may be speculated if the deposit formed near the outlet from a former freshwater or brackish water Baltic Sea, somewhat similar to the palaeogeographical situation in the early Holocene.

The assemblage of freshwater taxa comprises at least 12 species. Macrolimnophytes are represented by a species of Nymphaeaceae (water lily, 1 leaf hair) and *Stratiotes aloides* (water soldier, 3 leaf-margin spines). These water plants grow in shallow water, in lakes or in streams with slowly flowing water. Both are typical of mesotrophic to eutrophic waters. Freshwater ostracods are represented by *Darwinula stevensoni* and *Scottia tumida* (Fig. 3) and freshwater molluscs by the gastropod *Borysthenia naticina* (Fig. 4) and the bivalves

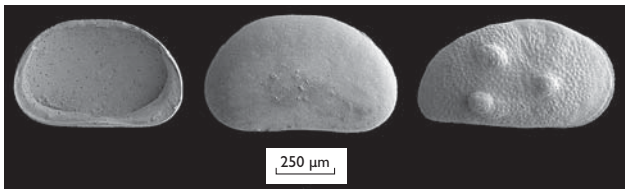

Fig. 3. Scanning electron microscope images of ostracode shells from Måløv. **A:** *Scottia tumida* (internal view). **B:** *Scottia tumida* (external view). **C:** *Cyprideis torosa* (external view, juvenile).

Fig. 4. Light photographs of two shells of *Borysthenia naticina* from Måløv.

Sphaerium cf. *solidum*, *Sphaerium* cf. *corneum*, *Pisidium supinum* and *Pisidium moitessierianum*. These are species characteristic of fluvial environments. Statoblasts of three species of bryozoans were found: *Cristatella mucedo*, *Plumatella* sp. and *Fredericella indica*. The bryozoans may have lived on water plants.

Fredericella indica is rarely recorded as a fossil, probably because its statoblasts are indistinctive. However, it has been found in Middle Weichselian interstadial deposits in Sweden, in late-glacial deposits in Norway and in Holocene deposits in Norway, Denmark and Greenland.

We cannot say if the remains of freshwater plants come from plants that grew in the depositional basin or if they were washed into the basin from freshwater environments in the catchment area. It is also possible that some of the remains of invertebrates, notably the statoblasts, may have been transported from lakes or streams into the basin. Most of the freshwater species can occur in many different freshwater biotopes, but overall they are characteristic of a low-energy fluvial environment. The presence of *C. torosa* suggests some influence by marine water.

The fine texture of the sediment (clay) implies deposition in a low-energy environment, such as a river with weak bottom currents. The presence of clay rather than gyttja indicates deposition in a river rather than in a lake.

Non-aquatic moss taxa are dominated by the mosses *Bryum* sp. and *Sphagnum* sp. but a leaf of the moss *Polytrichum* s.l. sp. was also recovered. Vascular land plants are represented by one achene of *Potentilla* sp., one seed of *Juncus* sp., two fruits of *Typha* sp. and four fruits of *Rumex maritimus*. The latter may indicate salt-water influence, supporting the evidence from *C. torosa*, although it is also found at inland sites today. Several of these species probably grew in mires along the shore of the former water body where the clay was deposited. In particular, *Sphagnum* sp. and *Typha* sp. are characteristic of mires.

The assemblage from Måløv is remarkably similar to that of the Sidestrand Hall Member of the Cromer Forest-bed Formation in Britain that has also yielded *Stratiotes aloides*, *Borysthenia naticina*, *Sphaerium solidum, Cyprideis torosa* and *Scottia* (Preece *et al*. 2009). The depositional environment and climate must have been extremely similar but these two deposits are not necessarily of the same age.

Palaeoclimate

Several of the species recovered are warmth-demanding, especially *S. aloides*, *Typha* sp. and *R. maritimus*. They are widespread in Denmark today and are also found in the southern and eastern parts of Sweden. The mean July temperature at the northern range limit of *Pisidium supinum* is around 15°C. *B. naticina* no longer lives in Denmark but has a wide modern range in central and eastern Europe, from southern and eastern Germany and Poland to Hungary, Rumania and south-western European Russia (Zilch & Jaeckel 1962). The presence of this species indicates a more continental climate with summer temperatures higher than those in Denmark today. *C. torosa* is also a warmth-demanding species (Frenzel *et al*. 2010).

Age estimate

The assemblage recovered from Måløv clearly indicates deposition during an interglacial rather than interstadial period as was previously suggested for deposits at Måløv (Frederiksen & Rosbirk 1999; probably the same deposit). Several of the thermophilous species present, such as *Borysthenia naticina*, *Sphaerium* cf. *solidum*, *Stratiotes aloides*, *Typha* sp. and *Rumex maritimus*, are unknown from interstadial contexts. Interstadial deposits so far described from eastern Denmark are characterised by arctic species, such as *Salix polaris*, *Dryas octopetala* and *Betula nana* (Bennike *et al*. 1994, 2007), none of which were found at Måløv.

Fruits of *Stratiotes* spp. are well known from interglacial deposits in Europe, and leaf-margin spines have also been reported (Bennike & Hoek 1999). In Denmark, fruits of *S. aloides* have been reported from the last interglacial, the Eemian and from reworked Pleistocene floras (Hartz 1909).

Outside Denmark the species is known from the last interglacial and from several older interglacials.

Biostratigraphically, *Borysthenia naticina* (Fig. 4) is the most important species. This species has not previously been reported from Denmark but is known as a Pliocene fossil from southern Russia, from the Early Pleistocene of northern France and The Netherlands and from the Middle Pleistocene of central and eastern Europe. There are Middle Pleistocene records to the north-west of its modern range in the Rhine Valley. In Britain it has been reported from deposits referred to the Cromerian Complex (marine isotope stages 15 and 13), the Hoxnian (marine isotope stage 11) and to marine isotope stage 9 (Roe *et al.* 2009). In The Netherlands, its youngest occurrence is in a deposit referred to marine isotope stage 7 (Meijer 2003). In north-western Europe, *B. naticina* is thus unknown from the last interglacial stage, the Eemian, which strongly suggests that the deposit at Måløv is of pre-Eemian age. *Scottia tumida* is an extinct species and so far only known from Pleistocene interglacial deposits from Germany, Poland, the United Kingdom, Hungary and Greece (Kempf 1971).

Other interglacial non-marine deposits on Sjælland

Interglacial deposits are quite common in Denmark, but most of them are found in the western and southern parts of the country where erosion by advancing glaciers and meltwater was less intense than in the eastern parts. From Sjælland, only a few interglacial deposits have been reported (Fig. 1). Most of them are marine deposits that have been referred to the Eemian or Holsteinian. Two interglacial lake deposits have been reported from Sjælland, at the Copenhagen free port and at Førslevgaard on southern Sjælland (Fig. 1). The mollusc fauna from these deposits includes the bivalve *Corbicula fluminalis* (Hartz 1909), which indicates an Early or Middle Pleistocene age (Meijer & Preece 2000).

Conclusions

We conclude that the clayey deposit found at Måløv was deposited in a low-energy fluvial environment influenced by weakly brackish water. The occurrence of the gastropod *Borysthenia naticina* suggests that the deposit is at least Middle Pleistocene in age. The mean July temperature was higher than in Denmark today, and the deposit is clearly interglacial rather than interstadial.

References

Bennike, O. & Hoek, W. 1999: Late-glacial and early Holocene records of *Stratiotes aloides* L. from north-western Europe. Review of Palaeobotany and Palynology **107**, 259–263.

Bennike, O., Houmark-Nielsen, M., Böcher, J. & Heiberg, E.O. 1994: A multi-disciplinary macrofossil study of Middle Weichselian sediments at Kobbelgård, Møn, Denmark. Palaeogeography, Palaeoclimatology, Palaeoecology **111**, 1–15.

Bennike, O., Houmark-Nielsen, M. & Wiberg-Larsen, P. 2007: A Middle Weichselian interstadial lake deposit on Sejerø, Denmark: macrofossil studies and dating. Journal of Quaternary Science **22**, 647–651.

Fredriksen, J. & Rosbirk, E. 1999: Fundering af bro i interstadialt søbassin. Varv **1999**(2), 59–63.

Frenzel, P., Keyser, D. & Viehberg, F.A. 2010: An illustrated key and (palaeo) ecological primer for Postglacial to Recent Ostracoda (Crustacea) of the Baltic Sea. Boreas **39**, 567–575.

Hartz, N. 1909: Bidrag til Danmarks tertiære og diluviale flora. Danmarks Geologiske Undersøgelse II. Række **20**, 292 pp.

Kempf, E.K. 1971: Ökologie, Taxonomie und Verbreitung der nichtmarinen Ostrakoden-Gattung *Scottia* im Quartär von Europa. Eiszeitalter und Gegenwart **22**, 43–63.

Meijer, T. 2003: The late Middle Pleistocene non-marine molluscan fauna of borehole Noorderhoeve-19E117 (province of Noord-Holland, the Netherlands). Cainozoic Research **2**, 129–134.

Meijer, T. & Preece, R.C. 2000: A review of the occurrence of *Corbicula* in the Pleistocene of North-West Europe. Geologie en Mijnbouw / Netherlands Journal of Geosciences **79**, 241–255.

Meisch, C. 2000: Freshwater Ostracoda of western and central Europe. In: Schwoerbel, J. & Zwick, P. (eds): Süßwasserfauna von Mitteleuropa **8**(3), 522 pp. Heidelberg: Spektrum Akademischer Verlag.

Preece, R.C., Parfitt, S.A., Coope, G.R., Penkman, K.E.H., Ponel, P. & Whittaker, J.E. 2009: Biostratigraphic and aminostratigraphic constraints on the age of the Middle Pleistocene glacial succession in north Norfolk, UK. Journal of Quaternary Science **24**, 557–580.

Roe, H.M., Coope, G.R., Devoy, R.J.N., Harrison, C.J.O., Penkman, K.E.H., Preece, R.C. & Schreve, D.C. 2009: Differentiation of MIS 9 and MIS 11 in the continental record: vegetational, faunal, aminostratigraphic and sea-level evidence from coastal sites in Essex, UK. Quaternary Science Reviews **28**, 2342–2373.

Zilch, A. & Jaeckel, S.G.A. 1962: Mollusca. Die Tierwelt Mitteleuropas **2**(1), 294 pp. Leipzig: Verlag von Quelle & Meyer.

Authors' addresses

O.B., E.L. & H.J. G., *Geological Survey of Denmark and Greenland, Øster Voldgade 10, DK-1350 Copenhagen K, Denmark*. E-mail: *obe@geus.dk*

R.C.P., *Department of Zoology, University of Cambridge, Downing St., Cambridge CB2 3EJ, UK.*

F.V., *Institute of Geology and Mineralogy, University of Cologne, Zülpicher Str. 49, 50674 Cologne, Germany.*

Mapping of raw materials and habitats in the Danish sector of the North Sea

Jørn Bo Jensen, Sara Borre, Jørgen O. Leth, Zyad Al-Hamdani and Laura G. Addington

In the summer of 2010, the Geological Survey of Denmark and Greenland (GEUS) mapped the potential raw materials and substrate types, over large parts of the Danish economic sector of the North Sea, in cooperation with Orbicon A/S. The mapping was carried out for the Danish Nature Agency; it is part of the general mapping of raw material resources within the territories of the Danish state and forms part of the input for the implementation of the European Union's Marine Strategy Framework Directive. The purpose was (1) to provide an overview of the distribution, volume and composition of available raw materials and (2) to identify, describe and map the distribution of the dominant marine bottom types.

Methods

During the first part of the field work a single beam echo sounder for bathymetrical data, a side scan sonar for mapping the seabed surface as well as a chirp (1–10 kHz) and a sparker (1 kHz) were used to map the layers below the seabed with up to 50 m penetration. After preliminary interpretation, the acoustic data acquisition was followed by sediment sampling using a vibrocorer with up to 6 m penetration and a grab sampler in order to investigate the characteristics of the sediments. In addition, the seabed was filmed using a video camera mounted on a remotely operated vehicle (ROV) to document the seabed sediment substrate and benthic fauna. The field work was divided into three phases (Fig. 1, Table 1): phase 1: mapping of both raw materials and bottom types, phase 2: mapping of bottom types alone and phase 3: geological mapping.

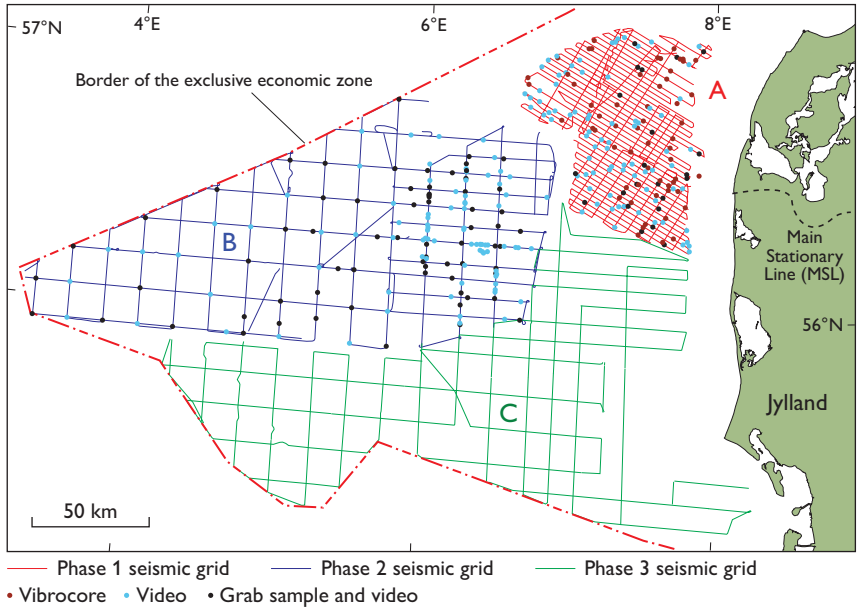

Fig. 1. Map of the economic sector of the Danish North Sea showing the seismic grids and sampling positions in the combined raw material and marine bottom-type mapping carried out in 2010. **A**: phase 1 area. **B**: phase 2 area. **C**: phase 3 area.

Bathymetry and geological model

The data from the phase 1 area made it possible to map the bathymetry and develop a geological model for the area. The bathymetric data show a NW–SE-trending ridge 25–30 m below present sea level interpreted as the offshore continuation of the Main Stationary Line (MSL) that formed during the last glacial maximum (Fig. 2A; Houmark-Nielsen & Kjær 2003). The high area comprises the core areas of Jyske Rev and Lille Fisker Banke. North of the MSL a series of ridges trending NNE–SSW that are 20–40 km long and 5–10 km broad dominate the bathymetry. The crests of the ridges are 18–24 m b.s.l. and the troughs around 40 m b.s.l. These large ridges are interpreted as early Holocene giant tidal sand ridges. Backstripping shows the pre-Holocene transgression surface and accentuates the MSL (Fig. 2B). South of the MSL the bathymetry shows a gentle south-western slope, which we interpret as drowned sandur deposits that formed in front of the melting Scandinavian ice sheet.

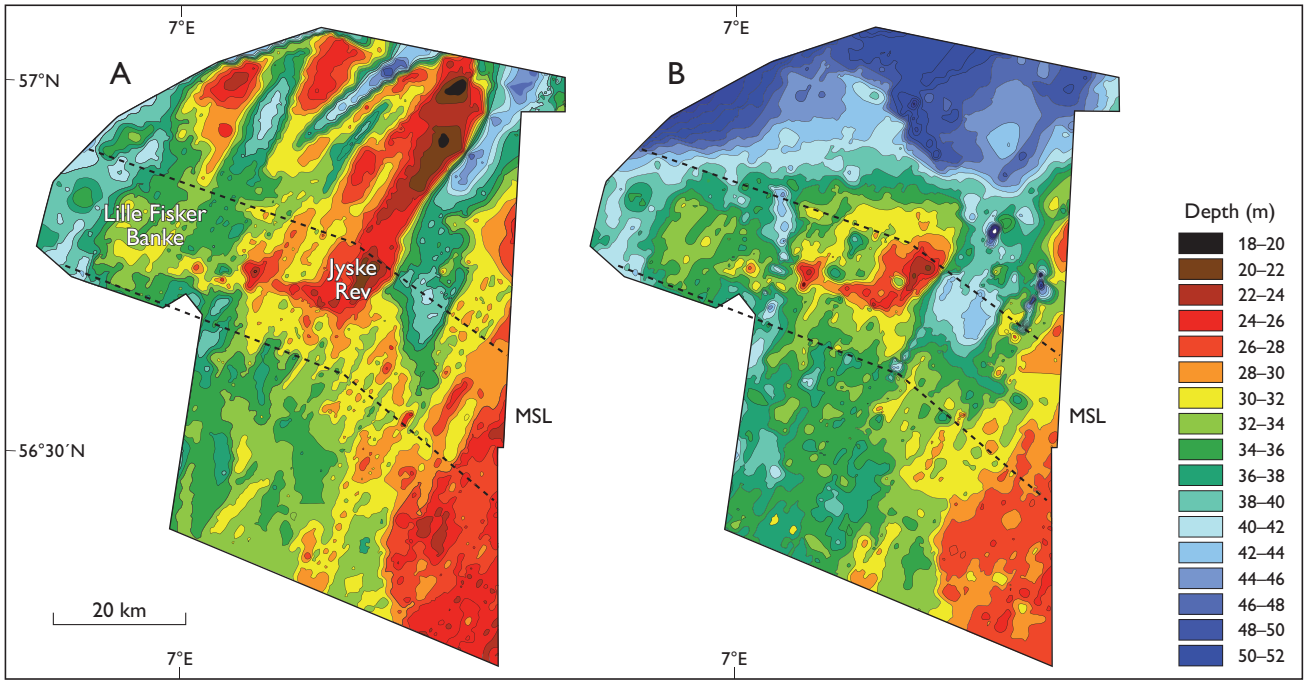

Fig. 2. Bathymetry and palaeo-morphology of the phase 1 area (Fig. 1), off north-west Jylland. **A**: Bathymetry. **B**: Palaeo-morphology in metres below present sea level of the pre-Holocene transgression surface. The Weichselian Main Stationary Line (MSL) is located in the Lille Fisker Banke – Jyske Rev area, between the stippled lines.

The pre-Quaternary surface is close to the seabed in the phase 1 area (Figs 3, 4; Nielsen *et al.* 2008) where it is overlain by a few tens of metres of Quaternary sediments. Thicker Quaternary deposits are found in local depressions connected with salt domes and in N–S-trending buried tunnel valleys that are incised into the pre-Quaternary deposits (Huuse & Lykke-Andersen 2000). The Quaternary sediments overlie Miocene sand and clay, Danian limestone and locally Cretaceous chalk.

The Quaternary stratigraphy in the North Sea is poorly known, but south of the MSL Elsterian and Saalian till deposits have been identified on the seismic sections and in sediment cores in a situation similar to that found in the onshore hill islands in western Jylland. To some extent the deeply incised valleys are filled with pre-Weichselian sand and Eemian marine silt and sand (Figs 3, 4).

To a large extent the Weichselian deposits are related to the MSL. They are partly seen as glaciotectonic deformations in the sparker data, and partly as till deposited below and at the margin of the ice sheet. Glaciofluvial sand and gravel are located in depressions in the Weichselian landscape and proximal to distal sandur sediments overlying glacial deposits south of the MSL (Figs 3, 4).

Late glacial marine deposits overlie the glacial deposits at present water depths greater than 40 m, which reflects the relative sea level around 17 000 years BP (Leth 1996), shortly after the last deglaciation (Fig. 3). From *c.* 17 000 years BP the relative sea level dropped to reach a minimum of about 50 m b.s.l. at *c.* 11 000 years BP. At that time only the northernmost part of the phase 1 area was below sea level (Fig. 2B) and a widespread hiatus is seen that lasted until submergence in connection with the Holocene transgression.

The relative sea level rose continuously from *c.* 11 000 to *c.* 6000 years BP to reach a maximum level at 1–3 m above the present sea level. Over the past 6000 years the relative sea level fell to its present level. The Holocene deposits can be divided into four units:

Table 1. Details of phases 1–3

Phase	Survey grid (km)	Acoustic profiles (km)	Vibrocores	Grab samples	Video data
1	2 × 5	*c.* 3000	60	24	85
2	7 × 7* / 7 × 15 #	*c.* 3000	–	31	67
3	7 × 7	*c.* 2500	–	–	–

* eastern area, #western area.

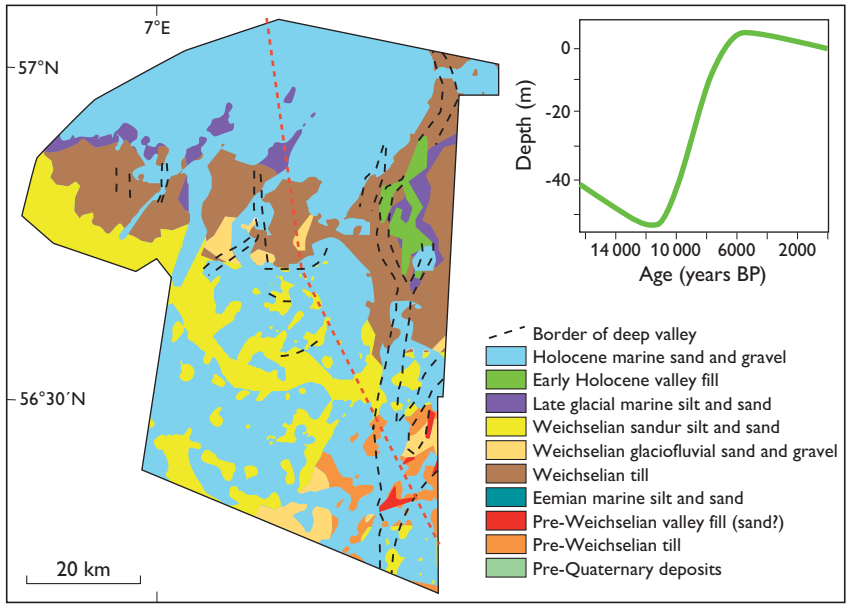

Fig. 3. Seabed surface sediments in the phase 1 area (Fig. 1). The location of the geological profile (Fig. 4) is shown with a red stippled line. The inset diagram is a model of relative sea-level changes after the last deglaciation in the study area.

Early Holocene giant tidal sand ridge deposits. The giant tidal sand ridges are connected to the MSL which trends NNE–SSW and attains heights up to 20 m (Figs 2–4). The architecture implies that the ridges were formerly connected to the shore and formed by tidal currents during the Holocene sea-level rise, mostly by trapping of sediment within tidal eddies generated by headlands or flow convergence. Similar giant sand ridges related to Holocene sea-level rise have been reported from the English Channel (Reynaud *et al.* 2003).

Early Holocene fine-grained marine and fjord sediments. Incised valleys formed in the easternmost part of the phase 1 area during the lowstand period and during the initial part of the Holocene transgression (Fig. 3). Fine-grained marine sediments were deposited in such valleys in protected areas east of Jyske Rev, and brackish fine-grained sedimentation took place in palaeo-fjords similar to the present Limfjorden (Agger Clay; Leth 1996).

Holocene beach ridge and spit deposits. These accumulations formed during the progressive transgression when the glacial deposits were isolated as islands in the open sea. Erosion, transport and deposition led to the formation of beach deposits on the lee side of Jyske Rev.

Sub-recent to recent mobile sand. Around 8000–7000 years ago the shallow parts (18–20 m b.s.l.) of the phase 1 area were transgressed by the sea. The present wave system and the Jutland Current developed (Gyllencreutz *et al.* 2006), which resulted in the formation of mobile sand waves and major sand banks in the Jyske Rev and Lille Fisker Banke region. The mobile sand deposits reached several metres in thickness and the bedforms can have wavelengths of over 100 m.

Potential for raw material

We have identified a number of stratigraphical units that could be of interest to the sand and gravel industry. Pre-Weichselian sand in buried tunnel valleys is of potential interest in areas where no or little cover sediment is found.

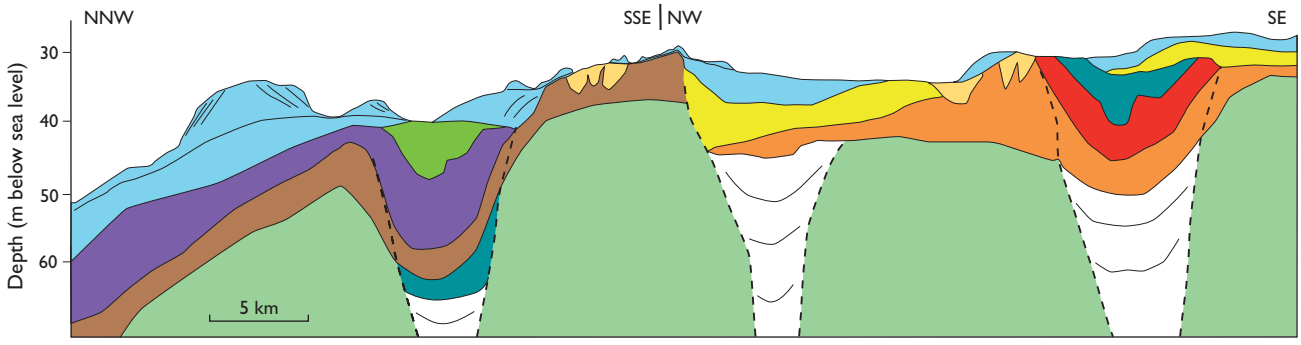

Fig. 4. NW–SE geological profile through the phase 1 area (Fig. 1) covered in the first phase. For legend and location of profile see Fig. 3.

This is seen in the south-eastern part of the phase 1 area, but little is known about the volume and quality of the material accumulated in the tunnel valleys.

Weichselian glaciofluvial sand and gravel deposits along the MSL are of great interest as a resource for concrete production. However, this resource occurs only sporadically and is often covered by several metres of Holocene sediments.

Giant Holocene sand ridges in the north-western part of the phase 1 area are the most noteworthy sand resource in the region because of their enormous volume of around 8×10^9 m^3. The resource is easily accessible and consists of medium-grained sand that is well suited for land reclamation, beach nourishment and concrete production.

Drowned coastal deposits are the traditional dredged resource in the Jyske Rev area. This resource consists of high-quality sand and gravel for concrete production as the high energy level during erosion and transport of the sediments has removed the light particles.

Recent mobile sand is often deposited in sand waves and the sediment consists of well-sorted, medium-grained sand that is excellent for beach nourishment. However, before this resource is removed it is crucial to ensure that the sand waves are not part of the present sand budget of the coast.

Geological seabed units as bottom types and possible sand-eel fishery areas

Bottom-type mapping was part of the seabed mapping task for the Danish Nature Agency. Since the seabed sediments form the habitat for marine benthic organisms and are of vital importance to the distribution of marine life, the seabed sediments have been used for mapping the dominant bottom types.

A number of additional parameters such as light penetration, salinity and temperature influence the distribution of faunal types, but a close link between till deposits on Jyske Rev and the Natura 2000 code 1170 stone reef type (Boedeker *et al.* 2006) is obvious. A close link is also seen between giant sand ridges and the Natura 2000 code 1110 sand bank type.

The mapping of the geological unit giant sand ridges as sand banks was compared with the distribution of sand-eel fishing grounds in the Jyske Rev and Lille Fisker Banke areas (Jensen *et al.* 2011) and a nearly perfect match was found.

Concluding remarks

We have developed a geological model that can form the basis of combined mapping of raw material and marine bottom types in the Lille Fisker Banke and Jyske Rev areas. Weichselian glaciofluvial deposits, early Holocene giant, tidal sand ridges, Middle Holocene drowned, coastal sand and gravel deposits and sub-recent to recent mobile sand waves and banks form potential or substantiated raw material geological units.

Examples of dominant bottom types are the Jyske Rev till deposits that are classified as a stone reef of the seabed type, and the early Holocene giant tidal sand ridges that represent a sand bank type. Sand-eel fishing grounds have been used as an example of the close linkage between geology, bottom types and fish habitats.

Acknowledgement

The Danish Nature Agency is thanked for permission to publish the paper.

References

Boedeker, D., Krause, J.C. & von Nordheim, H. 2006: Interpretation, identification and ecological assessment of the NATURA 2000 habitats 'sandbank' and 'reef'. In: von Nordheim, H., Boedeker, D. & Krause, J.C. (eds): Progress in marine conservation in Europe, NATURA 2000 sites in German offshore waters, 47–64. Berlin: Springer.

Gyllencreutz, R., Backman, J., Jakobsson, M., Kissel, C. & Arnold, E. 2006: Postglacial paleoceanography in the Skagerrak. The Holocene **16**, 975–985.

Houmark-Nielsen, M. & Kjær, K.H. 2003: Southwest Scandinavia 40–15 kyr BP: palaeogeography and environmental change. Journal of Quaternary Science **18**, 769–786.

Huuse, M. & Lykke-Andersen, H. 2000: Overdeepened Quaternary valleys in the eastern Danish North Sea: morphology and origin. Quaternary Science Reviews **19**, 1233–1253.

Jensen, H., Rindorf, A., Wright, P.J. & Mosegaard, H. 2011: Inferring the location and scale of mixing between habitat areas of lesser sandeel through information from the fishery. ICES Journal of Marine Science **68**, 43–51.

Leth, J.O. 1996: Late Quaternary geological development of the Jutland Bank and the initiation of the Jutland Current, NE North Sea. Geological Survey of Norway Bulletin **430**, 25–34.

Nielsen, T., Mathiesen, A. & Bryde-Auken, M. 2008: Base Quaternary in the Danish parts of the North Sea and Skagerrak. Geolological Survey of Denmark and Greenland Bulletin **15**, 37–40.

Reynaud, J.-Y., Tessier, B., Auffret, J.-P., Berné, S., de Batist, M., Marsset, T. & Walker, P. 2003: The offshore Quaternary sediment bodies of the English Channel and its Western Approaches. Journal of Quaternary Science **18,** 361–371.

Authors' address

Geological Survey of Denmark and Greenland, Øster Voldgade 10, DK-1350 Copenhagen K, Denmark. E-mail: *jbj@geus.dk*

Postglacial, relative shore-level changes in Lillebælt, Denmark

Ole Bennike and Jørn Bo Jensen

The brackish Baltic Sea and the more saline Kattegat are connected by three straits, Lillebælt, Storebælt and Øresund (Fig. 1). Of the three straits, Lillebælt is the narrowest, with 700 m at its narrowest point, widening out towards the south to around 25 km (Fig. 2). In the narrow parts of Lillebælt, water depths around 30–50 m are common. In the northern part of Lillebælt the depth is 16–18 m and in the southern part the depth is around 35 m. Storebælt and Øresund have played important roles as outlets during the history of the Baltic Sea, and their histories have been much discussed (Björck 1995; Bennike *et al.* 2004). In contrast, Lillebælt has received little attention. In this paper we present 11 new radiocarbon accelerator mass spectrometry (AMS) ages and propose a curve for Holocene relative shore-level changes in Lillebælt. We use the term shore-level changes rather than sea-level changes because we have constructed both lake-level and sea-level changes.

During the last deglaciation of the Lillebælt region, large channels were eroded by northward-flowing subglacial meltwater. These channels are now found at the bottom of the strait, and most of them are kept free of sediments by strong bottom currents. However, late and postglacial sediments are found in some parts of the channels. Several submerged settlements have been reported from the Lillebælt region (Andersen 1985). They are dated to the mid-Holocene from artefacts and by radiocarbon dating.

Methods

Combined high-resolution, sub-bottom profiling and sediment coring were carried out from R/V *Alexander von Humboldt*. The seismo-acoustic equipment included a sediment echosounder (Fig. 3), and the profiles obtained were used for the selection of the core sites (Fig. 4). A 6 m long vibrocorer was used for coring. We also had access to vibrocores and seismic profiles from a survey conducted in connection with a planned gas pipeline. This material was handed over to the Geological Survey of Denmark and Greenland (GEUS) from Dansk Olie og Naturgas A/S.

Selected cores with the most complete stratigraphy were sub-sampled for studies of macrofossils. The samples were wet sieved and analysed using a dissecting microscope. Re-

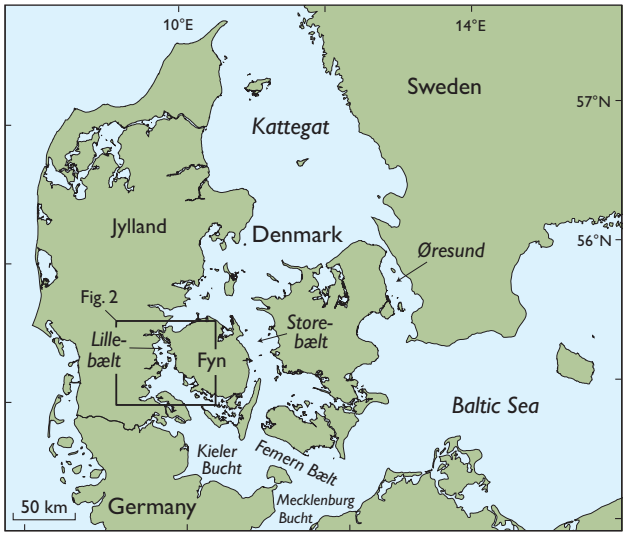

Fig. 1. Map of Denmark and surrounding area showing the location of Lillebælt and the other straits connecting the Baltic Sea to Kattegat, as well as place names mentioned in the text.

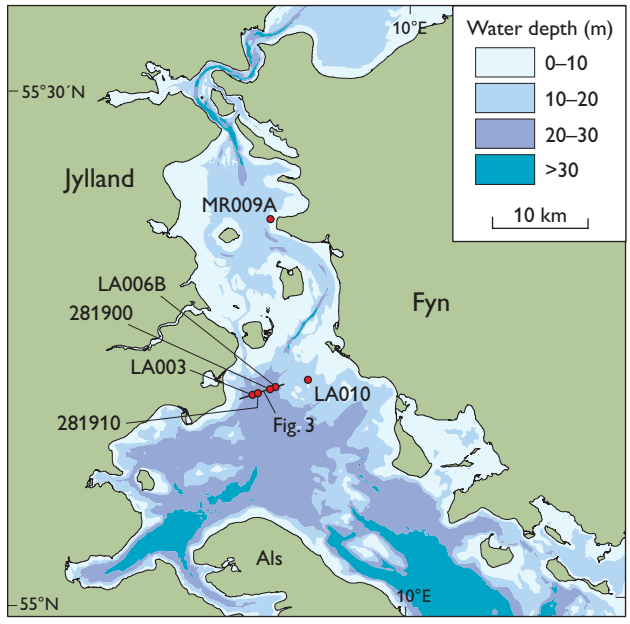

Fig. 2. Bathymetry of Lillebælt with the location of the vibrocores indicated.

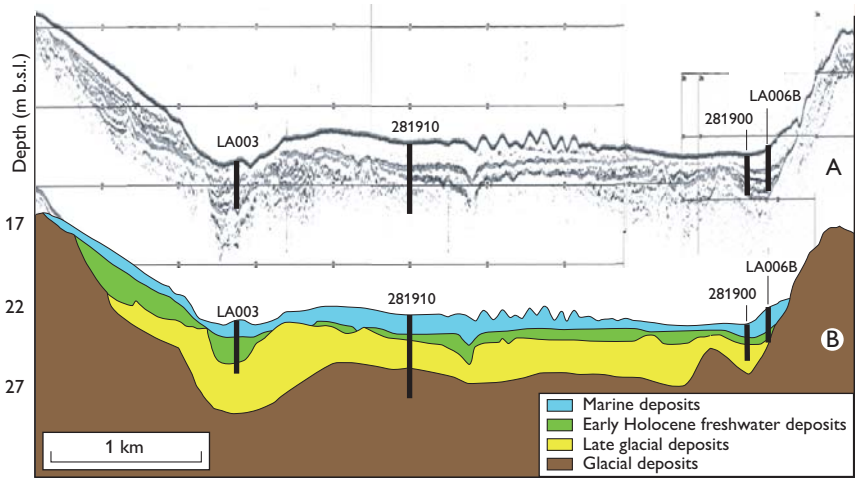

Fig. 3. **A**: Original seismic profile, obtained by a sediment echosounder. **B**: Interpretation below. For location see Fig. 2. Cores labelled 2819xx were collected from R/V *Alexander von Humboldt*, and cores labelled LA were collected for Dansk Olie og Naturgas A/S.

mains of plants and marine molluscs were submitted for AMS radiocarbon dating (Table 1). Several published dates were also used for the reconstruction of shore-level changes (Table 2; K-samples are conventional ages, and the LuS-sample is an AMS age). We have used a reservoir age of 400 years for the marine samples, however, the reservoir age may have varied somewhat during the Holocene (Olsen *et al.* 2009).

Sediments, palaeoecology and chronology

The oldest sediments consist of till that shows an internal, chaotic reflection pattern and a sharp upper boundary. A few cores also penetrated meltwater sand. Till and meltwater sand accumulated during the last glaciation and deglaciation of the region.

The glacial deposits are locally overlain by late glacial sediments, which are found in the channels. The late glacial sediments show conformable internal reflectors, and consist of clay, silt and fine-grained sand. One sample has been dated to 11 400–11 900 cal. years BP, corresponding to a late Younger Dryas age (Table 1, Poz-8924). We suggest that the late glacial sediments were partly deposited in a branch of the Baltic Ice Lake.

In the deeper parts of Lillebælt, black, organic-rich sediments are widespread. The sediments are commonly laminated and may contain abundant fragments of small roots and fruits of telmatic plants. Some of this sediment is swamp peat, but most of it is coarse detritus gyttja. The organic-rich sediments are usually overlain by laminated calcareous gyttja clay. However, in core LA006B lake sediments are found below peat. This succession is interpreted as overgrowing of a basin. Samples from the lake deposits gave ages of *c.* 11 000–8800 cal. years BP (early Holocene, Table 1, Poz-5754, Poz-5755, Poz-5753, Poz-8859, Poz-8860).

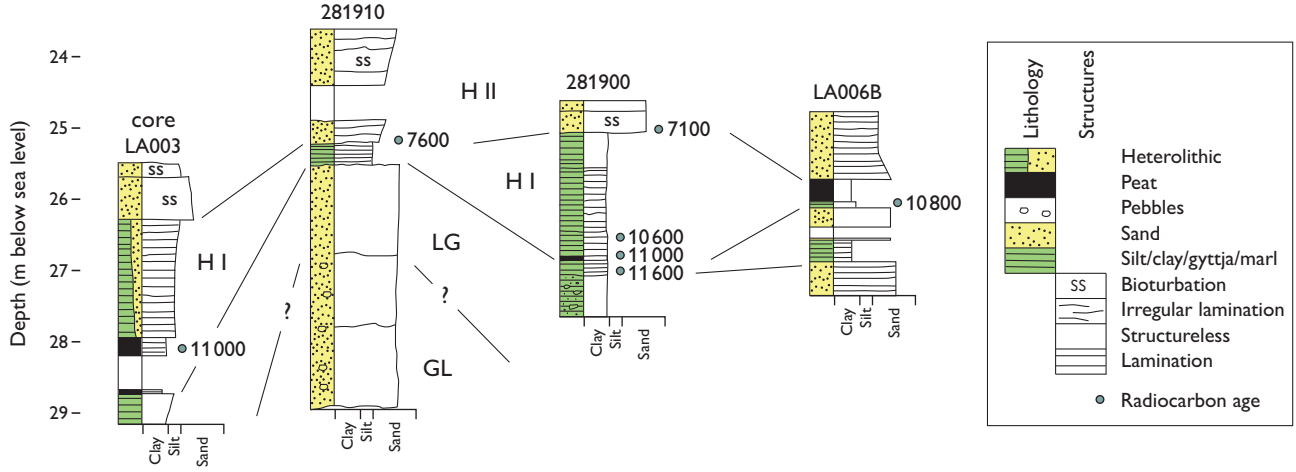

Fig. 4. Sedimentological logs from vibrocores from the Lillebælt. Radiocarbon ages are in calibrated calendar years BP. **GL**: glacial. **LG**: late glacial. **H I**: early Holocene freshwater. **H II**: brackish and marine Holocene deposits.

Table 1. New radiocarbon AMS age determinations from Lillebælt

Core no.	Laboratory no.	Species*	Sediment	Depth b.s.l. (m)	Age (^{14}C years BP)	Calibrated age (years BP)§
LA003	Poz-5754	*M. trifoliata, C. mariscus P. australis*	Detritus gyttja	28.10–28.20	9670 ± 50	10 789–11 210
LA006B	Poz-5755	*M. trifoliata, C. mariscus*	Lake marl	26.02–26.03	9460 ± 50	10 567–11 068
LA010	Poz-5767	*B. Albae, C. mariscus*	Brackish sand	16.60–16.70	7700 ± 70	8384–8599
LA010	Poz-5753	*M. trifoliata, C. mariscus*	Lake gyttja	16.72–16.78	7880 ± 50	8556–8976
MR009A	Poz-5790	*Mytilus edulis*	Marine mud	9.70	7280 ± 40	7842–7649
MR009A	Poz-5805	*B. Albae*	Peat	9.80–9.90	7420 ± 50	8074–8372
281900	Poz-8820	*Arctica islandica*	Marine sand	25.00–25.05	6590 ± 40	6994–7225
281900	Poz-8859	*P. tremula, B. nana*	Lake clay	26.50–26.60	9350 ± 50	10 419–10 702
281900	Poz-8860	*P. tremula, B. Albae*	Detritus gyttja	26.80–26.88	9670 ± 50	10 789–11 210
281900	Poz-8924	*Salix* sp.	Clay	26.98–27.08	10 110 ± 60	11 401–11 910
281910	Poz-8821	*M. edulis, M. balthica*	Marine sand	25.25–25.26	7140 ± 40	7528–7692

* Full names are: *Menyanthes trifoliata, Cladium mariscus, Phragmites australis, Betula* sect. *Albae, Betula nana, Populus tremula, Mytilus edulis, Macoma balthica.* §Calibration is according to the INTCAL09 dataset (terrestrial samples) and the Marine09 dataset (marine samples).

Marine sediments from protected areas consist of laminated or bioturbated, fine-grained, organic-rich mud. Sandy and silty sediments are found in shallow water areas and in areas with strong bottom currents (Fig. 3). Shells and shell fragments of marine molluscs are common. On the acoustic records, the marine deposits are mostly transparent or show continuous reflectors parallel to the lower boundary. In three cores we dated the lowermost shell of marine molluscs we could find. The oldest age determination is *c.* 7700 cal. years BP (Table 1, Poz-5790).

In core LA010 bioturbated sand is present in the upper part of the core. The fauna implies brackish conditions. A sample from the bottom of the sand unit was dated to *c.* 8500 cal. years BP (Table 1, Poz-5767). We suggest that the sand marks the first marine influence in the area.

Shore-level changes

On the basis of the available radiocarbon ages, we have reconstructed relative shore-level changes in the region (Fig. 5). The relative shore level was low during the early part of the Holocene and probably rose slowly throughout the early Holocene, and at the same time a large lake existed in the area. As the shore level rose this lake increased in size and at around 8500 cal. years BP it was transformed into a brackish water body. Two dates from core MR009A provide an important fix point for the shore-level evolution (Table 1). The dates show that a peat now found 9 m below sea level was transgressed by the sea between *c.* 8200 and *c.* 7700 cal. years BP, and around 8000 cal. years BP marine conditions were established.

Later sea-level changes are constrained by six published radiocarbon dates (Table 2). They comprise two dates of wood from marine gyttja, two dates from *Ostrea edulis* shells, an age from a bone found in a grave at a water depth of 2.7 m and a bone of harp seal from a submarine settlement. The two latter dates come from sites that were situated above the contemporary sea level.

Discussion

In Lillebælt, late glacial sediments are found in incised channels. The Younger Dryas sequence that consists of fine-grained laminated clay and silt is followed by a hiatus which was probably formed during the final drainage of the Baltic Ice Lake, when shore level dropped around 25 m over a few years (Björck 1995). The maximum shore level of the Baltic Ice Lake in the south-western Baltic Sea was around 20 m b.s.l., and this lake may have extended as far west as south-western Kieler Bucht (Jensen *et al.* 2002). The Baltic Ice Lake may also have extended into southern Lillebælt.

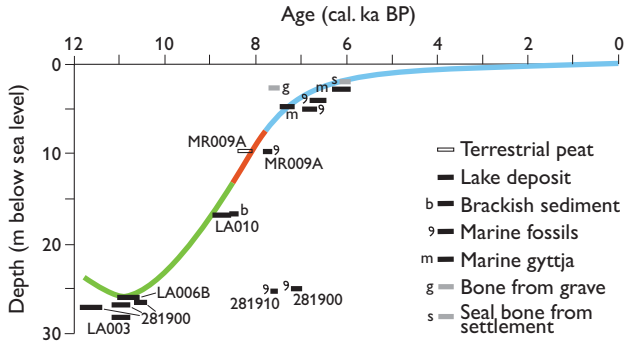

Fig. 5. Curve showing relative shore-level changes in southern Lillebælt during the Holocene. Green: lake phase. Red: brackish water phase. Blue: marine phase. **ka**: 1000 years.

Table 2. Published radiocarbon age determinations from Lillebælt

Laboratory no.	Material	Depth b.s.l. (m)	Age (^{14}C years BP)	Calibrated age (years BP)*	Reference
K-3558	Human bone	2.7	6740 ± 80	7459–7727	Andersen (1985)
K-4150	*Alnus* wood	4.7	6380 ± 100	7153–7480	Andersen (1985)
K-4149	*Tilia* wood	2.8	5370 ± 100	5922–6317	Andersen (1985)
K-5680	*Ostrea edulis* shells	5.0	5940 ± 70	6645–6995	Petersen & Rasmussen (1995)
K-5681	*Ostrea edulis* shells	4.0	5780 ± 70	6445–6797	Petersen & Rasmussen (1995)
LuS-6136	*Phoca groenlandica* bone	2.0	5595 ± 50	5885–6144	Bennike *et al.* (2008)

*Calibration is according to the INTCAL09 dataset (terrestrial samples) and the Marine09 dataset (marine samples).

During the earliest Holocene, large parts of Lillebælt were dry land, but local bogs and lakes must have existed in the deeper parts. As the shore level began to rise, local lakes and bogs became widespread. During continued shore-level rise, bogs were transformed into lakes, and a large lake developed in the southern part of Lillebælt. It was connected to another large lake to the south in Kieler Bucht, and to other large lakes in Femer Bælt, Mecklenburg Bucht and Storebælt.

Later, the ongoing eustatic sea-level rise led to brackish and then to marine conditions in Lillebælt. The first marine influence was via Storebælt when southern Lillebælt was a fjord. However, the fjord was transformed into the Lillebælt strait during continued rapid sea-level rise. The oldest dated marine shell from Lillebælt is from 7700 cal. years BP, but brackish water conditions are suggested at 8600–8384 cal. years BP. The youngest lake deposits (around 17 m below sea level) are dated to 8976–8556 cal. years BP. In Storebælt, the oldest dated marine shell gave an age of 8100 cal. years BP (Bennike *et al.* 2004), and in the Mecklenburg Bucht, the oldest shell date is *c.* 8000 cal. years BP (Rößler *et al.* 2011). The early Holocene deposits in Lillebælt show no indication of a lowering of the shore level before being inundated by marine waters.

Conclusions

Glacial till and Holocene marine deposits are widespread in Lillebælt. In the deeply incised channels late glacial and early Holocene non-marine deposits are found, these units are separated by an erosional boundary. The late glacial deposits were probably deposited during pre-Allerød and Allerød times, as well as during the Younger Dryas. The early Holocene non-marine deposits have yielded ages between 11 000 and 8800 cal. years BP.

The late glacial unit consists of lake deposits, and we suggest that the Baltic Ice Lake extended into southern Lillebælt. During the early Holocene, a large lake existed in southern Lillebælt; this lake expanded in size during shore-level rise. The oldest shell of a marine mollusc from Lillebælt is dated to 7700 cal. years BP, but brackish conditions were probably established at around 8500 cal. years BP.

Acknowledgement

The captain and crew of R/V *Alexander von Humboldt*, and in particular the cruise leader, the late Wolfram Lemke are thanked for their help during the marine cruise.

References

Andersen, S.H. 1985: Tybrind Vig, a preliminary report on a submerged Ertebølle settlement on the west coast of Fyn. Journal of Danish Archaeology **4**, 52–69.

Bennike, O., Jensen, J.B., Lemke, W., Kuijpers, A. & Lomholt, S. 2004: Late- and postglacial history of the Great Belt, Denmark. Boreas **33**, 18–33.

Bennike, O., Rasmussen, P. & Aaris-Sørensen, K. 2008: The harp seal (*Phoca groenlandica* Erxleben) in Denmark, southern Scandinavia, during the Holocene. Boreas **37**, 263–272.

Björck, S. 1995: A review of the history of the Baltic Sea, 13.0–8.0 ka BP. Quaternary International **27**, 19–40.

Jensen, J.B., Kuijpers, A., Bennike, O., Laier, T. & Werner, F. 2002: New geological aspects for freshwater seepage and formation in Eckernförde Bay, western Baltic. Continental Shelf Research **22**, 2159–2173.

Olsen, J., Rasmussen, P. & Heinemeier, J. 2009: Holocene temporal and spatial variation in the radiocarbon reservoir age of three Danish fjords. Boreas **38**, 458–470.

Petersen, K.S. & Rasmussen, K.L. 1996: The impact of radiocarbon datings on natural historical sciences in Denmark: especially paleozoological and shore-line datings. Pact **49**, 117–130.

Rößler, D., Moros, M. & Lemke, W. 2011: The Littorina transgression in the southwestern Baltic Sea: new insights based on proxy methods and radiocarbon dating of sediment cores. Boreas **40**, 231–241. Doi: 10.1111/j.1502-3885.2010.00180.x.

Authors' address

Geological Survey of Denmark and Greenland, Øster Voldgade 10, DK-1350 Copenhagen K, Denmark. E-mail: *obe@geus.dk*

Detection of terrain changes in southern Denmark using persistent scatterer interferometry

Stig A. Schack Pedersen, Geraint Cooksley, Marc Gaset and Peter Roll Jakobsen

Since 1991, a number of European satellites have acquired data of the Earth's surface for environmental monitoring. In general, a satellite will orbit the Earth in about 1½ hours and it takes 35 days before an ERS or ENVISAT satellite repeats radar scanning of the same position. For younger generations of satellites, such as RADARSAT and TERRA, the scanning repeat interval has decreased to 24 and 11 days, respectively, so that hundreds of radar scenes of the same place, produced over the past *c.* 20 years, are now available.

Persistent scatterer interferometry (PSI) is a remote-sensing technique for measuring and monitoring land deformation that uses these radar scenes (Ferreti *et al.* 2001). The technique can be used to assess natural ground movements and displacement of man-made constructions.

Over the next three or more years the Geological Survey of Denmark and Greenland (GEUS) will participate in three satellite monitoring projects conducted under the auspices of the European Union. They are all funded under the Global Monitoring Environment System (GMES). The first project, which is the subject of this paper, is named TerraFirma and started in 2003 as a European Space Agency GMES service project. The second project, funded by the 7th Framework Programme, is named SubCoast, and it will monitor subsidence in coastal areas. In Denmark, it will concentrate on the southern part of the island of Lolland. Finally a large monitoring project named PanGeo with similar funding has begun early in 2011. Twenty-seven European geological surveys participate in PanGeo that focuses on ground movements in urban areas. Two cities in each of the participating countries are selected as targets for PSI analysis. Concerns about the effects of global climate changes are the main motivation for the GMES support to the satellite monitoring projects.

The TerraFirma project was extended with an additional three years of research and development and will continue until 2012. The project has five themes: (1) tectonic movements, (2) hydrological conditions, (3) flooding, (4) subsidence in abandoned mining areas and (5) wide-area satellite scanning. GEUS is involved in the flooding theme dealing with the increased risks of flooding of the low-lying areas in south-west Jylland, adjacent to the Danish Wadden Sea (Vadehavet). The main environmental and constructional concerns are the dykes that protect the low land areas along the coast of Vadehavet. In order to improve risk management

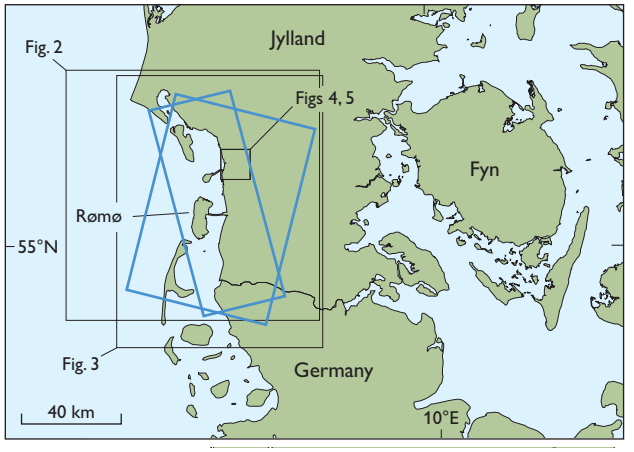

Fig. 1. Map of south-western Denmark showing the location of the investigated areas. The blue frames show areas for which data from the descending track 337 and the ascending track 403 were PSI processed.

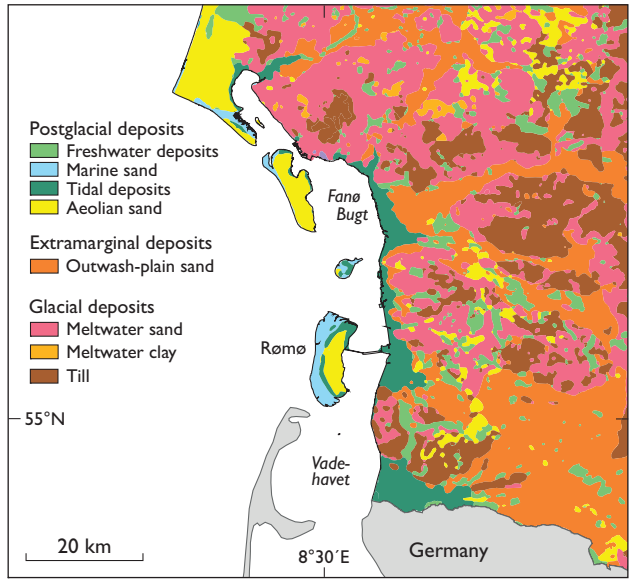

Fig. 2. Map of the surface deposits in the south-western part of Jylland. The region is dominated by glacial deposits of Saalian age. The glacial landscape is intersected by outwash plain deposits of Weichselian age. Holocene tidal deposits and recent aeolian deposits are found in the westernmost part of the map. Simplified from Pedersen (1989).

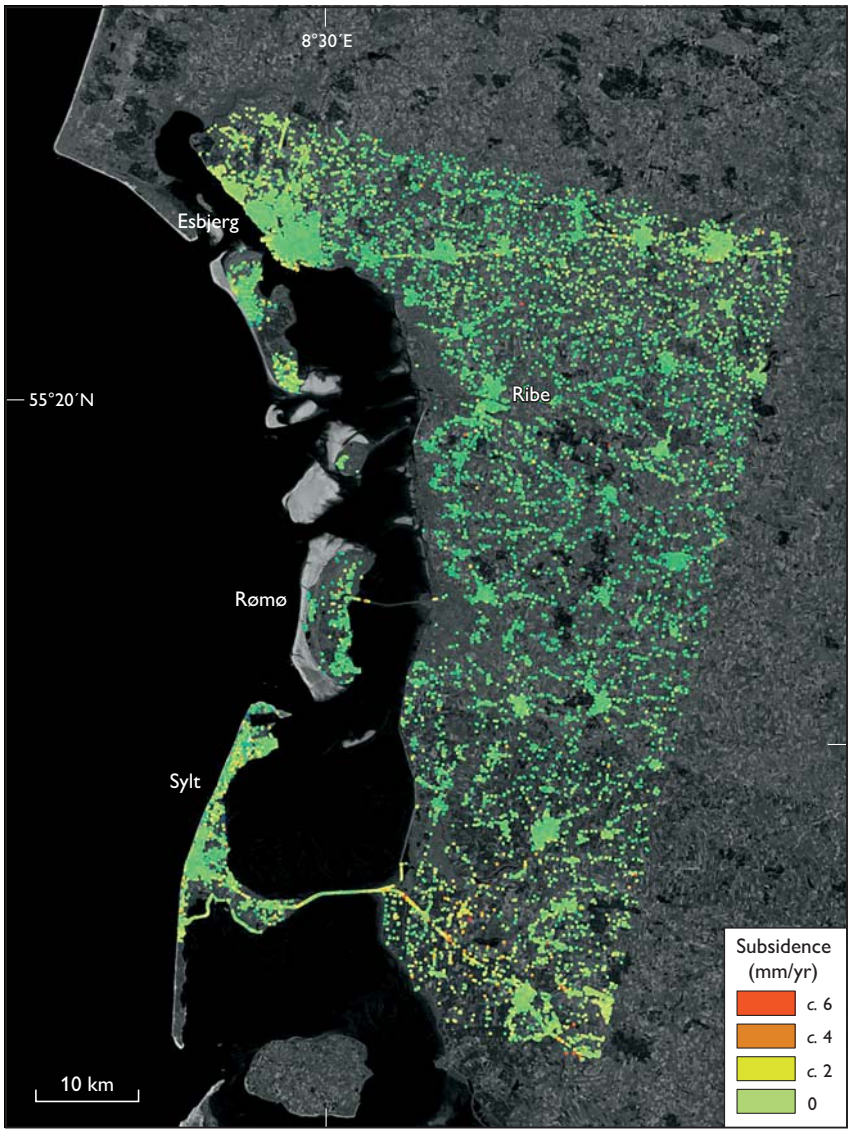

Fig. 3. Map of south-western Jylland showing PSI-processed radar data from the ERS descending track 337. Subsidence is seen along the causeway to Sylt and along the railway line east of Esbjerg. For location see Fig. 1.

and mitigation, it is also important to identify areas of land subsidence that can be caused by geological processes and by man-made impact.

The Danish flood theme site

The investigated area is located in the south-western part of Jylland, Denmark (Fig. 1) that is prone to flooding, when spring tides coincide with stormy weather. After identification of the appropriate satellite tracks for the area, GEUS provided position data for the partner Altamira Information responsible for the calibration and processing of the satellite data. The coverage by the two satellites ERS and ENVISAT and the PSI processing areas are shown in Fig. 1. The satellite line coverage consists of both descending and ascending tracks, which in broad terms means scanning by a satellite moving both from north to south and from south to north.

GEUS' role in the project is to contribute with a geological and geomorphological analysis of the region (Fig. 2). Furthermore GEUS provides Geographical Information System (GIS) data and interpretation of the data based on a geo-scientific understanding of the region. An important GEUS contribution to the project was the conclusion of the geological map of Rømø (Jakobsen 2011). Rømø is located in the centre of the area covered by the satellite imagery.

PSI data and GIS processing of satellite data

A preliminary example of PSI-processed data is shown in Fig. 3. The orange and red pixels in the satellite image represent places where elevation changes have been detected. The PSI data have been analysed using the program ARCGIS. The first step of this is to calibrate the data to fit relevant intervals. In the second step, the point data are statistically treated to cover the geographical area by average figures in equiva-

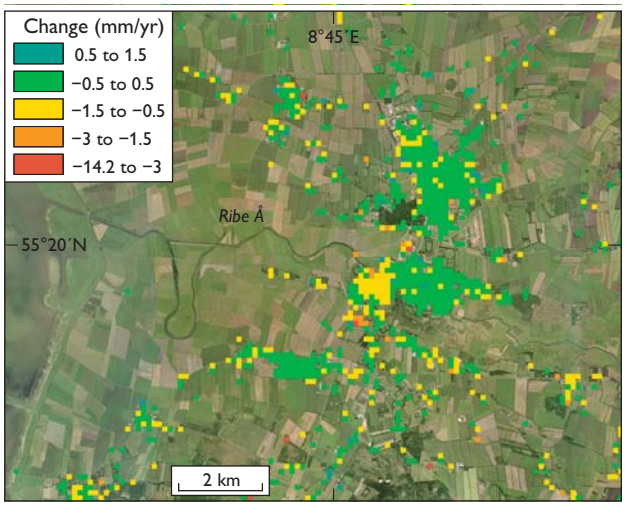

Fig. 4. Image of the area around Ribe (centre of image). The coloured pixels show places where elevation changes have been detected. The radar data have been PSI processed in a 500 × 500 m grid with average values of the PSI points representing the mean values of the vertical movements (differences in vertical displacement). The concentration of yellow pixels in the western part of Ribe town is interpreted as subsidence due to urban fill. For location see Fig. 1.

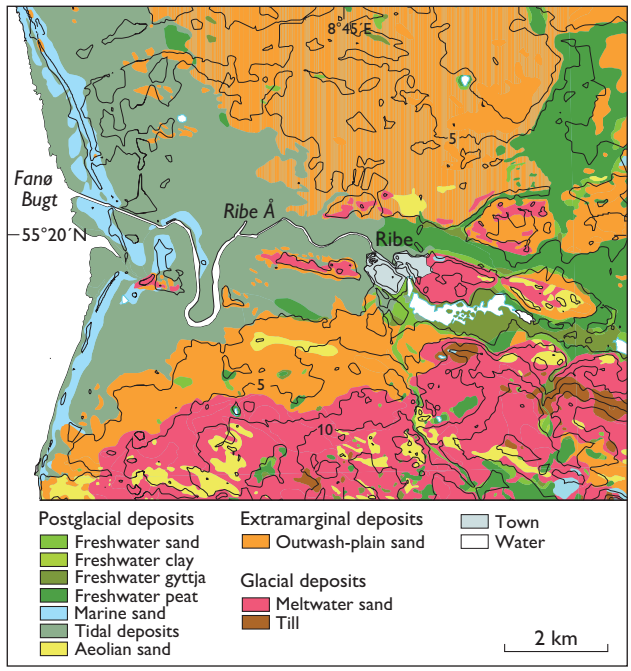

Fig. 5. Detailed geological map of Ribe and the Ribe Å area. Contour interval 2.5 m. For location see Fig. 1.

lent pixels. Finally the data are compared with other terrain data, such as topographical maps, orthophotographs or terrain models based on gradient variation or geological maps.

Interpretation of the persistent scatterer interferometry data

The obvious interpretations that can be made from the preliminary persistent scatterer interferometry processing of the satellite data are terrain movements related to man-made constructions. From this it is evident that the causeway connecting the German island of Sylt to the mainland is subject to subsidence, in particular at its eastern part (Fig. 3). There is also marked subsidence along the railway line east of Esbjerg, and some of the bridges that are built across small streams are settling (Jakobsen 2008).

Detailed analysis of a subsiding area: the Ribe case

The town of Ribe and the surrounding area are described as an example of a detailed analysis using ARCGIS programming (Figs 3–5). On the map of Ribe and its surrounding, a marked subsidence is seen in the western part of the old town (yellow to red colours in Fig. 4). The subsidence rate is −1 ± 0.5 mm/year, and appears to increase to *c.* −2–3 mm/year on the slopes close to the stream Ribe Å and a smaller stream south of the town (Figs 4, 5). The eastern part of Ribe appears to be comparatively stable with no significant movement recorded.

There is no obvious geological explanation for the subsidence in the western part of old Ribe. The town is located on the eastern part of an island of marine sand surrounded by meltwater sand deposited during the Saalian. During the Weichselian, the Ribe island became separated from the Saalian deposits to the north and south by eroding rivers flowing westwards from an ice margin 30 km to the east. Glaciofluvial sand and gravel were deposited by the rivers. In the Holocene, Ribe was situated at the boundary between an isolated sandy hill that formed an erosional remnant of the former glacial landscape surrounded by tidal flats to the west and freshwater deposits to the east. None of these geological features can explain the subsidence of western Ribe.

However, Ribe is an old town with a long and famous historical record going back to the early part of the Viking period. Around AD 1100 the town was a centre for trade with a well- developed harbour, and was favoured with privileges given by the Danish kings. During historical time, the estuary west of Ribe silted up due to accumulation of tidal deposits, and Ribe's value as a merchant town decreased. Several destructive events, including serious flooding, also affected Ribe, therefore the town has been rebuilt several times on the rubbles of former buildings. Dump and fill deposits up to 6 m thick lie beneath the present-day centre of old Ribe.

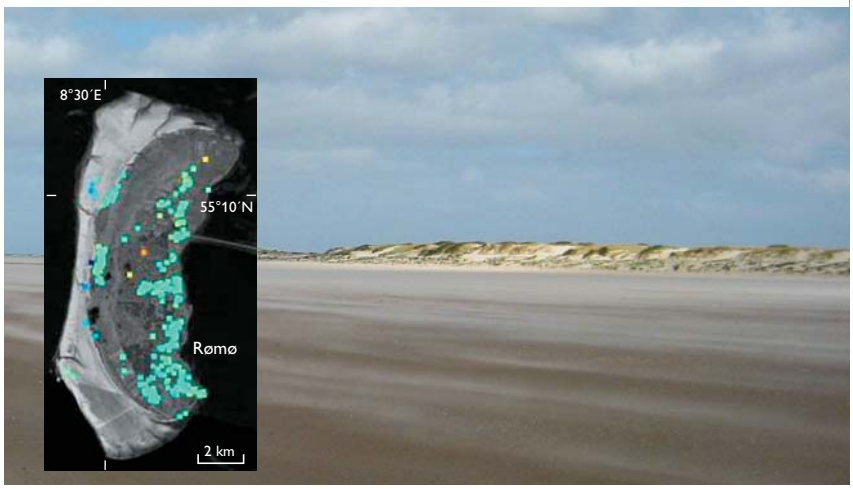

Fig. 6. Beach plain and sand dunes on the west coast of the island of Rømø. The growing dunes are identified by the persistent scatterer interferometry technique as an area with positive elevation change. Inset: Close up of the island of Rømø based on data from the ERS satellite track 401. The scattered blue points along the west coast of the island indicate an increasing elevation of *c.* 2 mm/year, caused by sand eroded from the beach and deposited on the dunes.

Therefore we interpret the subsidence of its western part as an effect of consolidation of the historical fill below younger buildings and constructions. However, we regard the more significant displacement on the slopes towards the river north and south of the centre as an effect of additional compaction of soft organic-rich sediments found at the transition between the freshwater drainage system and the tidal environment.

Detailed analysis of elevation changes: the Rømø dune field

One of the main geological features, expected to show up in the PSI-processed data, is the concealed Tønder Graben (Lykke-Andersen 1995: Gravesen *et al.* 2004). However, we could not identify this structure in the data. On the contrary, it appears that the data from the ascending satellite ERS track 401 indicate a small regional uplift. The data central to this problem are being analysed further, but we note that some points along the west coast of Rømø indicate uplift (Figs 6). An uplift rate of 2 mm/year is indicated from the PSI data along a row of points that coincide with the outermost dunes along the flat sandy beach plain. There are no houses or constructions in this area, so we interpret the points to represent crests of recent dunes. Thus the small elevation change is caused by sand accumulation on the crest of the dunes, and the magnitude of accumulation, 2 mm/year, is a realistic figure for aeolian deposition in this area.

Conclusions

PSI-processed satellite data from Vadehavet (the Danish Wadden Sea) in south-west Denmark have been analysed using ARCGIS and the first results indicate that no subsurface movements can be detected. A number of constructions and urban areas are subject to minor subsidence, in the order of 2–6 mm/year. A preliminary interpretation of elevation change data from the west coast of Rømø implies that accumulation of dune sand is the reason for movements of around 2 mm/year. We find that PSI processing of satellite data is a powerful tool for detecting elevation changes.

References

Ferreti, A., Prati, C. & Rocca, F., 2001: Permanent scatterers in SAR interferometry. IEE Transactions on Geoscience and Remote Sensing **39**, 8–20.

Gravesen, P., Jakobsen, P.R., Binderup, M. & Rasmussen, E.S. 2004: Geologisk set: Det sydlige Jylland, 188 pp. Copenhagen: Skov- og Naturstyrelsen.

Jakobsen, P.R. 2008: Geological evaluation of observed vertical terrain movements in the Esbjerg test area. A contribution to the ABSRATE/Terrafirma project. Danmarks og Grønlands Geologiske Undersøgelse Rapport **2008/18**, 11 pp.

Jakobsen, P.R. 2011: Geological map of Denmark, 1:50 000, 1112 III, Rømø og Mandø. Copenhagen: Geological Survey of Denmark and Greenland.

Lykke-Andersen, H. 1995: Neotektonik i Danmark. In: Nielsen, O.B. (ed.): Danmarks geologi fra Kridt til i dag, 19–30. Århus: Geologisk Institut, Aarhus Universitet.

Pedersen, S.A.S. 1989: Quaternary geological map of Denmark, 1:200 000, map sheet 3. Copenhagen: Geological Survey of Denmark.

Authors' addresses

S.A.S.P. & P.R.J., *Geological Survey of Denmark and Greenland, Øster Voldgade 10, DK-1350 Copenhagen K, Denmark*. E-mail: *sasp@geus.dk*

G.C. & M.G., *Altamira Information, Còrsega 381-387, E-08037 Barcelona, Spain*.

Does road salt affect groundwater in Denmark?

Søren M. Kristiansen, Flemming D. Christensen and Birgitte Hansen

Chloride (Cl) from dissolved salt is a major threat to groundwater quality in many regions of the world. In arid regions near present-day coastlines, where old seawater occurs in deeper sediments and where road salt is frequently used, Cl can be a significant pollutant (European Environmental Agency 2009). European Union member states have recently reported that next to nitrogen, Cl is the most commonly found pollutant and is often responsible for groundwater bodies being at risk or having a poor ecological status (European Commission 2010).

Intrusion of salty groundwater and infiltration by seawater near coastlines are well-known phenomena in Danish aquifers (Ødum & Christensen 1936; Bonnesen *et al.* 2009). Saltwater in aquifers may also come from human pollution such as landfills, road salt storage facilities, roads and agricultural activities (Panno *et al.* 2006). Since the 1970s, de-icing salt applied to roads has been recognised as a significant source of contamination that may deteriorate aquifers that are used as drinking water resources by increasing their Cl concentration and by harming stream and lake ecosystems (Jackson & Jabbogy 2005). Recent studies have suggested that the decade-long usage of road salt is becoming a rising threat to groundwater quality (Bester *et al.* 2006). Salt contamination from roads is therefore particularly problematic to aquifers already at risk (Lundmark & Olofsson 2007). The present paper explores the impact of road salt on groundwater quality in Denmark by means of a combination of chemical indicator analysis, temporal and spatial Cl analysis and numerical groundwater modelling.

The vulnerability of aquifers to road salt depends on the amount of salt applied per kilometre road, the degree of urbanisation and the percentage of salt lost to the subsurface. Based on a literature review, the estimated percentage of road salt lost to the groundwater is 10–20% of applied de-icing salt in Danish urban areas (Kristiansen *et al.* 2009). The average amount of road salt used during the winter in Denmark has risen since the late 1990s, but varies with weather conditions (Fig. 1). In comparison, Fig. 1 also shows that the atmospheric NaCl deposition for the entire Danish surface area is about 280 gigagrams (Gg) per year, which is tentatively estimated based on actual bulk deposition measurements (T. Ellerman, personal communication 2011). Thus, the total amount of applied road salt and the total atmospheric salt deposition in Denmark are of the same order of magnitude. However, the local surface load of road salt and atmospheric salt deposition vary widely across Denmark.

The Danish road salt project

This paper addresses the results from a recent assessment performed under the Danish groundwater mapping project in order to evaluate the impact and risk of road salt to the quality of Danish groundwater resources (Kristiansen *et al.* 2009). The project used groundwater quality data from the national database Jupiter. The data were downloaded in October 2008 and included approximately 140 000 analyses from approximately 24 000 groundwater sampling points corresponding to about one sample per 2 km^2. The oldest data are from 1890, the most recent from 2007. Data on the historical consumption of road salt were drawn from the Danish Road Directorate and involved municipalities.

Three different methods were used: (1) Evaluation of indicators to separate chloride sources in groundwater chemistry, (2) analysis of the distribution and variation of Cl in time and space, and (3) development of a numerical groundwater risk assessment tool in the hydrological modelling system MIKE SHE.

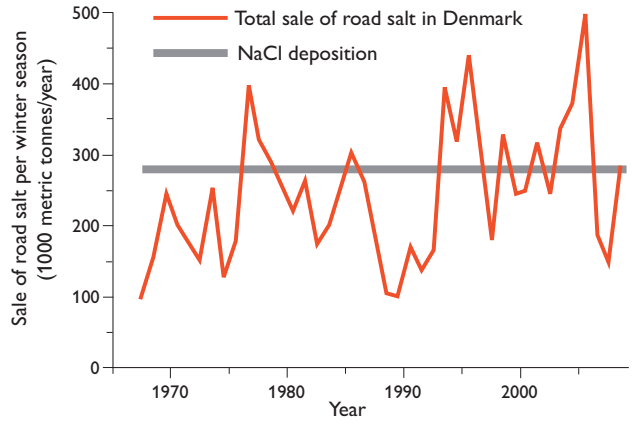

Fig. 1. Sale of road salt for highway use in Denmark from 1965/1966 to 2008/2009 in 1000 metric tonnes (Gg) per winter season based on data from the Danish Road Directorate. Atmospheric NaCl deposition in Gg per year is a tentative estimate for the entire Danish surface area based on bulk deposition measurements by T. Ellerman, University of Aarhus, 2011.

Chloride source indicators

Geochemical tools with mass ratios of especially the halides have proved useful for identifying different groundwater Cl sources (Davies *et al.* 1998). Groundwater salt origins were identified by a graphical technique that distinguishes between multiple sources (Panno *et al.* 2006). This approach discriminates sea salt from, for instance, vacuum salt used as road salt. An average of 40% of Danish de-icing salt is vacuum salt. Both Cl and Br form stable anions in water, which are usually not affected by sediment–water reactions. In addition, NaBr is less soluble than NaCl. As a consequence of the production process, vacuum salt has a Cl/Br mass ratio >1000. Sedimentary rock salt, and hence road salt coming from this source, has Cl/Br mass ratios similar to rain, as well as residual and infiltrating waters with a Cl/Br mass ratio <400 (Davis *et al.* 1998). Based on a literature review and own data analyses, we find that Cl/Br ratios are appropriate to detect the origin of dissolved Cl sources in Danish groundwater (Kristiansen *et al.* 2009).

The chemical indicator analysis shows that the potential impact of road salt on groundwater can be traced using a combination of Cl/Br mass and Na/Cl molecular ratios in groundwater where the Na/Cl ratio is affected by the exchange of sodium between the solid and liquid phases and the Cl/Br ratio is affected by the above-mentioned dissolution processes.

Groundwater chloride sources

Firstly, a prevalence of Br-poor groundwater (Cl/Br mass ratios >1000) was found in upper groundwater (<80 m below surface), which indicates that anthropogenic Cl sources (e.g. vacuum salt from roads, atmospheric deposition, or animal manure from farming) have a general impact on groundwater quality. Secondly, groundwater with reversed ionic exchange (Na/Cl molecular ratio <0.75) was also preferentially found in upper groundwater, which indicates infiltration of NaCl containing water into more fresh sediment. Thirdly, most

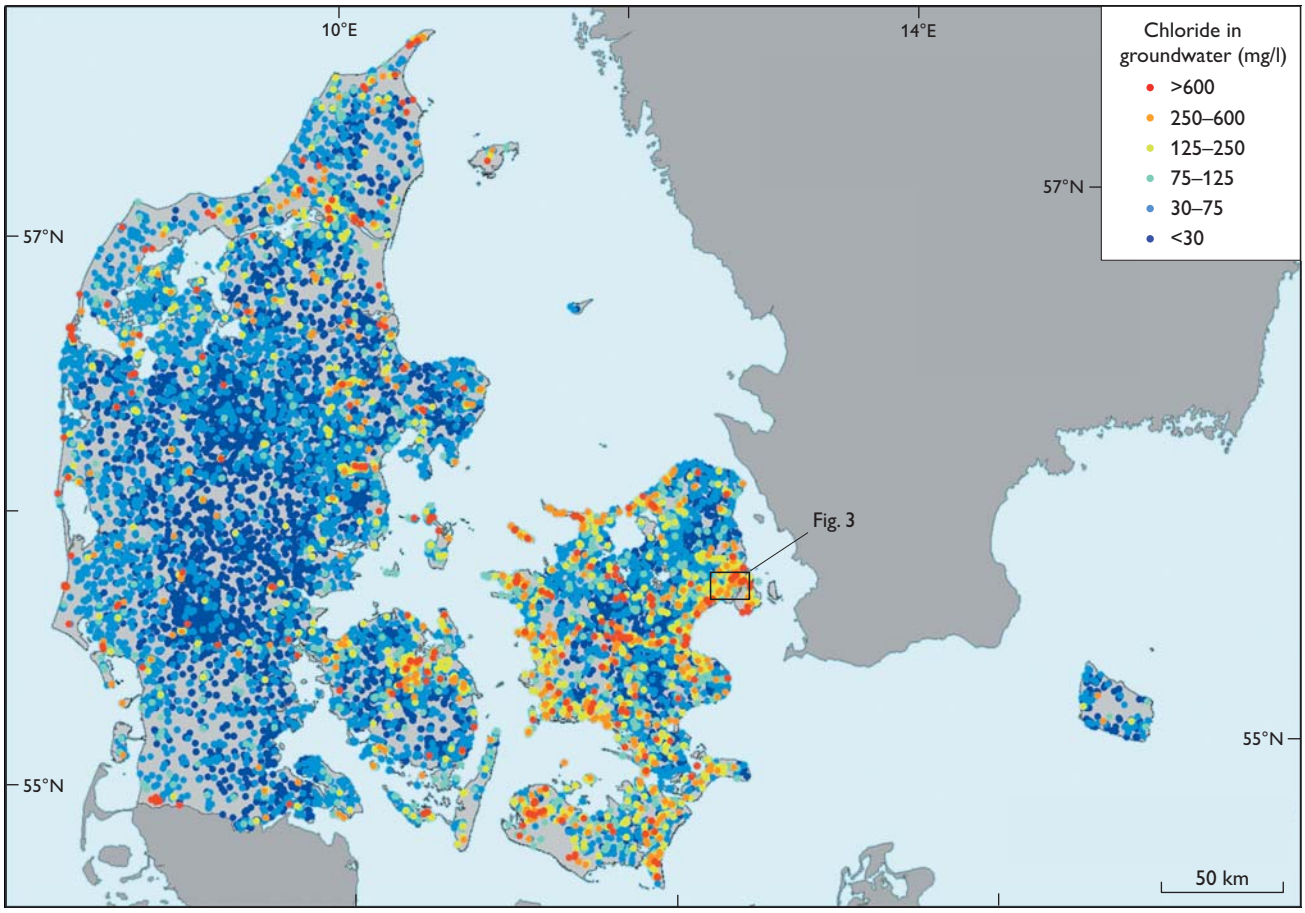

Fig. 2. Geographical distribution of the latest analysed chloride concentration in *c.* 24 000 Danish groundwater sampling points. The highest measured chloride concentration in wells with more than one measuring point is shown. Data were downloaded from the national database Jupiter in October 2008.

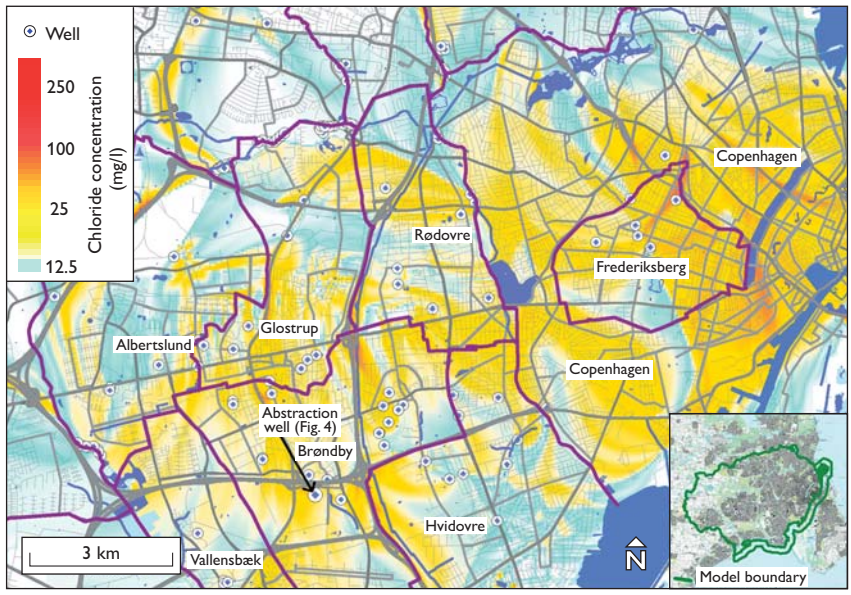

Fig. 3. Modelling results of chloride concentrations in the primary aquifer due to leaching of road salt estimated for a steady-state situation in 2060 in the greater Copenhagen area. The loss of historically used road salt is put to 15% and all factors are kept constant from 2008 to 2060. The background concentration of chloride is not included. For location see Fig. 2.

of the groundwater with high Cl concentrations was found in the upper groundwater with a gradual decrease from the surface to about 80 m below surface. These three different analyses support that the upper groundwater is affected by Cl sources at the soil surface. However, the analyses could not identify which specific type of Cl source at the surface influences groundwater quality.

In addition, the analyses showed that the deeper groundwater (>90 m below surface) often had Cl/Br mass ratios <550; moreover, a gradual increase in Cl concentrations with depth indicated that the primary Cl source in deeper Danish aquifers should be found in the underlying groundwater with much higher Cl concentrations.

Chloride distribution in Danish groundwater

The Cl concentration classes used in Fig. 2 are based on statistical analysis of the distribution of all the Cl analyses from Danish groundwater where four geochemical populations are found: <10, 10–30, 30–600 and >600 mg Cl/l. Background concentrations of Cl in Danish groundwater is below 30 mg/l. Groundwater with Cl concentrations above the drinking water standard of 250 mg/l is commonly found close to the coastline, especially in the eastern parts of Denmark (Fig. 2). However, elevated concentrations of Cl are also found in inland aquifers.

Trend analyses of the Cl concentration in the groundwater in the greater Copenhagen area show that 38% of the wells have experienced significantly increasing concentrations whereas only 9% have seen significantly decreasing concentrations (95% confidence interval) since the 1960s. Median Cl concentrations in groundwater rose from 40–80 mg/l in 1965–1978 to 80–160 mg/l in 1994–2007. A predominance of inversed ionic exchanged groundwater indicates that infiltration of salt water into a fresher aquifer comes from anthropogenic influenced sources such as road salt or intrusion by sea water due to drinking water abstraction.

Numerical modelling of road salt impact

A numerical assessment tool was developed for a large part of the greater Copenhagen area (274 km^2) in order to evaluate the impact of road salt on groundwater quality. We modelled losses of road salt to the environment at catchment scale from 1967 to 2060 (Fig. 3). The tool combines a surface load model with a well-calibrated 3D numerical groundwater model in MIKE SHE that simulates water flow and solute transport in the subsurface (Kristiansen *et al.* 2009). The surface load model consists of (1) the historic use of road salt since 2001 distributed on the road network where the type of road has been taken into consideration, (2) estimation of the loss of road salt to the groundwater, and (3) simple 1D modelling of the Cl transport through the unsaturated zone.

The loss of road salt to the surroundings is difficult to estimate, but Tvedt *et al.* (2001) estimated that 15–30% of the road salt is lost under Danish conditions. However, not all the lost road salt infiltrates the groundwater as some percolating water is removed by drainage or sewage. In the modelling, we decided to use a loss of 15% of the road salt to groundwater, which can be considered as a best estimate based on available knowledge.

Simulations indicate that with a loss of 15% of the applied road salt, the chloride concentrations below urban areas gen-

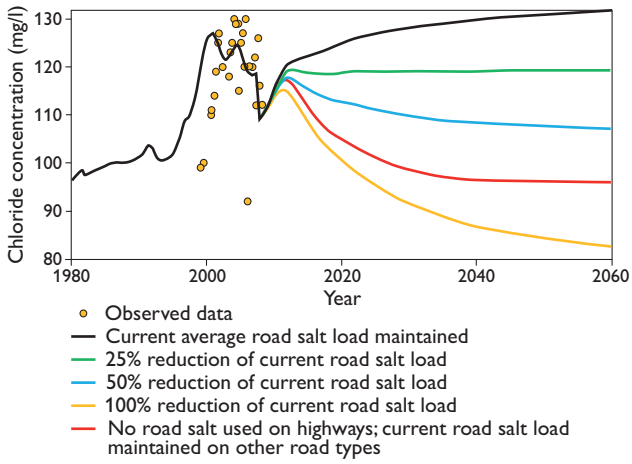

Fig. 4. Modelled and measured chloride concentrations in groundwater in an abstraction well in the greater Copenhagen area. For location see Fig. 3. Breakthrough curves are shown for different scenarios whereby road salt losses to groundwater are reduced.

erally will show a 25–40 mg/l increase, whereas increases can reach 125 mg/l at some major road junctions. Simulated breakthrough curves for a shallow well are shown in Fig. 4 for different scenarios compared to measured values. A background Cl concentration of 80 mg/l is added for the simulated results which contains Cl from natural sources as atmospheric deposition and marine residual water. The upper curve, where the current load of road salt is maintained, shows that it takes decades before a steady state situation is reached. The rest of the curves show the development of the groundwater Cl concentrations at steady state for different reduction scenarios in relation to current road salt usage.

Conclusions

The results show that the upper groundwater Cl concentrations (<80 m below surface) are affected by Cl sources such as road salt, atmospheric deposition and animal manure. Precise identification of the Cl sources at the surface requires more analyses of chemical indicator species in the groundwater. Numerical groundwater modelling in the greater Copenhagen area shows that road salt can result in a significant increase of the Cl concentration in groundwater, particularly near major road junctions. The aquifer used for water supply may be degraded because of the accumulated impact from several Cl sources such as road salt, residual salt groundwater and recent seawater intrusion. The applied model assumes that the loss to groundwater of road salt is 15%. But if the loss was 30%, then the resultant Cl concentration should be doubled. More precise quantification of the loss of road salt and knowledge on Cl sources other than salt applied to public roads are therefore required in order to reduce the uncertainty of the current estimate of the effect of road salt on groundwater quality, for example by establishing study sites in urban areas.

Acknowledgement

The project was supported by the former Environmental Centres under the Danish Ministry of the Environment.

References

Bester, M.L., Friend, E.O., Molson, J.W., Rudolph, D.L. 2006: Numerical investigation of road salt impact on an urban well-field. Ground Water **44**, 165–175.

Bonnesen, E., Larsen, F., Sonnenborg, T., Klitten, K. & Stemmerik, L. 2009: Deep saltwater in chalk of north-west Europe: origin, interface characteristics and development over geological time. Hydrogeology Journal **17**, 1643–1663.

Davis, S., Cecil, D.W., Zreda, M. & Sharma, P. 1998: Uses of chloride/bromide ratios in studies of potable water. Ground Water **36**, 338–350.

European Commission 2010: Report from the commission in accordance with article 3.7 of the groundwater directive 2006/118/EC on the establishment of groundwater threshold values, 10 pp. Brussels: European Commission.

European Environmental Agency 2009: Water resources across Europe – confronting water scarcity and drought, 60 pp. Copenhagen: European Environmental Agency.

Jackson, R.B. & Jabbogy, E.G. 2005: From icy roads to salty streams. Proceedings of the National Academy of Sciences of the United States of America **102**, 14487–14488.

Kristiansen, S.M., Christensen, F.D. & Hansen, B. 2009: Vurdering af danske grundvandsmagasiners sårbarhed overfor vejsalt, 107 pp. København: De Nationale Geologiske Undersøgelser for Danmark og Grønland.

Lundmark, A. & Olofsson, B. 2007: Chloride deposition and distribution in soils along a deiced highway – assessment using different methods of measurement. Water, Air & Soil Pollution **182**, 173–185.

Ødum, H. & Christensen, W. 1936: Danske Grundvandstyper og deres geologiske Optræden. Danmarks Geologiske Undersøgelse III. Række **26**, 183 pp.

Panno, S.V., Hackley, K.C., Hwang, H.H., Greenberg, S.E., Krapac, I.G., Landsberger, S. & O'Kelly, D.J. 2006: Characterization and identification of Na-Cl sources in ground water. Ground Water **44**, 176–187.

Tvedt, T., Randrup, T.B., Pedersen, L.B. & Gludsted, S. 2001: Planter & vejsalt, 19 pp. København: Trafikministeriet, Vejdirektoratet and Miljø- og Energiministeriet, Skov & Landskab.

Authors' addresses

S.M.K., *University of Aarhus, Department of Earth Sciences, Høegh-Guldbergs Gade 2, DK- 8000 Aarhus C.* E-mail: *smk@geo.au.dk*

F.D.C., *Rambøll, Hannemanns Allé 53, DK-2300 Copenhagen S, Denmark.*

B.H., *Geological Survey of Denmark and Greeland, Lyseng Allé 1, DK-8270 Højbjerg, Denmark.*

Comprehensive Nuclear-Test-Ban Treaty – a peace-keeping initiative with scientific impact

Tine B. Larsen, Peter H. Voss, Trine Dahl-Jensen and Søren Gregersen

Any major shaking of the Earth can be recorded on a seismograph regardless of the nature of the source. Earthquakes and large explosions generate waves with similar frequency content. This fact has been used for decades to construct systems to monitor detonations of underground nuclear explosions. The quality of the monitoring system has increased significantly in recent years, and we demonstrate here that the data are useful in Danish earthquake research.

One important difference between explosions and earthquakes is the depth of the source, most earthquakes occurring at much larger depths than explosions. Thus the depth determination is important in both fields. However, accurate depth determination of earthquake hypocentres is a challenge even when it comes to large well-recorded earthquakes. The uncertainty of the calculated depth of a Danish earthquake is of the same magnitude as the depth itself when using standard location techniques. A technique utilising crustal phases recorded at large distances has been introduced at the Geological Survey of Denmark and Greenland to improve the determination of the hypocentre depths.

Only the largest earthquakes in Denmark and its immediate surroundings produce sufficiently strong signals to be recorded at teleseismic distances, i.e. larger than 3000 km. The signals are discernable at low-noise seismic array stations as far away as North America and Africa. Some of these stations are operated by the United Nations Comprehensive Nuclear-Test-Ban Treaty Organisation (CTBTO). Data from many of these stations are available for scientific purposes. We demonstrate here how data from Canada and Niger can significantly improve the depth estimates for two earthquakes, one in Skåne, Sweden in 2008 and the other in the Danish part of the North Sea in 2010 (Figs 1, 2).

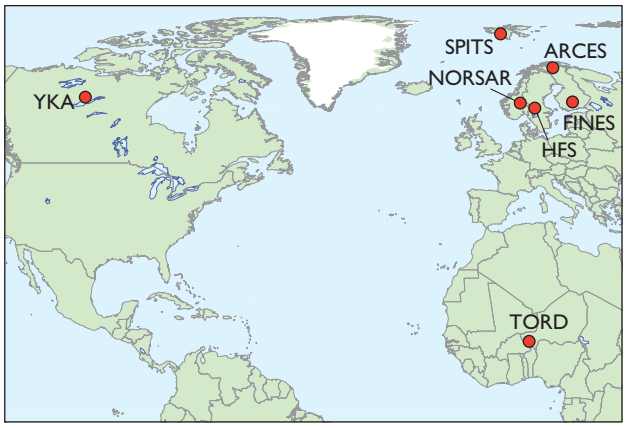

Fig. 1. Map of the North Atlantic region showing the locations of seismic array stations used by GEUS to locate earthquakes in Denmark and Greenland. YKA, Canada. SPITS, NORSAR and ARCES, Norway. FINES, Finland. HFS, Sweden. TORD, Niger.

CTBTO and IMS

The Comprehensive Nuclear-Test-Ban Treaty was adopted by the general assembly of the United Nations (UN) in September 1996. The treaty bans all nuclear explosions on Earth whether for military or for peaceful purposes. Denmark signed the treaty in 1996, and it was ratified by the Parliament of Denmark in 1998. The treaty will enter into force once it has been signed and ratified by all nuclear powers of the world. However, the ratification is still pending in several key countries such as China, Pakistan, India and United States of America.

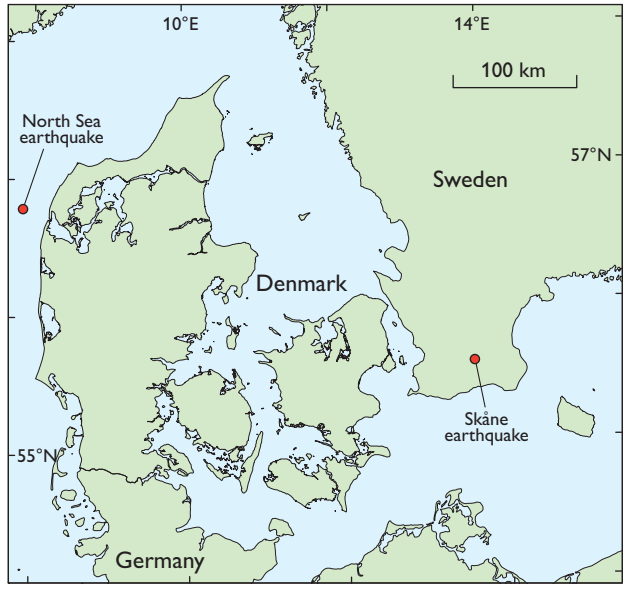

Fig. 2. Teleseismic array data have been used to locate earthquakes and measure their depths in Skåne on 16 December 2008 and in the North Sea on 19 February 2010.

Significant resources are being allocated to the development of a large international monitoring system (IMS), so that all technical systems as well as procedures, manuals and other agreements are in place once the treaty enters into force. The IMS is a UN-controlled monitoring system based on four technologies: seismology, radio nuclides, hydroacoustics and infrasound. The system consists of a worldwide network of high-quality monitoring stations, supplementing the existing national networks of detectors, and it has improved the detection threshold for explosions as well as earthquakes in large parts of the Earth. Data from the stations are transmitted via secure satellite links to a UN data centre in Vienna.

All the data are processed at the centre in Vienna. The data centre is completely neutral and is not permitted to judge if an event is natural, such as an earthquake or a volcanic eruption, or caused by a man-made explosion. Instead the data centre makes raw data as well as processed data available to the individual countries, and then it is up to the national authority in each country to decide whether an event is suspicious or not.

Should an event be deemed suspicious by a country, any country has the right to request further processing by the IMS and ultimately request an on-site inspection at the location of the suspicious event. In recent years, nuclear test explosions have been easy to identify, as the involved nations have openly announced the tests and provided information about location and time of the explosions (Pakistan 1998, India 1998, North Korea 2006 and 2009).

GEUS and CTBTO

In Denmark, GEUS houses both the national data centre and is also the National Authority for the CTBTO. GEUS is responsible for running two monitoring stations in the IMS network. One is a seismograph in Kangerlussuaq, West Greenland; it is part of the auxiliary (secondary) seismic network. The other is an infrasound station near Qaanaaq, North-West Greenland, that is a primary IMS station. The Danish Meteorological Institute takes part in the daily maintenance of the infrasound station.

Together with diplomats from the Danish embassy in Vienna, GEUS is also involved in the preparatory work on operational manuals and procedures for waveform processing that is carried out at the UN centre. This involves discussions on how to tune the detection system to automatically filter out as many earthquake signals as possible, so that the system triggers on explosions only. This part of the system still needs significant improvements.

In order to be as familiar as possible with the data from the IMS before the treaty enters into force, seismologists at GEUS make experiments with the incoming data for other purposes. Recently we have found that the IMS raw seismological data are useful for determining accurate depths of Danish earthquakes. The IMS seismographs are of a very high quality and it is possible to identify signals from relatively weak earthquakes at distant stations.

Earthquake depth analysed using CTBTO array data

For several decades we have supplemented with data from seismic stations in the countries around Denmark and Greenland to help detect and localise earthquakes. Seismic array stations produce data of particularly high quality. A seismic array station consists of a large number of sensors installed in a small area. The ability to detect an earthquake decreases when the strength of the seismic noise increases relative to the strength of the seismic signal. Seismic noise can be reduced significantly in earthquake data recorded by an array by summing the signals recorded at the sensors, thus enabling the detection of smaller events than is possible on a station with just one sensor. The closest seismic arrays that contribute to the monitoring of earthquakes in Denmark and Greenland are the NORSAR and ARCES arrays in Norway, the HFS array in Sweden, the FINES array in Finland and the SPITS array at Svalbard (Fig. 1).

Previously, array data have been used to locate earthquakes in Denmark and Greenland from observations of *P* and *S* phase travel times only. For the two earthquakes in Skåne on 16 December 2008 and in the North Sea on 19 February 2010, however, a new technique was used to improve the estimate of the depth of the earthquakes. This

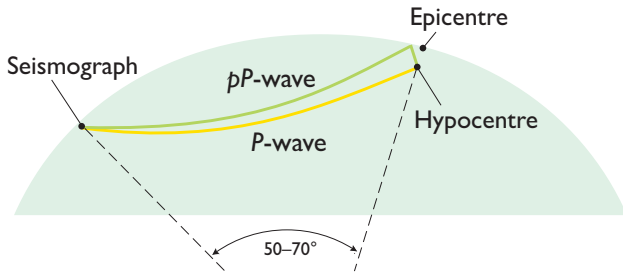

Fig. 3. The slightly different paths taken by the *P*- and the *pP*- (or *sP*-) waves can be used to calculate the depth of an earthquake. The *P*-wave (yellow) travels directly from the hypocentre to the seismograph, whereas *pP*- and *sP*-waves (green) travel from the hypocentre to the surface near the epicentre and from there reflected to the seismograph. The paths of the *pP*- and *sP*-waves differ slightly due to the crustal structures near the earthquake.

technique uses teleseismic observations of travel-time differences between the *P* phase and the *pP* and/or *sP* phases to calculate the depth of the earthquake. The *pP* and *sP* phases are reflections at the Earth's surface of the shaking from the earthquake hypocentre. These phases are recorded slightly after the *P* wave arrival (Fig. 3). The technique requires measurements with a high signal-to-noise ratio and good knowledge of the geological structures near the epicentre. The principles of the teleseismic depth-determination technique are very simple. At teleseismic distances the difference in travel length is negligible for the *P*-wave travelling directly from the hypocentre to the seismograph and the part of the *pP*-wave travelling from the epicentre to the seismograph (Fig. 3). The difference in travel time between the phases is assumed to be caused by the *pP*-wave travelling almost vertically through the crust from the hypocentre to the surface. If the velocity structure in the crust below the epicentre is well known, the travel time difference between *P* and *pP* and/or *sP* can be converted to a depth. An accurate crustal velocity model is therefore critical for the analysis since errors in the crustal model will give a wrong determination of the depth. A teleseismic recording is needed as the paths of the *pP* and *sP* phases must be near vertical at the source. However, the distance between the earthquake and the seismic array must be sufficiently short for the phase not to be effected by the core–mantle boundary. We find that a distance of around 50 to 70 degrees is optimal for this technique.

A significant number of the IMS stations are seismic arrays. The stations are installed at locations with low ambient noise, in order to record data of high quality. In our analysis we use data from the Yellowknife Array (YKA) in Canada and the Toridu Array (TORD) in Niger (Fig. 1). The Yellowknife Array consists of 19 short-period sensors and 4 broadband sensors. The sensors are installed in a cross with an aperture of 25 km. The array was installed in 1962 with the main purpose of monitoring underground nuclear explosions (source: Natural Resources Canada). The Toridu Array is a modern array constructed specifically for the CTBTO (Estabrook *et al.* 2009). It consists of 16 broadband sensors deployed in three concentric rings with a central node. The sensors are not radially aligned, as this layout leads to the largest noise reduction (e.g., Schweitzer *et al.* 2002).

As described above, the energy release of the majority of the earthquakes in Denmark and Greenland is too low to generate clear signals even at the best IMS stations. The two earthquakes, Skåne, 16 December 2008 and the North Sea, 19 February 2010, measuring 4.8 and 4.7 on the Richter scale, respectively, are our best candidates for this technique (Fig. 2). The geological structures are well mapped in Denmark where we have a good knowledge of *P*-wave velocity (Thybo 2001). For the *S*-wave velocity we have used $Vp = 1.73 \times Vs$ to estimate the earthquake depth. Using this technique in Greenland will be less reliable in most areas, because the crustal structures are not as well mapped.

We have analysed the measurements of the Skåne earthquake on the YKA Array (Fig. 4). The measurements show a good signal-to-noise ratio and we find a difference in the *P* and *sP* travel times of *c.* 4 sec., equivalent to an earthquake depth of 9 km. The previously calculated depth of this earthquake was 18.1 ± 5.2 km using the standard location method (SNSN 2010), and the result from moment-tensor inversion was 8 km (Regel 2010). The standard location method is based on an approach that searches for the hypocentre that gives the best fit to measured travel times of *P*- and *S*-waves within *c.* 1000 km of the earthquake, using a 1D Earth model. The larger depth obtained by SNSN might be due to the velocity model, which is not well calibrated for the Skåne

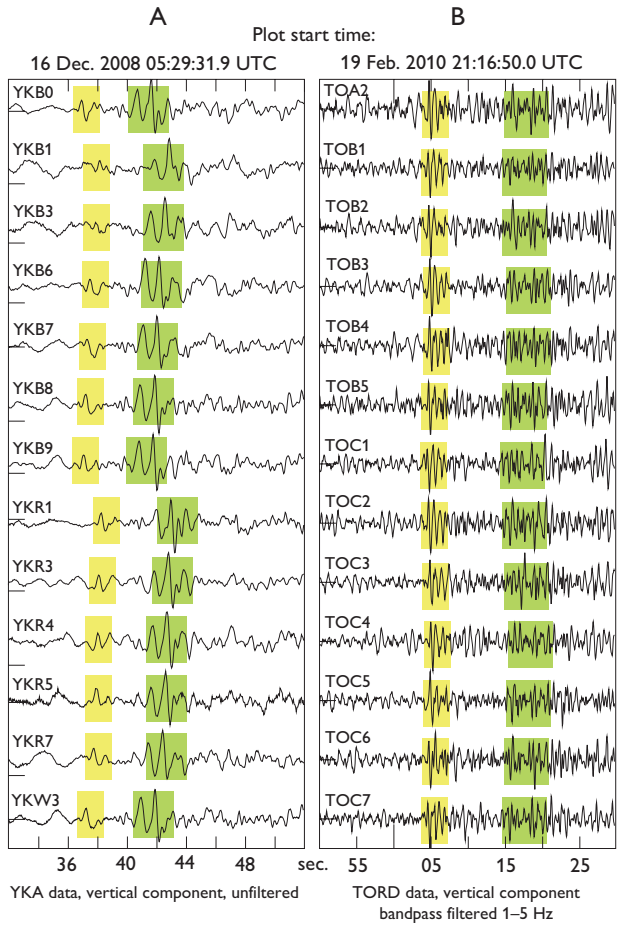

Fig 4. **A**: The *P*-wave train from the Skåne earthquake on the Yellowknife Array (YKA). Yellow is the direct *P* phase and green is the *sP* phase. **B**: The *P*-wave train from the North Sea earthquake on the Toridu Array (TORD). Yellow is the direct *P* phase and green is the *pP* phase. The high number of sensors improves the possibility of identifying different phases.

area (B. Lund, personal communication 2010) and the use of measurements far from the epicentre.

The North Sea earthquake measurements on the YKA have a low signal-to-noise ratio on many of the sensors, but on the best five sensors we observe a signal *c.* 15 sec. after the P phase. Interpreting this as the *sP* phase yields a depth of 35.2 km. The high noise level in the YKA data carries a risk of misinterpretation of the data. We therefore supplement with data from the TORD array (Fig. 4), to verify the depth of this earthquake. From the measurements of the TORD array we find a difference in the *P* and *pP* travel time of *c.* 11 sec., corresponding to an earthquake depth of 38.5 km. The previously calculated depth was 38.7 ± 10.3 km using the standard location method. The depth uncertainty is larger than that of the Skåne earthquake due the larger distance of the nearest seismometer. The depths of the two earthquakes are comparable with the depths of previous earthquakes in these areas (Gregersen *et al.* 1999). The higher noise level of the North Sea event (Fig. 4) is a source of error in the analysis. The higher noise level could be due to an energy radiation pattern of the earthquake that is low in the direction of TORD or a different frequency content of the released shaking.

Concluding remarks

Teleseismic array data have produced consistent depth estimates for two recent earthquakes in the Danish area. This raises the possibility that we might find other earthquakes suitable for this technique in the GEUS database, especially from Greenland.

The seismological involvement in detection and discrimination of nuclear explosions has spurred significant Nordic collaboration since the 1960s, and a yearly Nordic seismological meeting is held. GEUS has made a special contribution together with the UK Foreign and Commonwealth Office, NORSAR, the Swedish National Defence Research Establishment and the University of Helsinki to improve data exchange between the International Monitoring System and the International Seismological Centre. This has resulted in the development of a collection of interactive seismological tools for merging and manipulating the two largest and most complete seismological databases (Gaspa *et al.* 2010). In the future this will hopefully help improve and ease the scientific use of the International Monitoring System data.

References

Comprehensive Nuclear Test-Ban Treaty (www.ctbto.org).

Estabrook, C., Bergsson, B., Soumana, S., Boureima, O. & Moumouni, M. 2009: Results from IMS Seismic Array in Niger. Poster presented at the EGU meeting in Vienna, April 2009.

Gaspa, O., Bondar, I., Harris, J. & Storchak, D. 2010: The CTBTO link to the ISC Database. The 41st Nordic Seminar on Detection Seismology, Århus, 6–8 October, 2010. Program with abstracts, 14 only.

Gregersen, S., Hjelme, J. & Hjortenberg, E. 1998: Earthquakes in Denrnark. Bulletin of the Geological Society of Denmark **44**, 115–127.

Regel, J. 2010: Moment tensor of the 16 Dec[ember] 2008 earthquake in Skåne, Sweden. The 41st Nordic Seminar on Detection Seismology, Århus, 6–8 October 2010. Program with abstracts, 39 only.

Schweitzer, J., Fyen, J., Mykkeltveit, S. & T. Kværna, T. 2010: Seismic Arrays. In: New Manual of Seismological Observatory Practice, Chapter 9. Doi: 10.2312/GFZ.NMSOP_rl_ch9.

SNSN 2010: Swedish National Seismic Network (http://snsn.geofys.uu.se/).

Thybo, H. 2001: Crustal structure along the EGT profile across the Tornquist Fan interpreted from seismic, gravity and magnetic data. Tectonophysics **334**, 155–190.

Authors' address

Geological Survey of Denmark and Greenland, Øster Voldgade 10, DK-1350 Copenhagen K, Denmark. E-mail: *tbl@geus.dk*

Free, online Danish shallow geological data

Martin Hansen and Bjarni Pjetursson

Geological data at the Geological Survey of Denmark and Greenland (GEUS) have been available on the internet for more than 10 years. The first step in making geological data available online was the launch of web access to data from water supply wells (Tulstrup 2004). The database is called Jupiter, and currently data from more than 260 000 shallow wells are available to the public. Figure 1 shows an example of a map from the Jupiter database available in a web-browser.

The first web access was via a text-based search form which supplied data lists and graphical well reports. In recent years, the interface has been extended with more data, map interfaces and extra functionality. This paper describes this development and illustrates the increasing value of the digital data at GEUS.

In its current form, the Jupiter webpage offers: (1) data on wells, geology, water level and groundwater chemistry, (2)

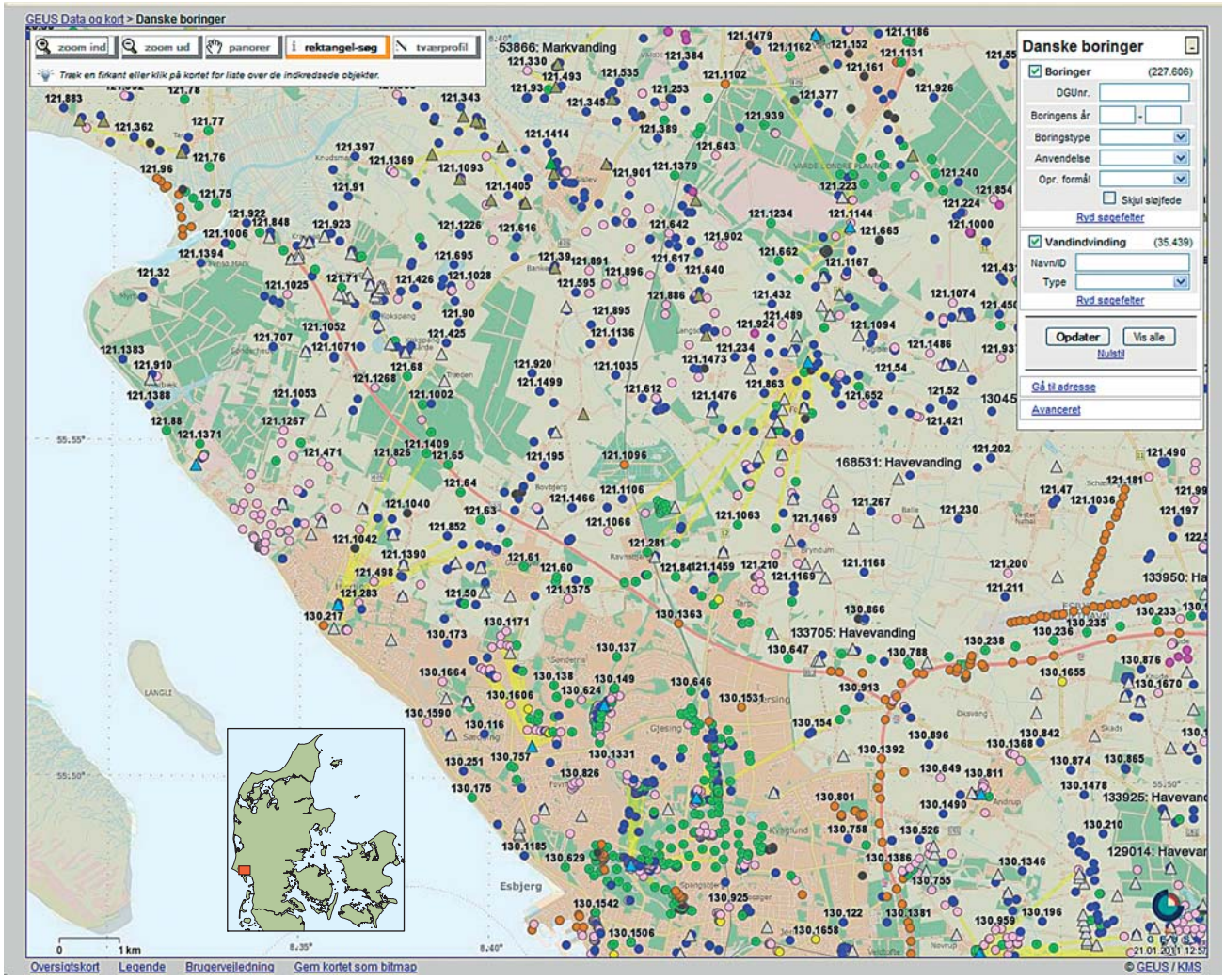

Fig. 1. Map interface showing boreholes (dots) and water extraction plants (triangles). The inset map shows the location in south-western Denmark.

data about water supply, water abstraction licences, yearly abstraction, exchange of drinking water between waterworks installations as well as drinking-water chemistry and (3) the possibility to download complete data sets in various database formats.

The simple text-based search form has been extended with new functions and supplied with different types of map interfaces. Data can now be accessed via web map services, web feature services and in Google Earth format. In 2007, after implementation of a local government reform in Denmark, Jupiter became the national database for shallow geology, groundwater and drinking water. A data model based on the Jupiter database was established and all the data were made available to the public. A set of simple object access protocol web services was launched giving full read-only access to all data in the public domain data model. Editing was allowed for the part of the data model that is maintained outside the Survey.

After the reform of the local government system, tasks involving shallow geology and hydrogeology were divided between (1) the state, which is responsible for hydrogeological mapping and groundwater monitoring, (2) the regions for dealing with soil pollution and remediation and (3) the municipalities (kommuner) for issuing groundwater abstraction licences and checking drinking-water quality.

With the demand for geological data at three administrative levels the ability to share knowledge is important. In addition to geological and hydrogeological information from the Jupiter database, shallow geophysical data from the Survey's GEophysical Relational DAtabase (GERDA) can now

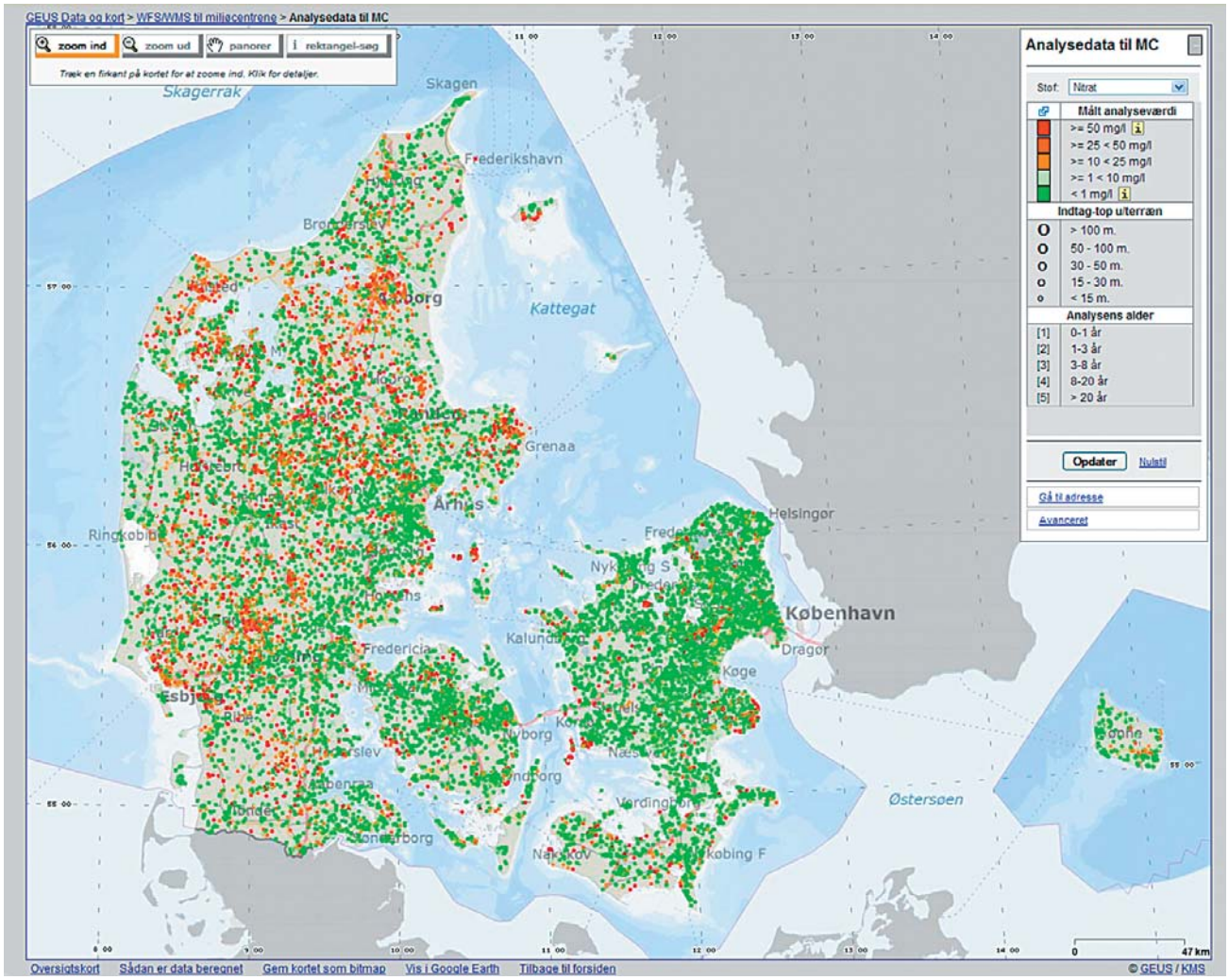

Fig. 2. Map of Denmark showing nitrate analyses from groundwater samples. These data are made available through web map services, web feature services and a simple map interface. Thirty-five other types of analyses are available in the same form.

Table 1. The databases can be accessed via different interfaces

Data set	Website	Map interface	Download	Google Earth format	WMS/WFS[$]	SOAP[#] web services
Jupiter	Yes	Yes	Yes	Yes	Yes	Yes
GERDA	Yes	Yes	Yes	No	Yes	No
Report database	Yes	Yes	Yes	No	Yes	No
Database for geological models	Yes	Yes	Yes	No	No	No
Groundwater chemistry for 36 selected parameters	Yes*	Yes	Yes*	Yes	Yes	No

[$]web map services/ web feature services, *part of Jupiter, [#]Simple object access protocol.

be used free of charge (Møller *et al.* 2009). Databases with hydrological reports and geological models were also established. The reports and models are also available at no cost.

At the same time, more than 750 000 documents from the Surveys' old Well Data Archive, and files from well archives held by the former Danish counties (amter) were added to the website, all linked to the wells they describe.

The data in the Jupiter database are in accordance with Danish legislation updated by GEUS and by local authorities. As an example, laboratories must deliver analyses of

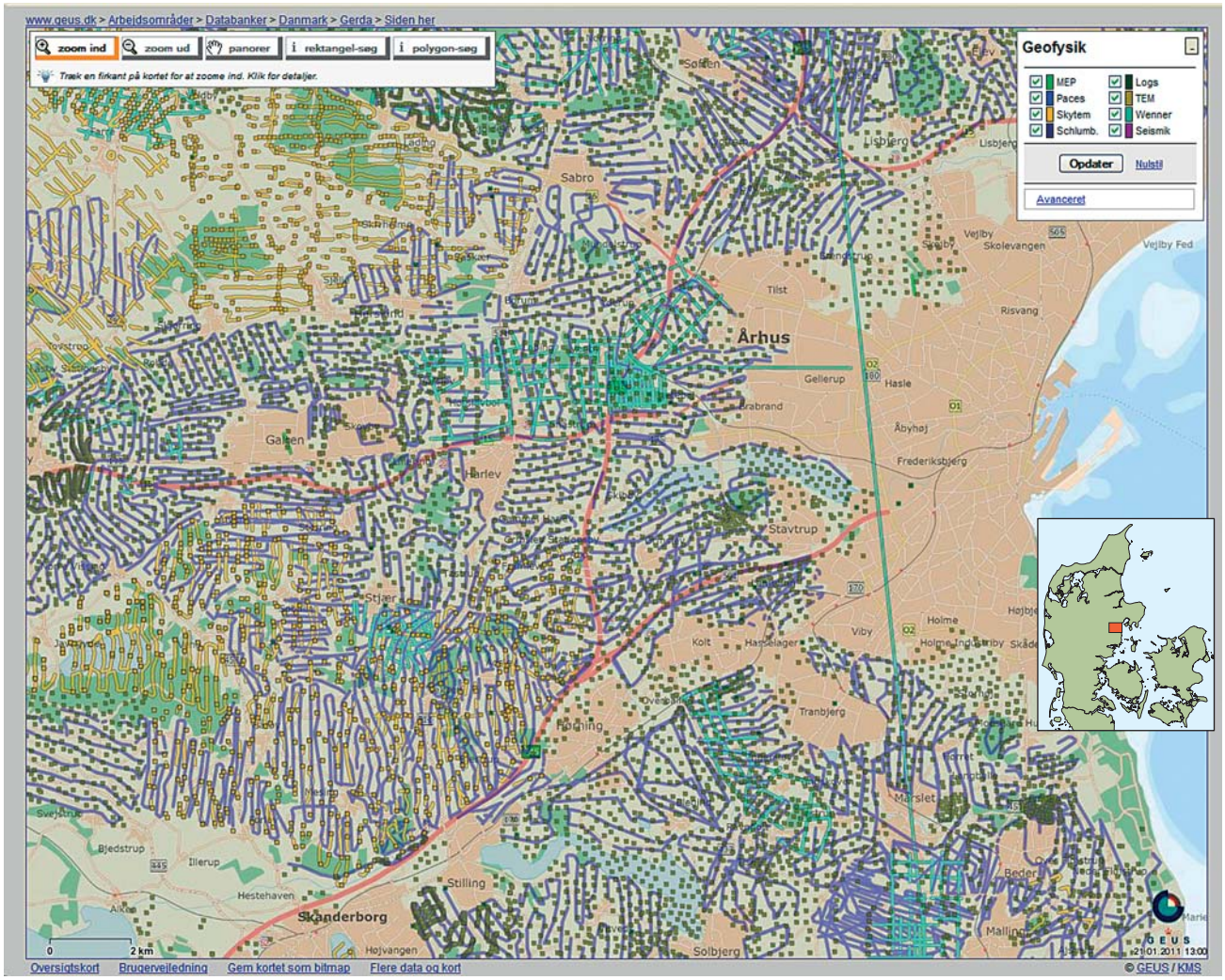

Fig. 3. A close-up of the area west of Aarhus showing GERDA data coverage of different geophysical data types. The inset map shows the location in central Denmark.

drinking and groundwater conducted for waterworks directly to the database. When data are entered into the Jupiter database, users responsible for drinking-water quality receive notification by e-mail, and after quality control the data are immediately available online.

Users of the data

The Jupiter data are used by a wide range of people. By storing data in a central database, the data of one municipality are available not only to the neighbouring municipalities but also to users of drinking water, to the educational system as well as to advisors working for the environmental centres in Denmark.

Different users with different needs and skills call for different user-interface types. At present, data can be accessed through a variety of interfaces. Maps and Google Earth can be used by the public, whereas web map services and web feature services are mainly for professional users (Fig. 2). The web services give full reading access through specially designed software and allow editing possibilities for public employees with the appropriate privileges. It is also possible to download complete databases that can be used for complex analyses and to develop geological and hydrogeological models.

Online shallow geophysical data

The geophysical relational database (GERDA) contains geophysical data acquired during hydrogeological mapping in Denmark over the past decade. The GERDA data became available to the public on 1 January 2007. GERDA comprises a wide range of geophysical data, geoelectric and geoelectromagnetic data, both raw and processed, reflection seismic data and borehole logging data (Fig. 3). Inverted 1D and 2D models are included with the geoelectric and electromagnetic data, and the processed sections are available with the seismic data. All information on data acquisition, data processing and inversion procedures can be stored, thus facilitating full reprocessing and inversion of data when required, which makes the inversion and interpretation of data transparent.

Hydrological reports and geological models

GEUS also hosts a database with hydrogeological reports and a database for geological models. Both databases have been developed in cooperation with the Danish environmental centres. Reports from hydrological surveys are stored in the report database, which was established to allow easy exchange of information between administrators at different levels. Reports can be accessed from a search form or from a map interface, if the report is geocoded.

The database containing geological models was established to store geological and hydrological models in a tool-independent format. The database is closely connected with the borehole, geophysical and report databases to give the users easy access to reports describing the models and to the data on which the models are based. All models developed by or for the environmental centres during the mapping of the Danish groundwater are stored in the model database.

Concluding remarks

Most of the Danish environmental data are available free of charge and most of them can be found through different Danish interfaces (Table 1). Users can access data through websites, where they can search for specific data sets; they can find data through different types of map interfaces, download parts of databases or complete databases. Through web services users can read directly from the database and privileged users can update data belonging to their own administrative unit.

The easy access to data makes it easy to share data between different administrative units, between individuals and between consultant companies. Private companies, often working for the public administration, have benefitted from the central data storage as they can now access most of the relevant data from one website. In addition, the data are updated and always in the same formats.

References

Møller, I., Søndergaard, V.H. & Jørgensen, F. 2009: Geophysical methods and data administration in Danish groundwater mapping. Geological Survey of Denmark and Greenland Bulletin **17**, 41–44.

Tulstrup, J. 2004: Environmental data and the internet: openness and digital data management. Geological Survey of Denmark and Greenland Bulletin **4**, 45–48.

Authors' address

Geological Survey of Denmark and Greenland, Øster Voldgade 10, DK-1350 Copenhagen K, Denmark. E-mail: *mh@geus.dk*

Remnants of Mesoarchaean oceanic crust in the Tartoq Group, South-West Greenland

Kristoffer Szilas, Vincent J. van Hinsberg, Alexander F. M. Kisters, Thomas F. Kokfelt, Anders Scherstén and Brian F. Windley

The Tartoq Group is located in the Sermiligaarsuk fjord region in South-West Greenland in an area of approximately 20 × 50 km (Fig. 1). The Tartoq Group consists of several discrete, fault-bound blocks of metavolcanic rocks, surrounded by Archaean tonalite-trondhjemite-granodiorite-type (TTG) gneisses. A zircon age of 2996.3 ± 5.9 Ma of a TTG intrusion provides a minimum age for the formation of the Tartoq Group (Fig. 2). The metavolcanic rocks probably show the lowest degree of metamorphism found anywhere in the Archaean craton of Greenland. Here we present a new model for the origin of the metavolcanic rocks of the Tartoq Group based on geochemical, metamorphic and structural data. The samples used for this study were collected by the Geological Survey of Denmark and Greenland (GEUS) in 2009 and 2010. The study is part of a joint project between the Greenland Bureau of Minerals and Petroleum and GEUS on the mineral potential of south-western Greenland.

Geology of the Tartoq Group

The Tartoq Group can be divided into five main lithological units: (1) subaqueous, mafic pillow lavas, (2) mafic dykes and sills with semi-ophitic textures, (3) gabbros with relict magmatic textures and tonalite-trondhjemite-granodiorite composition, (4) ultramafic rocks that are mainly serpentinites and (5) felsic schists that commonly show high strain with mylonitic textures. In addition, a marble unit occurs in the Nuuluk block; gneiss of quartz dioritic composition lies in a large breccia zone with intrusive tonalite-trondhjemite-granodiorite-type (TTG) gneisses that have been fractured and chloritised; and undifferentiated pegmatites are found in the Bikuben and the Iterlak blocks. The lithologies and their relations were described by Higgins (1968), Berthelsen & Henriksen (1975), Petersen (1992) and van Hinsberg *et al.* (2010).

Greenschist facies rocks with pseudo-sections indicating peak metamorphic conditions of 380°C at 2 kbar dominate the Nuuluk block in the west (Fig. 1). The metamorphic grade increases to upper amphibolite facies with pressure and temperature calculated to 650°C at 6–7 kbar in the Bikuben block in the east. Evidence for partial melting is seen for at least one locality in the Bikuben block, where leucosomes occur in fold hinges of amphibolites. Peak metamorphic assemblages generally correlate with the different lithological units, which means that pillow lavas and shallow dykes or sills are at a lower grade and gabbro and serpentinite units at a higher grade (van Hinsberg *et al.* 2010).

The Tartoq Group is thrust (top to the SE) and imbricated with younger TTG gneisses. Kilometre-scale nappes, low-angle shear zones, and younger cataclastites formed as a

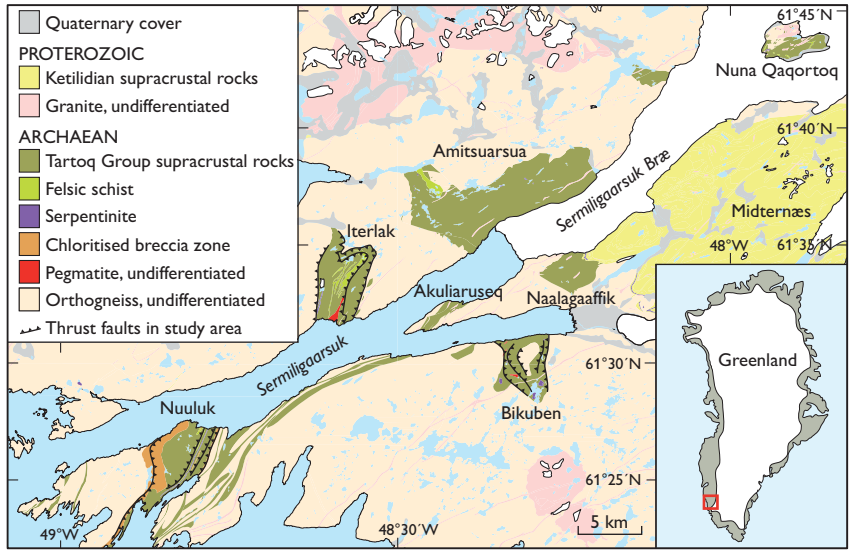

Fig. 1. Simplified geological map of the Sermiligaarsuk fjord area, with the names of seven blocks with supracrustal rocks belonging to the Tartoq Group. The undifferentiated orthogneiss surrounding TGG gneisses has ages ranging from about 2500 Ma to 3000 Ma. The Ketilidian supracrustals overly the Tartoq Group unconformably (van Hinsberg *et al.* (2010). The Tartoq Group is mostly in tectonic contact with the surrounding orthogneiss, but a few intrusive relations are preserved at south Iterlak and north Amitsuarsua blocks. The supracrustal blocks form thrust sheets and lateral ramps with internal top to the SE kinematic indicators.

result of the accretion and progressive exhumation of these rocks. Deformation was associated with hydrothermal alteration (with Au mineralisation at *c.* 450°C) that overprinted regional metamorphic parageneses and intense carbonation in high strain zones.

Felsic, 1–80 m thick schist bodies in the mafic sequence represent high-strain zones where TTG gneisses have been preferentially sheared in the metavolcanic rocks. Some of these mylonitic, felsic schists gave zircon ages of *c.* 2800 Ma to 3700 Ma which indicate the subsurface presence of old crustal material. These ages also suggest that the felsic schists are not part of the Tartoq Group, but are tectonic in origin.

Geochemistry

The geochemical data were screened and samples showing evidence of post-magmatic alteration were rejected. Microscopy of thin sections was used to identify the least altered samples. Samples with quartz and carbonate veining and samples showing excessive large-ion lithophile elements (LILE) enrichment were discarded. Pillow lavas are prone to sea-floor alteration during extrusion, and therefore this group of rocks may be under-represented in the screened dataset.

The Tartoq Group metavolcanic rocks (pillow lavas, dykes or sills and gabbro units) all have tholeiitic basaltic compositions. Trace-element variations within the volcanic sequence broadly show that the incompatible trace elements increase with decreasing MgO content and the compatible trace elements decrease with falling MgO, consistent with trends of fractional crystallisation of olivine, clinopyroxene and perhaps plagioclase. The major elements show trends similar to what would be expected for a tholeiitic fractionation series. The scatter seen within the data may be due to metamorphic or slight hydrothermal background alteration. The metavolcanic rocks generally have flat, primitive, mantle-normalised trace-element patterns with La_N/Sm_N = 0.8–1.0, but they show negative Nb anomalies with Nb_N/La_N = 0.4–0.9 (Fig. 3). In tectonic discrimination diagrams, which rely on immobile trace elements, the metavolcanic rocks plot in the mid-ocean ridge basalt (MORB) or island-arc tholeiite (IAT) fields. La, Y and Nb abundances are similar to those of some modern back-arc basalts (BAB).

The serpentinites have median values of SiO_2 (45 wt%), MgO (37 wt%), FeO_T (14.5 wt%), Cr (3100 ppm), Ni (600 ppm) and essentially no CaO or Al_2O_3, combined with a large negative chondrite-normalised Eu anomaly (Fig. 3). The serpentinites mainly consist of normative olivine and hypersthene (3:1 ratio) and are thus harzburgitic in composition.

The felsic schist units show complete overlap in major and trace elements with the surrounding gneisses. This is consistent with the structural interpretation that they are deformed rocks along thrust faults, and hence unrelated to the volcanic sequence.

Discussion

The metavolcanic rocks in the Tartoq Group have similar trace-element patterns, with pronounced negative Nb anomalies (Fig. 3). Their overall major and trace-element variations are consistent with fractional crystallisation processes. These features suggest that the metavolcanic rocks are co-magmatic. The dykes and sills have the highest concentration of incompatible trace elements. This is consistent with the fact that they have the lowest MgO content and they thus form the more evolved portion of the magma pile. The four pillow lavas show a narrow compositional range that

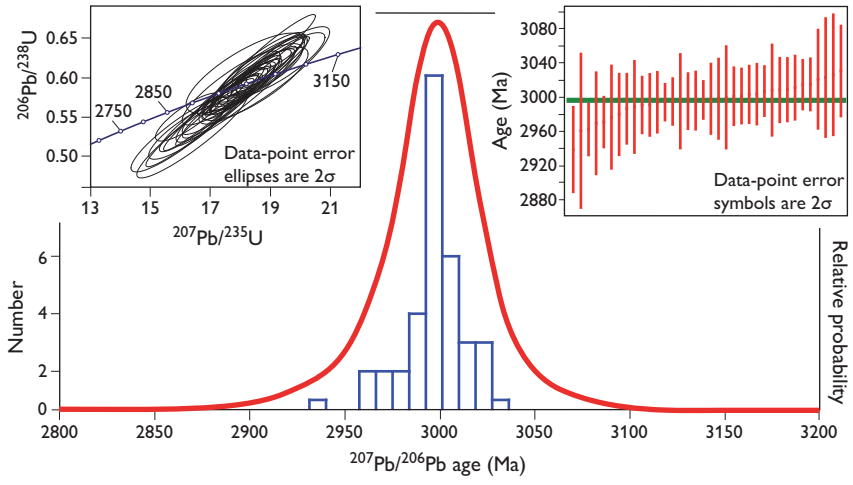

Fig. 2. Zircon U/Pb age of sample GGU 510771 using laser ablation inductively coupled mass spectrometry. The sample is an intrusive orthogneiss from the northern contact in the Amitsuarsua block and the age was 2996.3 ± 5.9 Ma (95% confidence interval). The zircons in the sample are prismatic and show oscillatory growth zonation. Only the zircon cores were analysed. Spots that are concordant within ± 10% have been used and they form a tight normal distribution with a mean square weighted deviation of 0.76 and a probability of 0.85. The mean was weighted by data point errors only (no points were rejected). The analyses cut the concordia with minimal signs of lead loss and thus provide a robust age.

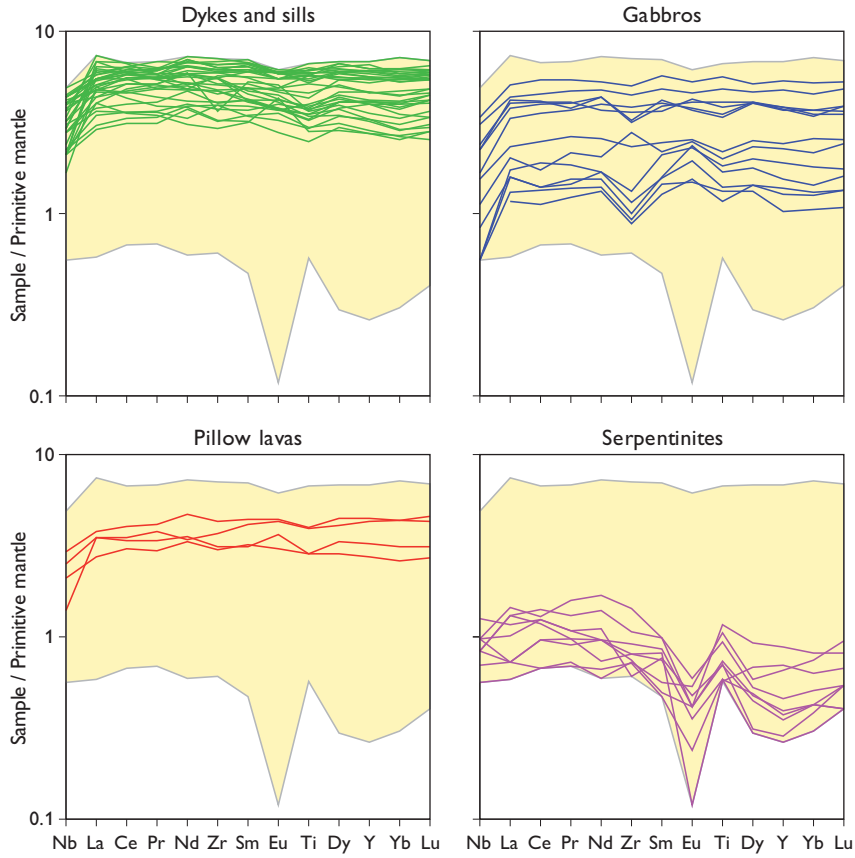

Fig. 3. Spidergrams showing primitive mantle-normalised trace-element compositions of samples from the Tartoq Group (normalisation after Sun & McDonough 1989). Only the relatively immobile trace elements are shown due to the likely mobility of the large ion lithophile elements during metamorphism and seafloor alteration. The pillow lavas, dykes and sills form fairly well-constrained compositional groups. In contrast, the gabbros show greater compositional variation, reflecting variable effects of fractionation and accumulation processes. The serpentinites show low concentrations and a large negative Eu anomaly, which imply melt or mineral equilibrium processes involving plagioclase. The yellow areas shown in the spidergrams represent the total data field of the Tartoq Group.

overlaps with the dykes and sills, as to be expected if the latter represent the feeding channels of lava flows. A broader compositional range is observed for the gabbros. Positive Eu anomalies, low trace element concentrations combined with high contents of CaO, Al_2O_3 and Sr suggest some accumulation of plagioclase.

The serpentinites show low incompatible trace-element concentrations, major element contents and normative compositions. These features are consistent with harzburgite that could represent either cumulates of the volcanic sequence or the residual source mantle. PGE patterns show depletion in Pt and Pd which is also observed in peridotite xenoliths from kimberlites in the area (Wittig *et al.* 2010). The serpentinites probably represent a sub-continental lithospheric mantle, which experienced high degrees of melt extraction and was exhumed together with the supracrustal rocks of the Tartoq Group.

No co-genetic, calc-alkaline rocks have been found in the Tartoq volcanic sequence and it is therefore unlikely that the volcanic rocks erupted through continental crust or formed in a mature arc setting. At first glance the geochemical features of the metavolcanic rocks resemble those of the modern MORB, but they differ distinctly by having a negative Nb anomaly and by their pattern of undepleted light rare-earth elements. The tectonic discrimination diagrams point to a IAT setting, but the lack of co-genetic, calc-alkaline rocks argues against this. The La, Y and Nb concentrations indicate a BAB setting, which is in agreement with the arc 'flavour' that is suggested by the IAT affinity.

The major and trace-element values for the Tartoq Group are similar to data from Archaean tholeiitic rocks from the Superior Province of Canada, which formed in a BAB setting according to the interpretation of Sandeman *et al.* (2006). Another explanation for Archaean tholeiites is that they formed in an oceanic plateau setting similar to the recent Ontong Java plateau (Arndt *et al.* 1997). All examples of Archaean tholeiites are associated with abundant komatiites. However, komatiites are rare in the supracrustal belts of Greenland and absent in the Tartoq Group, which argues against an oceanic plateau setting. Rocks from a BAB setting are also more likely to be preserved over time, because the crust in BAB settings is thin and located in a collision setting, like the present-day Lau and Mariana back-arc crust (Martinez & Taylor 2003).

It is mainly the higher degree of partial melting estimated for Archaean tholeiites compared to present day MORB settings that have led some authors to argue for an oceanic plateau setting, whereas the LILE enrichment and negative

Nb anomaly have led others to suggest a BAB environment. However, Rollinson (2010) suggested that the differences between modern MORB and Archaean non-arc tholeiites simply reflect high temperatures of the Archaean mantle. Rollinson's model provides a robust explanation for the geochemical features of the Tartoq Group. The Tartoq Group may be a product of a hotter mantle giving rise to a thicker melting column, which affected the composition and differentiation of MORB magmas and resulted in the observed discrepancies compared with the modern MORB.

Regardless of the precise setting of ocean crust formation, the similar flat trace-element patterns and fractional crystallisation trends of all the metavolcanic rocks of the Tartoq Group, together with the presence of serpentinites, indicate that the rocks form a co-magmatic assemblage resembling an ophiolitic ocean floor sequence. Two possible scenarios can explain the metamorphic and structural observations: (1) shallow subduction followed by TTG formation due to slab melting made the oceanic crust sufficiently buoyant to cause exhumation in a subduction channel and subsequent incorporation into the overriding plate; (2) the Tartoq Group formed from the overriding plate in an oceanic flake-style subduction setting that was dragged down with a shallow *PT*-trajectory by the subducting plate and later rebounded during aborted subduction (or slab break-off?), which could initiate TTG formation by decompression melting of the lower crust. In both scenarios we envisage that subduction took place in an intra-oceanic setting, resulting in the lack of continent-derived material in the Tartoq Group. Both tectonic environments could give rise to the observed peak metamorphic assemblages and later retrogression by fluid input together with inter-thrusting with the TTG gneisses, which resulted in the tectonic slices and slabs that we see today.

Conclusions

Based on geochemical, metamorphic and structural data we have developed a new model according to which the Tartoq Group is a slab of oceanic crust. We interpret the protolith of the Tartoq Group as a structurally dismembered section of Archaean oceanic crust of either MORB or BAB affinity, which might provide valuable insight into Archaean geodynamics.

References

Arndt, N.T., Kerr, A.C. & Tarney, J. 1997: Dynamic melting in plume heads: the formation of Gorgona komatiites and basalts. Earth and Planetary Science Letters **146**, 289–301.

Berthelsen, A. & Henriksen, N. 1975: Geological map of Greenland, 1:100 000, Ivigtut 61 V.1 Syd. Descriptive text, 169 pp. Copenhagen: Geological Survey of Greenland.

Higgins, A.K. 1968: The Tartoq Group on Nuna qaqortoq and in the Iterdlak area, South-West Greenland. Rapport Grønlands Geologiske Undersøgelse **17**, 17 pp.

Martinez, F. & Taylor, B. 2003: Controls on back-arc crustal accretion: insights from the Lau, Manus and Mariana basins. In: Larter, R.D. & Leat, P.T. (eds): Intra-oceanic subduction systems: tectonic and magmatic processes. Geological Society Special Publications (London) **219**, 19–54.

Petersen, J.S. 1992: Nuuluk-Iterlak gold and massive-sulfide project, Taartoq Archaean greenstone belt, SW Greenland, 164 pp. Unpublished field report, Nunaoil A/S.

Rollinson, H. 2010: Coupled evolution of Archean continental crust and subcontinental lithospheric mantle. Geology **38**, 1083–1086.

Sandeman, H.A., Hanmer, S., Tella, S., Armitage, A.A., Davis, W.J. & Ryan, J.J. 2006: Petrogenesis of Neoarchaean volcanic rocks of the MacQuoid supracrustal belt: a back-arc setting for the northwestern Hearne subdomain, western Churchill Province, Canada. Precambrian Research **144**, 140–165.

Sun, S. & McDonough, W. F. 1989: Chemical and isotopic systematics of oceanic basalts: implications for mantle composition and processes. In: Saunders, A.D. & Norry, M.J. (eds): Magmatism in the ocean basins. Geological Society Special Publications (London) **42**, 313–345.

van Hinsberg, V.J., Szilas, K. & Kisters, A.F.M. 2010: The Tartoq Group, SW Greenland: mineralogy, textures and a preliminary metamorphic to hydrothermal history. Danmarks og Grønlands Geologiske Undersøgelse Rapport **2010/120**, 40 pp.

Wittig, N., Webb, M., Pearson, D.G., Dale, C.W., Ottley, C.J., Hutchinson, M., Jensen, S.M. & Luguet, A. 2010: Formation of the North Atlantic Craton: Timing and mechanisms constrained from Re–Os isotope and PGE data of peridotite xenoliths from S.W. Greenland. Chemical Geology **276**, 166–187.

Authors' addresses

K.S. & T.F.K., *Geological Survey of Denmark and Greenland, Øster Voldgade 10, 1350 Copenhagen K, Denmark*. E-mail: *ksz@geus.dk*

V.J.H., *Department of Earth Sciences, University of Oxford, South Parks Road, Oxford OX1 3AN, UK*.

A.F.M.K., *Department of Earth Sciences, Stellenbosch University, Matieland 7602, South Africa*.

A.S., *Deptartment of Earth and Ecosystem Sciences Division of Geology, Lund University Sölvegatan 12, 223 62 Lund, Sweden*.

B.F.W., *Department of Geology, University of Leicester, University Road, Leicester, LE1 7RH, UK*.

Palaeogene deposits in North-East Greenland

Henrik Nøhr-Hansen, Lars Henrik Nielsen, Emma Sheldon, Jussi Hovikoski and Peter Alsen

Scattered occurrences of Palaeogene sediments are found in North-East Greenland, where they overlie unconformably Cretaceous sediments and are capped by Palaeogene basalts. These sediments have received little attention (Watt 1994), except for relatively recent studies (Nøhr-Hansen & Piasecki 2002; Jolley & Whitham 2004; Larsen *et al.* 2005; Heilmann-Clausen *et al.* 2008). As part of an ongoing petroleum geological study that focuses on the Jurassic–Cretaceous succession, the Palaeogene sediments were included to better constrain their age, depositional environment and relation to the basalts. Several localities were investigated on Wollaston Forland, Sabine Ø and Hold with Hope, a few of which are described here (Fig. 1).

Eastern Wollaston Forland and Sabine Ø

Discontinuous outcrops of mostly loose and un-cemented Palaeogene sediments occur in Haredal, eastern Wollaston Forland. A N–S-striking normal fault with 100–125 m of downthrow to the east separates the main outcrop in the southern slope into two blocks. The best exposed succession is situated in the western footwall block, where the succession dips 20° to the SW (Fig. 2). It overlies marine mudstones of Late Albian age (*Wigginsiella grandstandica* Subzone (V1) of Nøhr-Hansen 1993) in the footwall block and of Early to Middle Campanian age (indicated by the dinocysts *Alterbidinium ioannidesii* and *Cerodinium diebelii*) in the hanging wall block; however, the contact to the Cretaceous is not exposed. A poorly exposed Palaeogene succession in the northern slope is probably from the hanging wall block; the base of the succession and underlying strata are not exposed.

Haredal, southern slope. Approximately 200 m of Palaeogene sediments are partly exposed in the footwall block, forming two upward-coarsening units overlain by basalts (Fig. 2). The lower unit consists of more than 70 m of dark grey mud overlain by 54 m of fine- to medium-grained sand beds alternating with thinner heteroliths topped by more than 2 m of coarse-grained sand. The succession is of earliest Ypresian age based on the presence of the dinocyst *Apectodinium augustum* (Fig. 3) and the nannofossil *Discoaster lenticularis*. The palynological assemblage is dominated by reworked material from Upper Jurassic (e.g. *Gonyaulacysta jurassica*), mid to Upper Cretaceous (e.g. *Hapsocysta benteae*, *Chatangiella* spp. and *Wodehouseia spinata*) and lower Paleocene (e.g. *Alisocysta margarita*). The presence of *A. augustum* may correlate with the *A. augustum* (P6b) Subzone described from the central North Sea (Mudge & Bujak 1996) and correlated

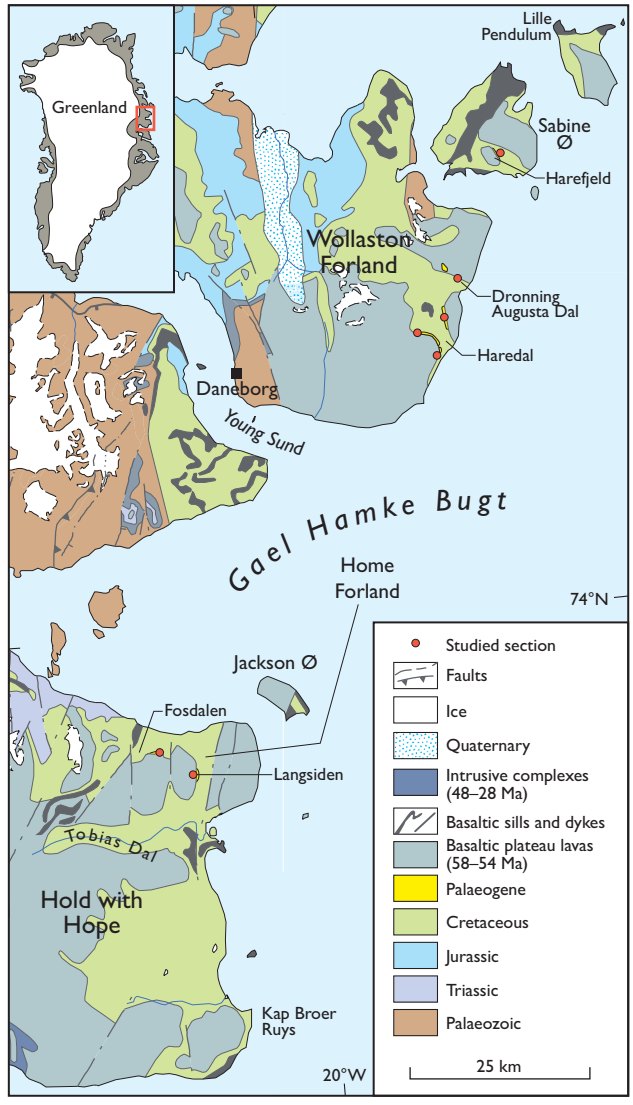

Fig. 1. Geological map of the Wollaston Forland – Hold with Hope study area in North-East Greenland. The location of the studied sections corresponds to the distribution of Palaeogene sediments.

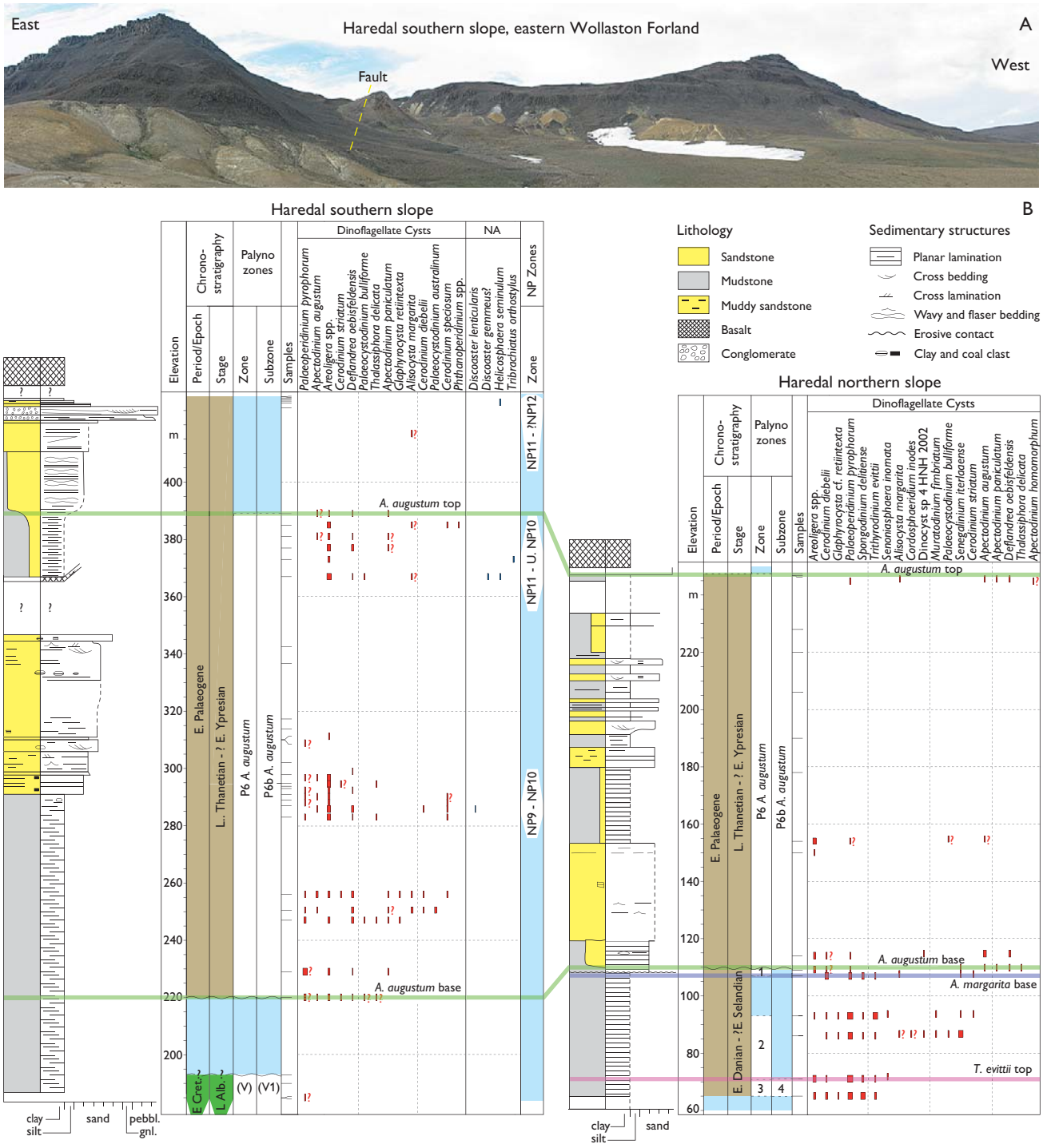

Fig. 2. **A**: Southern slope and fault at Haredal. The highest mountain is *c.* 700 m high. **B**: Sedimentological logs and range charts of selected *in situ* dinocysts and calcareous nannofossils. Numerals in the zones of the northern slope are: **1**: *Alisocysta margarita* Zone, **2**: *Senegalinium iterlaaense* Zone or *Palaeocystodinium bulliforme* Zone, **3**: *Trithyrodinium evittii* Zone and **4**: *Spongodinium delitiense* Subzone (Nøhr-Hansen *et al.* 2002). **NA**: Nannofossils, **NP**: Palaeogene nannoplankton zone. **V**, **V1**: *Subtilisphaera kalaalliti* Zone and *Wigginsiella grandstandica* Subzone (Nøhr-Hansen 1993).

with the Paleocene–Eocene thermal maximum (PETM) which occurred at about 56 Ma and lasted for *c.* 170 kyr (Harding *et al.* 2011). The upper, coarser-grained part only yielded two dinocyst species *Cerodinium* sp. and *Areoligera* sp. and no nannofossils.

The upper unit consists of more than 20 m of dark grey silty and sandy mud overlain by slightly heterolithic, fine-grained sand (22 m), fine-grained sand (10 m), conglomerate and pebbly sandstone (8 m) topped by a few metres of sand, mud and carbonaceous mud or coal. The palynologi-

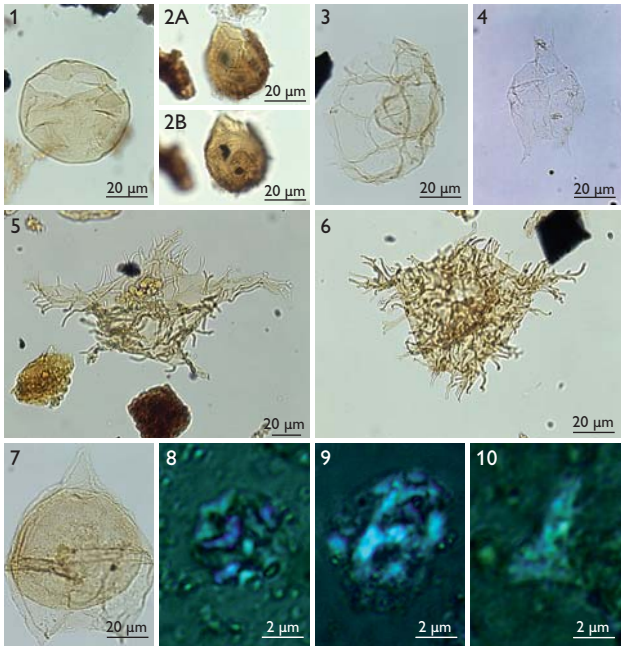

Fig. 3. Images of selected dinocysts (1–7) and nannofossils (8–10). **1**: *Trithyrodinium evittii*. **2A**, **B**: *Alisocysta margarita*. **3**: *Thalassiphora delicata*. **4**: Gen et sp. indet. of Piasecki *et al.* (1992). **5**: *Apectodinium augustum*. **6**: *Apectodinium paniculatum*. **7**: *Deflandrea oebisfeldensis*. **8**: *Discoaster gemmeus*? **9**: *Helicosphaera seminulum*. **10**: *Tribrachiatus orthostylus*.

cal assemblages below the conglomerate are dominated by reworked material of mid – Late Cretaceous age and a few specimens of Paleocene age. The succession is of early Ypresian (Early Eocene) age based on poorly preserved specimens of the dinocysts *Apectodinum augustum*, *Apectodinium paniculatum, Deflandrea oebisfeldensis* and the nannofossil *Tribrachiatus orthostylus* (Fig. 3). Samples above the conglomerate yielded a few reworked Upper Cretaceous and Paleocene dinocysts together with a few indeterminate algae and the nannofossil *Helicosphaera seminulum* (Fig. 3). The latter indicates an age not younger than mid Ypresian for the youngest dated sediments in Haredal; this is compatable with a mid Ypresian radiometric $^{39}Ar/^{40}Ar$ age of 55.02 ± 0.49 Ma for the oldest lava analysed from Wollaston Forland (L.M. Larsen personal communication 2008).

Haredal northern slope. Approximately 180 m of sediments were studied on the northern slope of Haredal (Fig 1). The lower 40 m consist of dark grey mud with a palynological assemblage dominated by reworked material from mid – Upper Cretaceous strata (e.g. *Hapsocysta benteae*, *Chatangiella* spp. and *Aquilapollenites* spp.). The presence of *Trithyrodinium evittii*, *Spongodinium delitiense* and a few specimens of *Senoniasphaera inornata* in the two lowermost samples indicates an Early Paleocene age and may correlate with the lower Danian *Trithyrodinium evittii* Zone (Fig. 2) established from West Greenland (Nøhr-Hansen *et al.* 2002). The presence of common *Senegalinium iterlaaense* and *Palaeocystodinium bulliforme* in the two overlying samples indicates a mid to late Danian age correlating with the *Senegalinium iterlaaense* and *Palaeocystodinium bulliforme* zones (2 and 3 in Fig. 2), whereas the next sample contains a few specimens of the dinocysts *Alisocysta margarita* and *Cerodinium striatum* indicating a late Danian/?early Selandian age correlating with the *Alisocysta margarita* Zone (Nøhr-Hansen *et al.* 2002; 1 in Fig. 2). The upper 130 m of sand and mud contain very few *in situ* palynomorphs, however the presence of *Apectodinium augustum* indicates correlation with the *Apectodinium augustum* (P6b) Subzone, indicating an ?early Selandian – Thanetian hiatus.

Outer Haredal, Dronning Augusta Dal and Sabine Ø. Palaeogene sediments from the southern slope of the easternmost part of Haredal, on the eastern slope of Dronning Augusta Dal, and on the north-eastern slope of Harebjerg, Sabine Ø were also studied and sampled (Fig. 1).The successions all contain the PETM dinocyst marker *Apectodinium augustum*.

North-eastern Hold with Hope

Langsiden. Interbedded in dark grey mud at Langsiden (Fig. 1) occurs an 8 m thick unit with sharp-based, upward-fining successions of conglomerate and pebbly sand, up to a few metres thick containing large reworked mudstone clasts. The palynological assemblage from the underlying mud is dominated by a reworked flora of late Maastrichtian age indicated by the presence of *Triblastula wilsonii* and *Wodehouseia octospina*. The presence of *in situ Trithyrodinium evittii*, *Spongodinium delitiense* and a few specimens of *Senoniasphaera inornata* indicates correlation with the lower Danian *Trithyrodinium evittii* Zone (Nøhr-Hansen *et al.* 2002). The mudstone clasts yielded a mid Cretaceous flora. The palynomorph assemblage of two samples from the overlying mud is likewise dominated by a reworked Upper Cretaceous flora; however, the lower sample also contains a few specimens of the dinocysts *Alisocysta margarita* and *Cerodinium striatum*, indicating correlation with the upper Danian/?lower Selandian *Alisocysta margarita* Zone (Nøhr-Hansen *et al.* 2002). The presence of *Thalassiphora delicata* in the upper sample indicates a latest Danian/early Selandian age (Nøhr-Hansen & Piasecki 2002).

East of Fosdalen. Approximately 6 m of loose, white-grey, fine- to medium-grained sand with scattered small clay clasts

overlain by a less than 2 m thick bed of dark grey mud covered by volcanic rocks overlies mid Cretaceous sandy mudstone east of Fosdalen (Fig. 1). The palynological assemblage of the mud bed is dominated by spores and pollen and some reworked dinocysts of mid to Late Cretaceous age. *In situ* specimens of the dinocyst gen. et sp. indet. of Piasecki *et al.* (1992; Fig. 3) also occur, suggesting fresh to brackish water. The species is common in wells offshore eastern Canada just above the *Apectodinium augustum* P6b Subzone (H. Nøhr-Hansen, unpublished data). The occurrence of the species immediately below the basalts may indicate an earliest Ypresian age.

Discussion

The new biostratigraphic dating shows that the Palaeogene sediments on Wollaston Forland, Hold with Hope and Sabine Ø comprise Paleocene and earliest Eocene strata with a hiatus that probably spans the major part of the Selandian and Thanetian. The age of the underlying Cretaceous deposits east of the fault in Haredal is Early–Middle Campanian, much younger than the Middle Albian previously described from Wollaston Forland (Nøhr-Hansen 1993). The stratigraphic gap between the Cretaceous and Palaeogene sediments thus decreases towards the basin to the east. The large amount of reworked Cretaceous marine palynomorphs including a Late Maastrichtian flora documents uplift of Cretaceous marine sediments and major erosion during the Early Palaeogene. The ages of the youngest Palaeogene sediments and the oldest flood basalts appear to be almost identical; however, the nature of the contact between the sediments and basalts needs to be further investigated to determine whether the contact is angular, as is suggested in places by a relatively steep dip of the sediments.

Discontinuous conglomerate beds with rounded quartzite pebbles and boulders up to 20 cm, as well as cross-bedded sandstones, terminate the upper unit in Haredal and are interpreted as fluvial channel deposits. The absence of basaltic clasts indicates that deposition occurred prior to the volcanic events. The thin overlying succession with a coaly bed is interpreted as an aggrading coastal plain subject to marine inundations. However, the principal part of the Palaeogene sediments accumulated in a marine environment as indicated by marine dinocysts and the presence of scattered marine trace fossils. Thin, fine-grained sandstone beds with flute casts and a massive lower part overlain by beds with parallel lamination and cross-lamination in outer Haredal indicate deposition from turbidite currents. The sharp-based, fining-upward conglomerate beds and pebbly sand from Langsiden embedded in mud are interpreted as channelised gravity flow deposits. The two upward-coarsening units in Haredal suggest that the Palaeogene sediments mainly accumulated during two major depositional phases. Potential by-pass surfaces are identified at the Cretaceous–Palaeogene boundary, at the top of the lower unit, at the base of the fluvial conglomerates and possibly at the sediment–basalt boundary. Coarse-grained sediments may have been transported toward the basin area to the east along these surfaces.

References

Harding, I.C. *et al.* 2011: Sea-level and salinity fluctuations during the Paleocene–Eocene thermal maximum in Arctic Spitsbergen. Earth and Planetary Science Letters **303**, 97–107.

Heilmann-Clausen, C., Abrahamsen, N., Larsen, M., Piasecki, S. & Stemmerik, L. 2008: Age of the youngest Paleogene flood basalts in East Greenland. Newsletters on Stratigraphy **43**, 55–63.

Jolley, D.W. & Whitham, A.G. 2004: A stratigraphical and palaeoenvironmental analysis of the sub-basaltic Palaeogene sediments of East Greenland. Petroleum Geoscience **10**, 53–60.

Larsen, M., Heilmann-Clausen, C., Piasecki, S. & Stemmerik, L. 2005: At the edge of a new ocean: post-volcanic evolution of the Palaeogene Kap Dalton Group, East Greenland. In: Doré, A.G. & Vining, B. (eds): Petroleum geology: North-West Europe and global perspectives. Proceedings of the 6th Petroleum Conference London **2**, 923–932. London: Geological Society.

Mudge, D.C. & Bujak, J.P. 1996: Paleocene biostratigraphy and sequence stratigraphy of the UK central North Sea. Marine and Petroleum Geology **13**, 295–312.

Nøhr-Hansen, H. 1993: Dinoflagellate cyst stratigraphy of the Barremian to Albian, Lower Cretaceous, North-East Greenland. Grønlands Geologiske Undersøgelse Bulletin **166**, 171 pp.

Nøhr-Hansen, H, & Piasecki, S. 2002: Palaeocene age of sub-basaltic sediments at Savoia Halvø, East Greenland. Geology of Greenland Survey Bulletin **191**, 111–116.

Nøhr-Hansen, H., Sheldon, E. & Dam, G. 2002: A new biostratigraphic scheme for the Paleocene onshore West Greenland and its implications for the timing of the pre-volcanic evolution. In: Jolley, D.W. & Bell, B.R. (eds): The North Atlantic Igneous Province: stratigraphy, tectonic, volcanic and magmatic processes. Geological Society, Special Publications (London) **197**, 111–156.

Piasecki, S., Larsen, L.M., Pedersen, A.K. & Pedersen, G.K. 1992: Palynostratigraphy of the Lower Tertiary volcanics and marine clastic sediments in the southern part of the West Greenland Basin: implications for the timing and duration of the volcanism. Rapport Grønlands Geologiske Undersøgelse **154**, 13–31.

Watt, W.S. 1994: Stratigraphy and correlation of the Tertiary plateau basalts in North-East Greenland. Rapport Grønlands Geologiske Undersøgelse **162**, 185–194.

Authors' address

Geological Survey of Denmark and Greenland, Øster Voldgade 10, DK-1350 Copenhagen K, Denmark. E-mail: *hnh@geus.dk*

Analysis of Palaeogene strike-slip tectonics along the southern East Greenland margin (Sødalen area)

Pierpaolo Guarnieri

This paper describes structural data collected during field work in southern East Greenland, a region characterised by a complex tectonic history. Here, 3D photogeology based on aerial and oblique photographs using high-resolution photogrammetry of a 150 km^2 area in Sødalen in southern East Greenland shows ESE–WNW-trending faults cross-cutting Paleocene rift structures and flexure-related normal faults. The kinematic analysis highlights oblique and left-lateral strike-slip movements along faults oriented 120°. Strike-slip and dip-slip kinematic indicators on the walls of the chilled contacts between alkaline E–W-oriented dykes and the volcanic host rocks suggest that the faults and dykes formed at the same time, or maybe the faults were re-activated at a later stage. Palaeostress analysis, performed by inversion of fault-slip data, shows the presence of three different tectonic events. Coupling the 3D photogeological tool with structural analysis at key localities is a fundamental way to understand better the tectonic history of such a large area.

Geological setting

The Blosseville Kyst in southern East Greenland is characterised by a thick sequence of flood basalts and mafic intrusions (Fig. 1). The Skaergaard layered gabbro, the Miki Fjord macrodyke and dolerite sill complexes were formed during the continental break-up and the initial opening of the North–East Atlantic ocean at 55 Ma (Nielsen 1975; Karson & Brooks 1999; Tegner *et al.* 2008).

In the Sødalen region pre-basaltic sediments characterise the Kangerlussuaq Basin and the lower part of the Blosseville Group (Wager 1947; Nielsen *et al.* 1981). Sedimentological studies recognise different facies associations of late Aptian to late Paleocene age (Larsen, M. *et al.* 1999). The youngest part of the basin comprises interfingering Paleocene volcanic units. Based on stratigraphy, geochemistry and petrography, the lavas of the Blosseville Group have been divided into two main series: (1) a 2 km thick sequence of volcanic rocks that formed in a continental rift environment (Nielsen *et al.* 1981), and (2) a 6 km thick sequence of plateau basalts (Larsen, L.M. *et al.* 1989). Furthermore, the Blosseville Kyst is characterised by different generations of dykes and sills, partly related to the break-up and post-break-up history (Wager 1947; Hanghøj *et al.* 2003).

Southern East Greenland is a type example of a volcanic rifted margin (Geoffroy 2005). The geological evolution of the margin is interpreted as the result of a NE–SW-oriented Late Cretaceous rifting phase that led to the onset of oceanic spreading in the Late Paleocene – Early Eocene (*c.* 55 Ma) after a period of syn-rift continental tectonism and volcanism. The general south-east dip of the basalts, the presence of landward-dipping normal faults and the coastal dyke swarm suggest a regional lithosphere flexure (Larsen, H.C. & Saunders 1998).

Sødalen region

Sødalen is an 8 km long, NW–SE-oriented, U-shaped glacial valley extending SE–NW up to the 'Sødalengletscher' (Fig. 2A). The bedrock of the area is characterised by gneiss basement, locally overlain by syn-rift sedimentary and volcanic rocks that form a monocline that dips south-eastwards. The late Paleocene syn-rift sedimentary rocks crop out along the western side of the valley; they are unconformably overlain by sedimentary rocks belonging to the Vandfaldsdalen Forma-

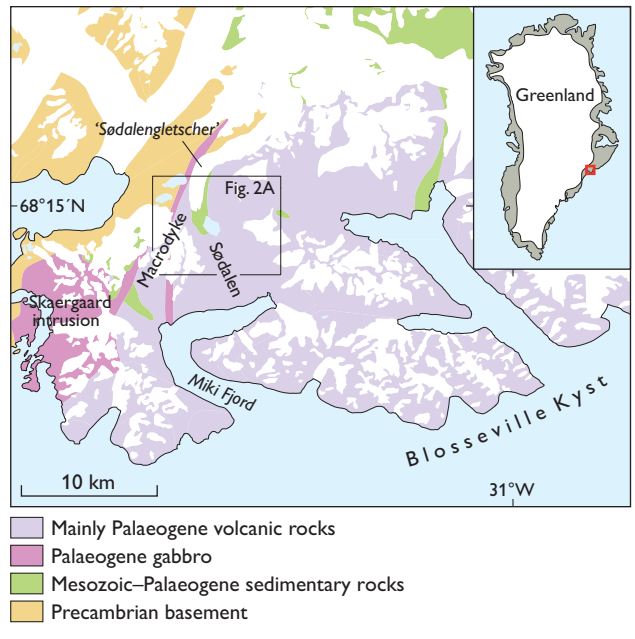

Fig. 1. Simplified geological map of the Sødalen region in southern East Greenland.

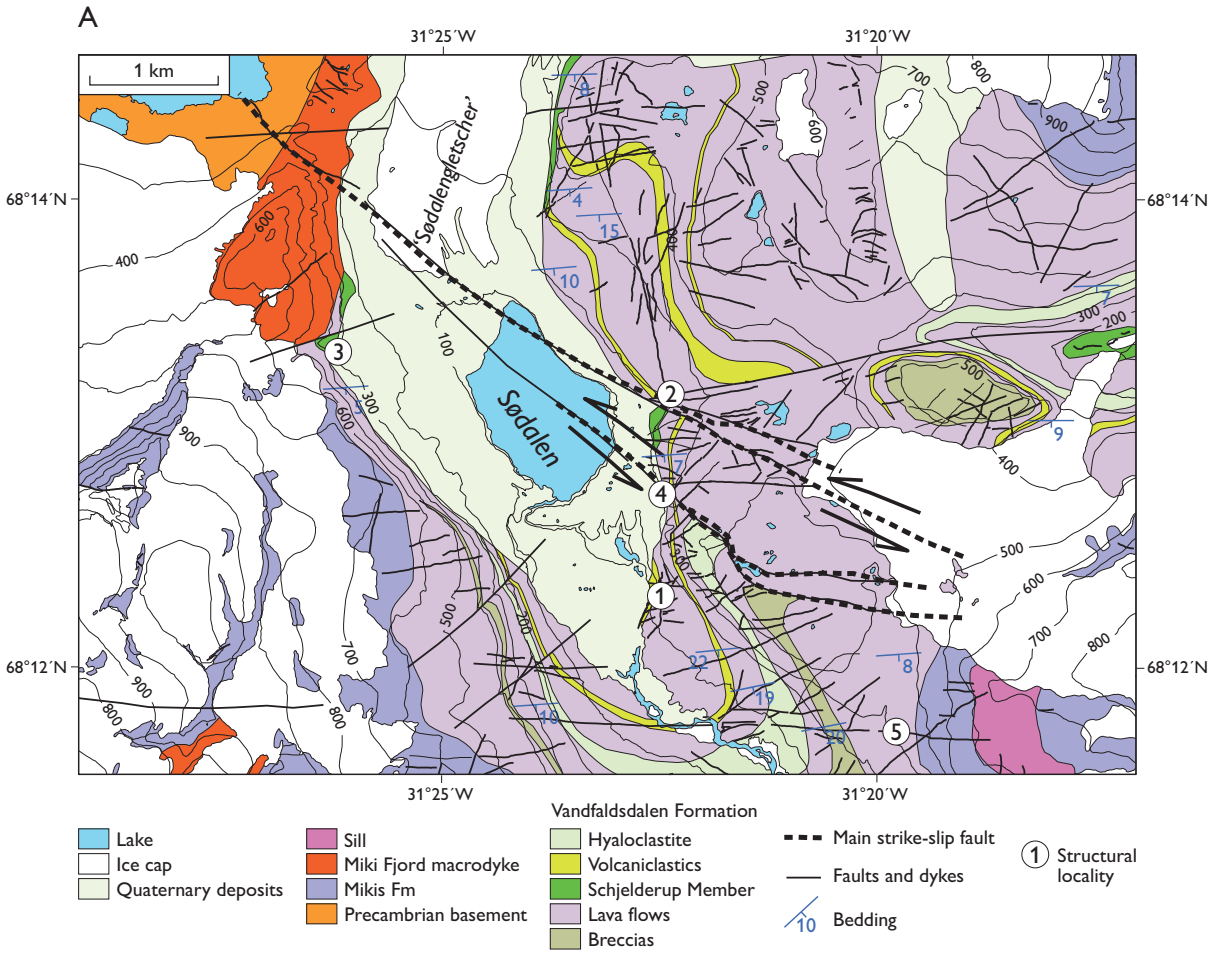
A
31°25´W
31°20´W
68°14´N
68°12´N
1 km
Søndalengletscher
Søndalen
Lake
Ice cap
Quaternary deposits
Sill
Miki Fjord macrodyke
Mikis Fm
Precambrian basement
Vandfaldsdalen Formation
Hyaloclastite
Volcaniclastics
Schjelderup Member
Lava flows
Breccias
Main strike-slip fault
Faults and dykes
Bedding
Structural locality
B
N
n = 111
max = 13%
Faults and dykes
(vertical photographs)
n = 66
max = 18%
Faults
n = 82
max = 17%
Dykes
(oblique photographs)
n = 92
max = 15%
Faults
(outcrop data)
C
normal faults
reverse faults
left-lateral faults
right-lateral faults
D
all faults (n = 92)
phase 1
phase 2
phase 3
S1> S2> S3

tion (Nielsen *et al.* 1981). The unconformity may be related to pre-volcanic uplift, coeval with the NE–SW-oriented rifting, followed by a rapid subsidence that accommodated the volcanism (Larsen, M. *et al.* 1999). The continental breakup is contemporaneous with the emplacement of layered gabbro bodies dated to *c.* 55 Ma, which formed at *c.* 2 km depth in the continental crust. The Skaergaard intrusion and the Miki Fjord macrodyke (Nielsen *et al.* 1981; Tegner *et al.* 2008) are contemporaneous with the up to 6 km thick sequence of plateau basalts (Larsen, L.M. *et al.* 1989).

Structural data

A total of 350 measurements for structural analysis were collected, from two sources: (1) from outcrops (metre scale) at five sites used for kinematic analysis and (2) from 3D photogeology to evaluate strike and dip direction and cross-cutting relationships of faults and dykes using vertical aerial photographs (kilometre scale) and oblique photographs (100 m scale). A new tool for photogeology and mapping is developed and implemented at GEUS to collect geological features as 3D polylines with a descriptive GIS database suitable for 3D modelling (Vosgerau *et al.* 2010).

Dykes – Three main generations of dykes are found in the area. Their relative ages can be established from cross-cutting relationships, which show that the oldest generation (D_1) is mainly NE–SW-oriented, orthogonal to bedding or landward-dipping; the trend is parallel to the Miki Fjord macrodyke. The average trend of the second generation (D_2) is ENE–WSW and these dykes are almost vertical (Fig. 2B). The third generation of dykes found in the area (D_3) trends E–W (Fig. 2B).

Faults – Two main trends of fault traces, up to 2 km long, can be followed on the vertical aerial photographs (Fig. 2B). The oldest generation (F_1) is characterised by ENE–WSW-oriented normal faults. These faults are mainly landward-dipping and are interpreted as flexure-related faults (Wager 1947; Nielsen *et al.* 1981). At site 3 (Fig. 2A), the Miki Fjord macrodyke contact is downfaulted by a landward-dipping (F_1) normal fault with an average vertical offset of 400 m. The youngest (F_2) faults trend ESE–WNW. South-east of localities 2 and 4 (Fig. 2A), the fault traces are curved in planar view typical of strike-slip fault systems.

Kinematic analysis

Field data suitable for fault-slip analysis include measurements of fault plane orientations, slip directions, senses of slip and bedding orientations. The slip direction of faults is determined using slickensides and calcite fibres on the fault plane. Sense of slip indicators include tails and scratches and crescentic marks formed by intersection of the fault plane with secondary fractures such as: R, R', P and T (Petit 1987).

Data collected in the canyon at locality 2 (Fig. 2A) define the kinematics of a 120°-trending fault corresponding to a major left-lateral strike-slip fault that cuts the basalts. The fault zone is *c.* 50 m wide and contains a >50 cm thick calcite vein. Double movement along the fault plane with well-developed dip-slip and strike-slip slickensides and calcite fibres suggests a reactivation of the fault (Fig. 3). The estimated vertical offset, based on the tectonic contact between two stratigraphic markers, is around 250 m, whereas the horizontal offset is estimated to 500 m. This results in a more than 50–150 m wide, 120°-trending, rhomb-shaped fault zone, 1 km long in map view (Fig. 2A, locality 2) and with a negative flower structure in cross-section. To the south-east, the fault trace disappears below an ice cap and to the north-west it is covered by the moraine in front of 'Sødalengletscher', but it is exposed on the western side of Sødalen, where a well-

Fig. 3. Evidence of multiple re-activation of a fault testified by well-developed dip-slip and strike-slip slickensides on a fault plane (locality 2 in Fig. 2A).

Facing page:
Fig. 2. Structural data analysis. **A**: Geological map of the Sødalen area (modified from Nielsen *et al.* 1981). Arrows show the direction of movement along strike-slip faults; contour lines 100 m. **B**: Rose diagrams for orientation of faults and dykes. **C**: Lower hemisphere stereographic projection of faults grouped by kinematics; arrows show the slip vector. **D**: Palaeostress analysis of 92 fault-slip measurements. Black arrows indicate maximum horizontal shortening/extension; $\sigma 1$, $\sigma 2$, $\sigma 3$ = principal axes of stress. Visualisation of the right dihedral method (red = pressure, blue = tension) shows planes that are likely to have been re-activated (the three diagrams to the right).

developed vertical cleavage, locally with strike-slip slickensides, cross-cuts the Miki Fjord macrodyke.

At locality 5 (Fig. 2A), a 4 km long E–W-oriented dyke crosses Sødalen; it is an example of the latest dyke generation (D_3). Slickensides are found on the chilled margins of the dyke, which show that both dip-slip and strike-slip movements have taken place. The trend of the dykes, coupled with evidence of multiple reactivation of the contact, suggests a relationship between strike-slip faults and dykes in which normal faults intruded by dykes were re-activated as left-lateral faults in a NNE–SSW extensional regime associated with the ESE–WNW-trending shear-zone (Fig. 2A).

Palaeostress analysis

Palaeostress analysis of the heterogeneous fault-slip data set was performed using integrated software for structural analysis (Žalohar 2009). More than 90 fault-slip measurements were taken at five sites (localities 2A–C) and used for inversion to obtain palaeostress values. The Gauss Method associated with visualisation of P&T dihedra (Žalohar 2009) distinguishes three superimposed tectonic phases in the area (Fig. 2D): (1) a phase with strike-slip regime and a 20–30°-trending maximum horizontal shortening interpreted as oblique rifting; (2) a phase with a SSE–NNW-trending maximum horizontal extension that corresponds to the coastal flexure and (3) a phase with strike-slip regime and a 95°-trending maximum horizontal shortening that caused the inversion and uplift of the entire area.

Conclusions

The structural data collected in Sødalen indicate the presence of strike-slip faults related to two tectonic events separated in time by the coastal flexure. The youngest structures and dykes (phase 3; Fig. 2D) are associated with a NW–SE left-lateral shear zone that cross-cuts the Paleocene rift and the structures related to the coastal flexure of the continental margin (phase 2). The evidence of dyke intrusions related to N–S extension compatible with the strike-slip tectonic regime of phase 3, suggests a coexistence of the two phenomena as a superficial expression of deep-seated crustal structures. The oldest structures and dykes of phase 1 show a maximum horizontal extension coherent with the trend of the Miki Fjord macrodyke. This strike-slip tectonic regime could be related to an oblique rifting stage in Paleocene time. Finally, the accuracy of the 3D photogeological tool is tested over a range of kilometre to metre scale (Fig. 2B) showing the power of this method developed at the Survey.

Acknowledgement

Chevron is thanked for interest and financial support.

References

Geoffroy, L.: 2005. Volcanic passive margins. Comptes Rendus Geoscience **337**, 1395–1408.

Hanghøj K., Storey M. & Stecher O. 2003: An isotope and trace element study of the East Greenland Tertiary dyke swarm: constraints on temporal and spatial evolution during continental rifting. Journal of Petrology **44**, 2081–2112.

Karson, J.A. & Brooks, C.K. 1999: Structural and magmatic segmentation of the Tertiary East Greenland volcanic rifted margin. In: Ryan, P.D. (ed.): Continental tectonics. Geological Society Special Publications (London) **164**, 313–338.

Larsen, H.C. & Saunders A.D. 1998: Tectonism and volcanism at the southeast Greenland rifted margin: a record of plume impact and later continental rupture. Proceedings of the Ocean Drilling Program, Scientific Results **152**, 503–534.

Larsen, L.M., Watt, W.S. & Watt, M. 1989: Geology and petrology of the Lower Tertiary plateau basalts of the Scoresby Sund region, East Greenland. Bulletin Grønlands Geologiske Undersøgelse **157**, 164 pp.

Larsen, M., Hamberg, L., Olaussen, S., Nørgaard-Pedersen, N. & Stemmerik, L. 1999: Basin evolution in southern East Greenland: an outcrop analog for Cretaceous–Paleogene basins on the North Atlantic volcanic margins. AAPG Bulletin **83**, 1236–1261.

Nielsen,T.F.D. 1975: Possible mechanism of continental breakup in the North Atlantic. Nature **253**, 182–184.

Nielsen, T.F.D., Soper, N.J., Brooks, C.K., Faller, A.M., Higgins, A.C. & Matthews, D.W. 1981: The pre-basaltic sediments and the Lower Basalts at Kangerdlugssuaq, East Greenland: their stratigraphy, lithology, palaeomagnetism and petrology. Meddelelser om Grønland Geoscience **6**, 3–25.

Petit, J.P. 1987: Criteria for the sense of movement on fault surfaces in brittle rocks. Journal of Structural Geology **9**, 597–608.

Tegner, C., Brooks, C.K., Duncan, R.A., Heister, L.E. & Bernstein, S. 2008: ^{40}Ar-^{39}Ar ages of intrusions in East Greenland: rift-to-drift transition over the Iceland hotspot. Lithos **101**, 480–500.

Vosgerau H., Guarnieri P., Weibel R., Larsen M., Dennehy, C., Sørensen, E.V. & Knudsen, C. 2010: Study of a Palaeogene intrabasaltic sedimentary unit in southern East Greenland: from 3-D photogeology to micropetrography. Geological Survey of Denmark and Greenland Bulletin **20**, 75–78.

Wager, L.R. 1947: Geological investigations in East Greenland, Part IV: The stratigraphy and tectonics of Knud Rasmussens Land and the Kangerdlugssuaq region. Meddelelser om Grønland **134**(5), 62 pp.

Žalohar, J. 2009: T-TECTO 3.0 Professional. Integrated software for structural analysis of fault-slip data. Department of Geology, SI-1000 Ljubljana, Slovenia.

Author's address

Geological Survey of Denmark and Greenland, Øster Voldgade 10, DK-1350 Copenhagen K, Denmark. E-mail: *pgua@geus.dk*

Kennedy Channel and its geophysical lineaments: new evidence that the Wegener Fault is a myth

Thorkild M. Rasmussen and Peter R. Dawes

2010, the year under review, marks the centennial of perhaps the most controversial structure in the Arctic: the Wegener Fault, the 1000-km long fracture that is supposed to underlie Nares Strait and define the north-western margin of an independent Greenland plate (Fig. 1). The seaway between Greenland and Ellesmere Island, Canada, was branded a megashear by Frank Taylor who, purely on physiographic expression, postulated massive Tertiary strike-slip (Taylor 1910). This revolutionary idea fittingly found a place in Alfred Wegener's theory of continental drift and thereafter in plate-tectonic theory with Greenland drifting hundreds of kilometres from North America along what Tuzo Wilson subsequently dubbed the 'Wegener Fault' (Wilson 1963).

Today, the concept lives on. In modern palaeogeography, Nares Strait is given a long multiphase dynamic history with collision of Greenland and Canada in the Palaeogene (Fig. 1). A freely drifting Greenland plate unconstrained by ties to North America is now part of conventional wisdom as related in textbooks, review articles and educational material available on the internet. Accordingly, the Wegener Fault is a standard feature in international compilations of world geology (e.g. UNESCO 2010; Fig. 2).

Unfortunately, this 100-year acclamation from Taylor (1910) to UNESCO (2010) is fundamentally flawed: the rocks and their relationships at Nares Strait flatly contradict the existence of the structure.

Scope and aim of this paper

This paper's four-page limit prevents discussion of the pros and cons of the Wegener Fault. For this, we refer to two multi-author volumes (Dawes & Kerr 1982; Tessensohn *et al.* 2006) and to the latest papers (e.g. Hansen *et al.* 2011; Pulvertaft & Dawes 2011). Our aim is twofold: (1) to mark the centennial of a lithospheric structure disputed by the on-site geology, and (2) to add new evidence in the form of magnetic field variations across northern Nares Strait (Kennedy Channel) that define a lineament in harmony with previous interpretations of gravity data.

Regional setting

The most recent overview of Nares Strait geology is by Harrison *et al.* (2006). Bedrock provinces of five ages are common to Greenland and Canada (Fig. 2).

In the south, *Archaean–Paleoproterozoic crystalline shield* is overlain by deposits of two sedimentary basins: the *Mesoproterozoic Thule Basin* that straddles northern Baffin Bay and Smith Sound, and the E–W-trending *Palaeozoic Franklinian Basin* that stretches westwards across northern Canada into Alaska. The Cambrian–Devonian fill of this basin is characterised by north-westerly thickening into a deep-water trough while its shelf overlaps the Thule Basin at Smith Sound. *Neoproterozoic basic dykes* cut the shield

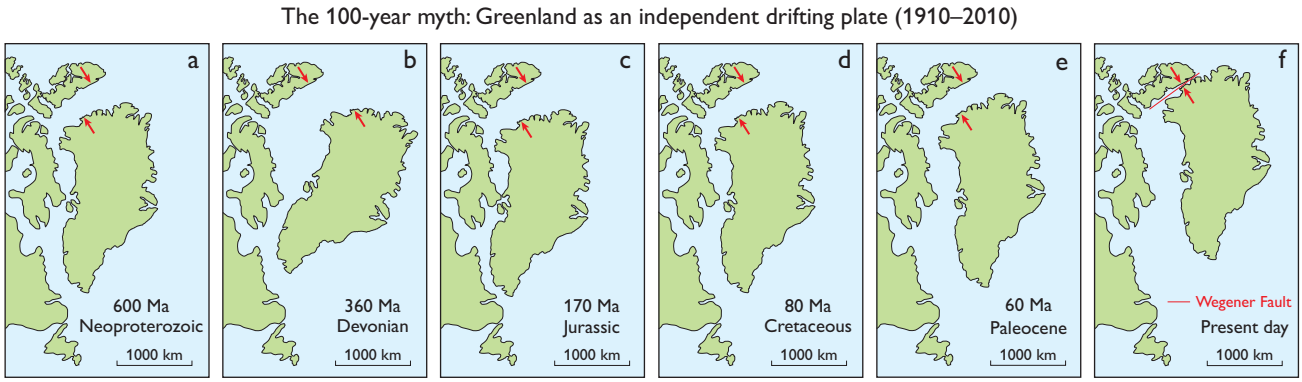

Fig. 1. Modern palaeogeography showing Greenland as a wandering plate detached from Canada throughout Phanerozoic time: **(a)** Cocks & Torsvik (2006), **(b–e)** Torsvik *et al.* in Eide (2002), **(f)** present-day with the Wegener Fault (after Taylor 1910; UNESCO 2010). Red arrows mark the coast locations of magnetic and gravimetric anomalies described in this paper.

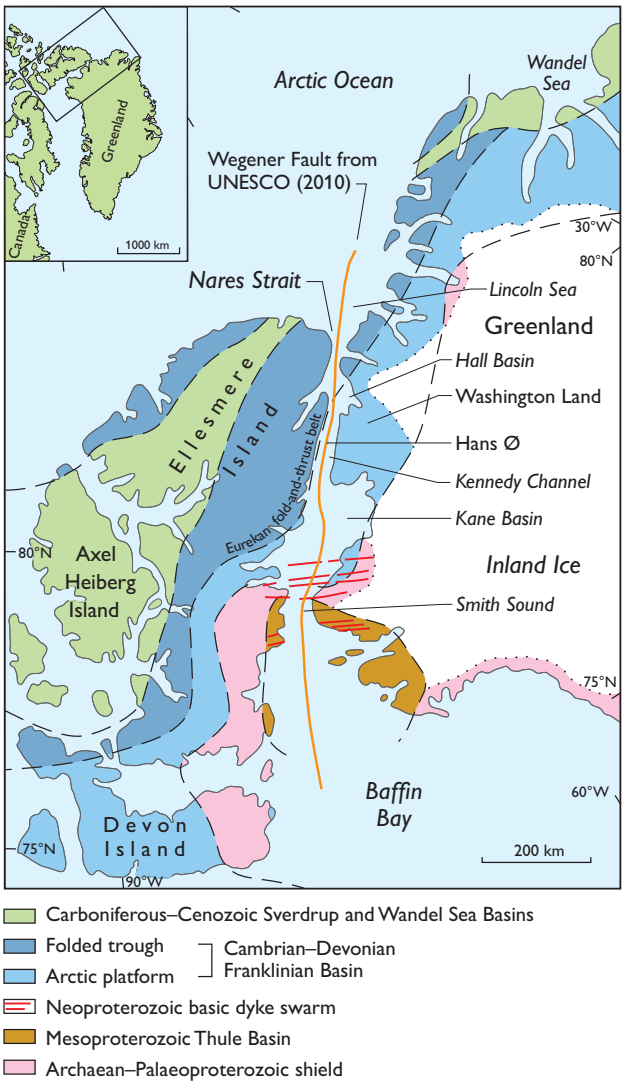

Fig. 2. Simplified geological map of the Nares Strait region. Note that a submarine Wegener Fault, such as UNESCO (2010), must bypass obstacles like those across Smith Sound and Kennedy Channel (see Fig. 4).

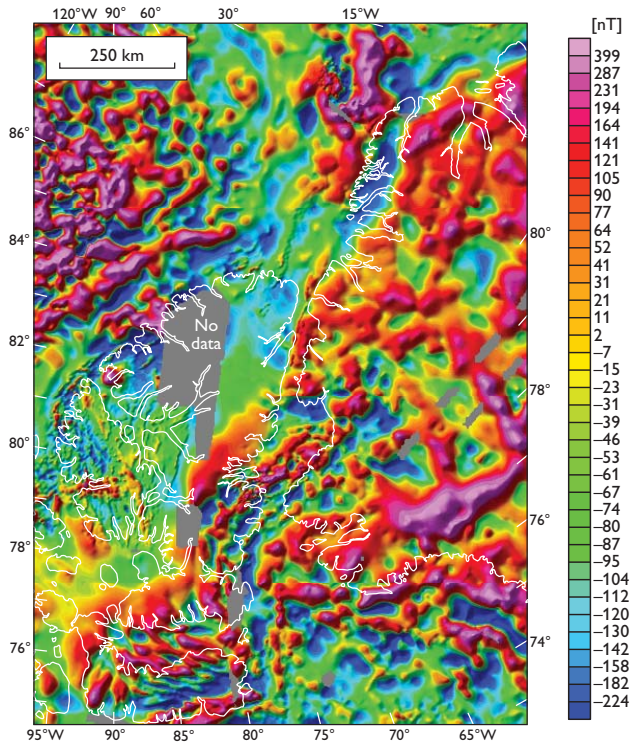

Fig. 3. Regional, total magnetic intensity showing the same region as Figs 2 and 4. Reproduced from Gaina *et al.* (2010).

and its Mesoproterozoic cover but are eroded off at the sub-Cambrian (Franklinian) unconformity. One E–W-trending basic dyke swarm has been mapped across southern Kane Basin and Smith Sound (Fig. 2; Oakey & Damaske 2006). In end-Devonian time, Ellesmerian deformation transformed the Franklinian trough into a fold belt flanked on the south by the homoclinal Arctic platform. The fifth province – *the Carboniferous–Cenozoic Sverdrup Basin* – developed across the eroded, folded Franklinian rocks but overlapped onto the platform. In Palaeogene time, Eurekan tectonism deformed the Sverdrup Basin and underlying Franklinian rocks into a composite structural belt (Innuitian orogen).

Geological relations at Kennedy Channel

Kennedy Channel is sited within the Franklinian Basin with homoclinal strata of the Arctic platform to the south-east and the folded trough to the north-west. Nares Strait trends roughly NNE and thus oblique to the Franklinian Basin (Fig. 2). However, the southern boundary of the folded trough has a sinuous form so that at Kennedy Channel structures roughly follow the coast, while to the south they swing westwards inland and to the north at Hall Basin, eastwards across Greenland. Limits of Ellesmerian and Eurekan diastrophism near the seaway roughly coincide producing a complicated fold-and-thrust belt of Palaeozoic rocks with fault-bound packets of Cretaceous–Palaeogene deposits on Ellesmere Island (Mayr 2008).

Homoclinal Ordovician and Silurian strata dipping 1–3° to the north-west underlie Kennedy Channel and these are involved in the Eurekan fold-and-trust belt (Harrison *et al.* 2007). In Greenland, the Cambro-Silurian sedimentary pile overlying the shield is up to 3500 m thick and all evidence suggests that this geology continues offshore without structural break, with mid-channel Hans Ø and other islands exposing the uppermost reefal part of the Silurian section (Dawes 2004). We stress that the latest maps portray a homoclinal Palaeozoic cover offshore unaffected by faulting (Harrison *et al.* 2007). This contrasts with the thesis of some, for

example, Jackson *et al.* (2006, fig. 15), who draw a sinistral strike-slip fault just west of Hans Ø, a dislocation that "is hypothesized to be the leading edge of the plate boundary between the North American and Greenland plates" (Jackson *et al.* 2006, p. 21). Its location in Kennedy Channel is roughly as shown in UNESCO (2010; Fig. 2).

The magnetic field anomalies

Our analysis is based on recently compiled magnetic and gravimetric data over the Arctic (Gaina *et al.* 2009; Fig. 3). Included are high-resolution data acquired by a Canadian–German project that in 2001 used a helicopter from an icebreaker to survey Kennedy Channel (Damaske & Oakey 2006) and data acquired in 2003 by the Geological Survey of Canada (Oakey & Damaske 2006). The data are low-pass filtered and levelled to provide a regional magnetic field representation of uniform spatial resolution.

Basically, a magnetic anomaly may be viewed as representing the response from a single isolated structure or the superimposed responses from several structures that merge into a well-defined anomaly. Which approach is applicable is mainly controlled by distance between observation level and the structures, and by the cut-off wavelength in any applied low-pass filtering. Our evaluation of continuity of anomalies is based on a tilt angle (Miller & Singh 1994) representation of a 5 km upward-continued version of the magnetic field. The upward continuation puts emphasis on structures having a regional extent but has the drawback of merging responses from adjacent structures. Responses from shallow isolated structures are attenuated. The tilt angle provides structural information that is independent or unbiased with respect to magnetisation intensity of the structures.

Our focus here is on magnetic anomalies that can be linked to the crustal scale of Kennedy Channel close to the above-mentioned hypothetical plate boundary of Jackson *et al.* (2006). Relevant features are marked in Fig. 4: a trend line based on peak values for the tilt angle and a previously published trend line of the Nares Strait Gravity Low (NSGL; Oakey & Stephenson 2008). We note that the magnetic trend line parallels the gravity trend for more than 1000 km along what is essentially the platform margin of the Franklinian Basin. This margin marks a drastic change in basin architecture from shallow shelf to deep trough with downwards flexuring of the substratum or surface of the shield. The magnetic trend line is interrupted at Kennedy Channel but extrapolation along line provides an excellent match between the extended sections. The yellow dashed line crossing Lincoln Sea in Fig. 4 represents merged responses from diverse *unconnected* magnetic structures seen both onshore

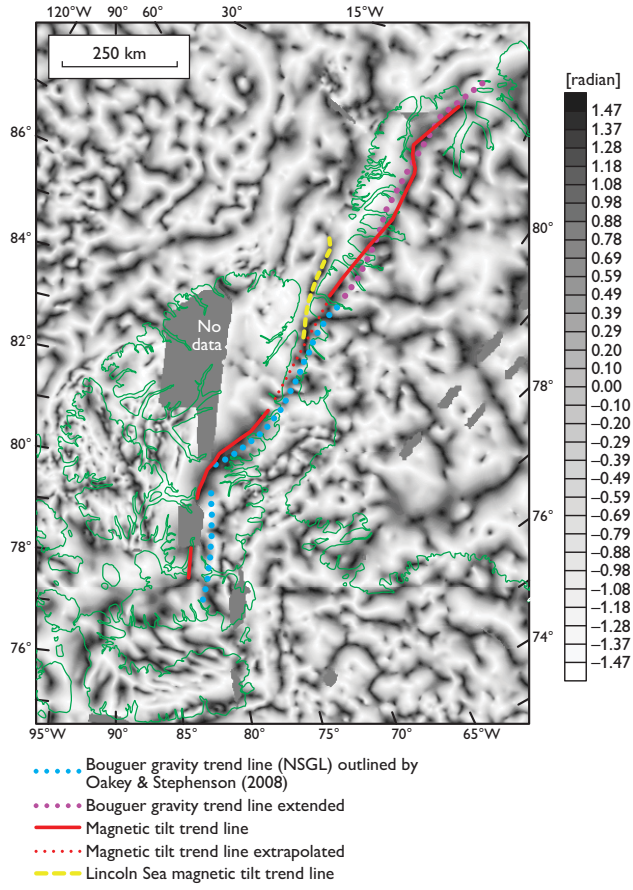

Fig. 4. Tilt-angle map derived from 5 km upward-continued, total magnetic field from data in Gaina *et al.* (2009).

and offshore on the total magnetic field map of Damaske & Oakey (2006, fig. 5) including responses from volcanogenic sandstones. Depiction of these unconnected structures as a single anomaly is simply due to the above-mentioned low-pass filter properties of the applied upwards continuation.

Oakey & Stephenson (2008) regard the NSGL to be an expression of low-density rocks within the Franklinian Basin and they demonstrate that the Palaeogene Eurekan frontal thrust (EFT) obliquely truncates it. Similarly, the magnetic trend is oblique to the EFT. We interpret the magnetic anomalies paralleling the NSGL to reflect the lateral contrast in magnetic properties between Franklinian Basin strata and the crystalline shield. The continuity of both the magnetic and gravimetric trends across Kennedy Channel in the vicinity of Hans Ø implies that this area is not affected by a crustal dislocation.

Farther south at Smith Sound, E–W-trending, offshore, linear, magnetic anomalies represent dykes that correlate with Neoproterozoic basic dykes onshore (Oakey & Damaske 2006). Correlation between several offshore and onshore dykes of Greenland is unequivocal, but on the oppos-

ing coast, although potential correlatives occur, there is a narrow coastal gap between magnetically identified offshore dykes and those onland (Fig. 2; Dawes 2009, fig. 5; Pulvertaft & Dawes 2011, fig. 3). We note here that on our magnetic tilt-angle map there is continuity in terms of texture of the magnetic tilt angle from the offshore area, intersected by dykes, to those onshore (Fig. 4).

Conclusions

A century after Frank Taylor's proposal, some two dozen geological–geophysical markers within Precambrian–Palaeozoic rocks have been identified that demonstrate stratigraphic and structural continuity across Nares Strait (Dawes & Kerr 1982, pp. 369–386; Tessensohn *et al*. 2006, pp. 129–160). The magnetic lineament brought to notice here represents one more marker that militates against plate-boundary strike-slip deformation through the seaway.

We take the persistence and parallelism of the magnetic and gravimetric anomalies to indicate crustal coherence between Greenland and Ellesmere Island and we conclude that these geophysical lineaments are incompatible with the Wegener Fault (Figs 1, 2). They confirm the story revealed by onshore outcrops that the Franklinian Basin is a structural entity stretching from Ellesmere Island to Greenland unhindered by a lithospheric break. We challenge advocates of the 100-year model to explain how a major dislocation can be reconciled with the geophysical lineaments, as well as other obstacles that cross the waterway, for example, the Neoproterozoic dyke swarm (Fig. 2). Furthermore, supporters of conventional reconstructions, such as those in Fig. 1, must explain the plate-tectonic mechanisms by which such features are repositioned into perfect alignment (without offset), how basic dykes can preserve their linearity (without deformation) and how the harmonious within-plate pattern of the regional geology is reassembled (without mismatch).

The Kennedy Channel geophysical lineaments – as well as two dozen previously defined markers – reflect intraplate geology that confirms the mythical character of the Wegener Fault which remains after a hundred years nothing more than a theory.

References

Cocks, L.R.M. & Torsvik, T.H. 2006: European geography in a global context from the Vendian to the end of the Palaeozoic. Geological Society of London Memoir **32**, 83–95.

Damaske, D. & Oakey, G.N. 2006: Volcanogenic sandstones as aeromagnetic markers on Judge Daly Promontory and in Robeson Channel, northern Nares Strait. Polarforschung **74**, 9–19.

Dawes, P.R. 2004: Explanatory notes to the Geological map of Greenland, 1:500 000, Humboldt Gletscher, Sheet 6. Geological Survey of Denmark and Greenland Map Series **1**, 48 pp. + map.

Dawes, P.R. 2009: Precambrian–Palaeozoic geology of Smith Sound, Canada and Greenland: key constraint to palaeogeographic reconstructions of northern Laurentia and the North Atlantic. Terra Nova **21**, 1–13.

Dawes, P.R. & Kerr, J.W. (eds) 1982: Nares Strait and the drift of Greenland: a conflict in plate tectonics. Meddelelser om Grønland Geoscience **8**, 392 pp.

Eide, E.A. (coord.) 2002: BATLAS – Mid Norway plate reconstruction atlas with global and Atlantic perspectives, 75 pp. Trondheim: Geological Survey of Norway.

Gaina, C., Werner, S.C. & the CAMP-GM group 2009: Circum-Arctic Mapping Project – gravity and magnetic maps. Geological Survey of Norway, Report **2009.010**, 21 pp.

Gaina, C., Werner, S.C., Mioara, M. & the CAMP-GM group 2010: Magnetic and gravimetric anomaly maps of the Arctic, 1: 5 000 000. UNESCO and Geological Survey of Norway.

Hansen, K., Dawes, P.R., Frisch, T. & Jensen, P.K. 2011: A fission track transect across Nares Strait (Canada–Greenland): further evidence that the Wegener Fault is a myth. Canadian Journal of Earth Sciences **48**, 819–840.

Harrison, J.C., Brent, T.A. & Oakey, G.N. 2006: Bedrock geology of the Nares Strait region of Arctic Canada and Greenland, with explanatory text and GIS content. Geological Survey of Canada Open File **5278**, 60 pp. + map.

Harrison, J.C., Dewing, K. & Mayr, U. 2007: Geology of Hans Island and adjacent parts of Kennedy Channel, northwest Greenland (Kalaallit Nunaat) and northern Nunavut (Canada). Geological Survey of Canada Open File **5321**, 33 pp. + map.

Jackson, H.R., Hannon, T., Neben, S., Piepjohn, K. & Brent, T.[A.] 2006: Seismic reflection profiles from Kane to Hall Basin, Nares Strait: evidence for faulting. Polarforschung **74**, 21–39.

Mayr, U. (ed.) 2008: Geology of northeast Ellesmere Island adjacent to Kane Basin and Kennedy Channel, Nunavut. Geological Survey of Canada Bulletin **592**, 404 pp.

Miller, H.G. & Singh, V. 1994: Potential field tilt – a new concept for location of potential field sources. Journal of Applied Geophysics **32**, 213–217.

Oakey, G.N. & Damaske, D. 2006: Continuity of basement structures and dyke swarms in the Kane Basin region of central Nares Strait constrained by aeromagnetic data. Polarforschung **74**, 51–62.

Oakey, G.N. & Stephenson, R. 2008: Crustal structure of the Innuitian region of Arctic Canada and Greenland from gravity modelling: implications for the Palaeogene Eurekan orogen. Geophysical Journal International **173**, 1039–1063.

Pulvertaft, T.C.R. & Dawes, P.R. 2011: North Atlantic spreading axes terminate in the continental cul-de-sacs of Baffin Bay and the Laptev Sea. Canadian Journal of Earth Sciences **48**, 593–601.

Taylor, F.B. 1910: Bearing on Tertiary mountain belts and on the origin of the Earth's plan. Bulletin of the Geological Society of America **21**, 179–226.

Tessensohn, F., Jackson, H.R. & Reid, I.D. (eds) 2006: Nares Strait and Wegener transform fault. Polarforschung **74**, 198 pp.

UNESCO 2010: Geological map of the World, scale 1:25 000 000, 3rd edition.

Wilson, J.T. 1963: Hypothesis of Earth's behaviour. Nature **198**, 925–929.

Authors' address

Geological Survey of Denmark and Greenland, Øster Voldgade 10, DK-1350 Copenhagen K, Denmark. E-mail: *tmr@geus.dk and prd@geus.dk*

Programme for Monitoring of the Greenland Ice Sheet (PROMICE): first temperature and ablation records

Dirk van As, Robert S. Fausto and the PROMICE project team*

The Greenland ice sheet is reacting to climate change. Yet, mass-budget estimates differ considerably, partly due to climatic variability and partly to uncertainties in the techniques of assessing mass change (IPCC 2007). Nevertheless, all recent estimates agree that the ice sheet is losing mass (e.g. 286 Gt/yr; Velicogna 2009) at an accelerating rate (Rignot *et al.* 2011). On top of this, the area with a negative mass budget is expanding rapidly (Khan *et al.* 2010). The mass loss is attributed equally to increases in both iceberg production and melting of the ice sheet (Van den Broeke *et al.* 2009).

The increasing mass loss in recent years has caught public attention and given rise to concern worldwide due to its potential impact on sea level. In the light of this, the Programme for Monitoring of the Greenland Ice Sheet (PROMICE) was initiated in 2007 (Ahlstrøm & PROMICE project team 2008), lead by the Geological Survey of Denmark and Greenland (GEUS). PROMICE undertakes surface mass-budget measurements using automatic weather stations, quantifies the mass loss by iceberg calving using remotely sensed data from satellites and airborne surveys and tracks changes in the extent of glaciers. In this paper, we focus on weather station measurements, which are crucial in calculating the energy exchange between the atmosphere and the ice sheet, and in validating model calculations of the surface mass budget. In particular, we present the observed temperatures and investigate how their high 2010 values affected ablation in southern Greenland.

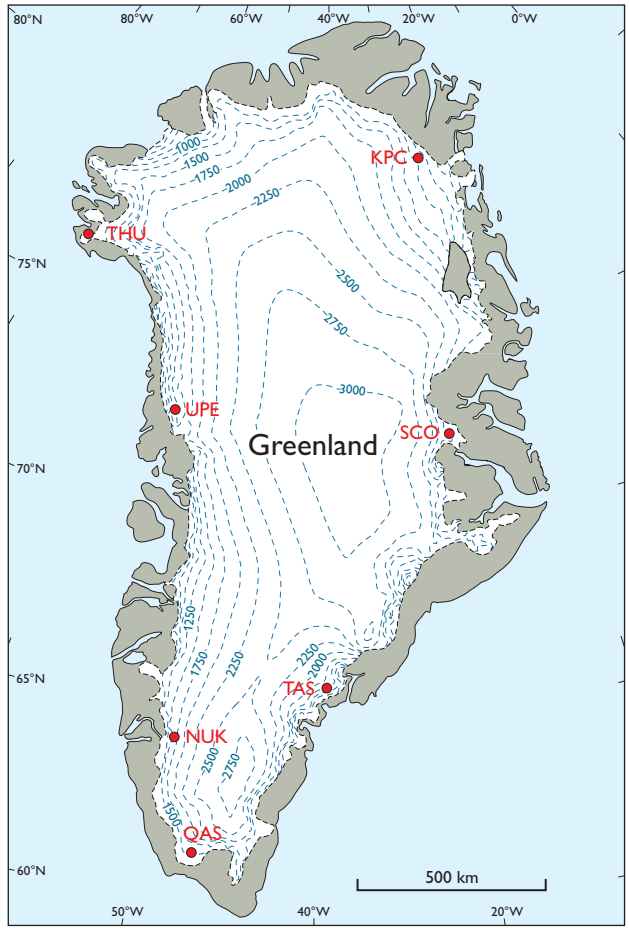

Fig. 1. Map of Greenland with the locations of the PROMICE automatic weather stations in 2010. Each dot represents a pair of stations. Station abbreviations as in Table 1. Dotted lines: elevation contours.

PROMICE automatic weather stations

The PROMICE weather station network started with five stations in 2007 and by summer 2010 consisted of seven station pairs (Fig. 1; Table 1). Typically, one of the stations in a pair is located in the upper ablation zone near the equilibrium line and the other at a lower elevation well into the ablation zone. The weather stations are equipped with the instruments shown in Fig. 2 which undergo continuous 10-minute measurement cycles. In summer, data are transmitted once per hour; in winter, transmissions are daily to reduce power consumption when solar power is limited.

PROMICE weather station data can be downloaded at no charge at www.promice.dk. In spite of the stations being placed in inhospitable places where strong winds, severe cold, icing as well as melting and highly uneven terrain are common, there was a success rate of 77–86% for the period up to February 2011. Not all data have been transmitted with success, so the success rate may reach 86% when also locally

*Andreas P. Ahlstrøm, Signe B. Andersen, Morten L. Andersen, Michele Citterio, Karen Edelvang, Peter Gravesen, Horst Machguth, Faezeh M. Nick, Søren Nielsen and Anker Weidick.

Table 1. PROMICE automatic weather station metadata (status 2010)

Station name	Latitude (°N)	Longitude (°W)	Elevation (m)	Start date
KPC_L*	79°55′	24°05′	380	17 July 2008
KPC_U	79°50′	25°10′	870	17 July 2008
SCO_L	72°14′	26°49′	470	21 July 2008
SCO_U	72°24′	27°15′	1000	21 July 2008
TAS_L	65°38′	38°54′	270	23 August 2007
TAS_U	65°42′	38°52′	580	15 August 2007
QAS_L	61°02′	46°51′	310	24 August 2007
QAS_U	61°11′	46°49′	890	7 August 2008
NUK_L	64°29′	49°32′	560	20 August 2007
NUK_U	64°30′	49°16′	1140	20 August 2007
UPE_L	72°54′	54°18′	230	17 August 2009
UPE_U	72°53′	53°32′	980	17 August 2009
THU_L	76°24′	68°16′	570	9 August 2010
THU_U	76°25′	68°09′	770	9 August 2010

*L: Lower station, U: upper station.

stored data have been collected. Strikingly, only few values are missing due to harsh climatic conditions such as wind damage. A prime cause of data gaps is data logger malfunction.

Temperatures over the ice sheet

In Fig. 3 we show the monthly mean near-surface air temperatures at those PROMICE stations for which data cover at least half a month. A clear annual cycle is present in the temperature records of all weather stations, and we see that the amplitude of the annual signal increases with latitude. This is explained by the fact that during summer the solar radiation increases with latitude due to the midnight sun, while the opposite is true during winter when central and northern Greenland experiences polar night. During the 'warm' season the presence of a melting ice surface at the stations does not allow near-surface temperatures to increase well above freezing. In southern Greenland, where day-time, free atmospheric temperatures can exceed 20°C during summer, the melting ice surface dampens the amplitude of the temperature cycle by about 10°C. The smallest amplitude and highest winter temperatures occur at the Tasiilaq stations (TAS_L and TAS_U), and the lower Qassimiut station (QAS_L; Fig. 1; Table 1). These stations are located at lower elevations close to the ice-sheet margin, and are exposed to the relatively warm wintertime atmospheric conditions of the Atlantic Ocean. The largest amplitude in the temperature cycle is seen at the upper Kronprins Christian Land station (KPC_U), where melting occurs in summer, but where mean temperatures drop below –30°C in winter. The lowest daily mean temperature recorded at this station was –40.6°C on 9 January 2010. Mid summer (July) monthly mean temperatures are above freezing at all stations, but never exceed 6°C.

Temperatures in Greenland have been rising since the 1980s, prior to which there was almost half a century of cooling (Box 2002). Still, 2010 was exceptionally warm over large parts of Greenland. It was the warmest year in Greenland on record at most of the land-based weather stations operated by the Danish Meteorological Institute. The only exception was seen in the north-east. Individual months and seasons showed record setting temperatures, with the longest instrument records in Greenland dating back to the 1870s (John Cappelen, personal communication, 2011). The PROMICE weather station network was not fully established until 2010 and thus comparison with previous years is limited. However, for our westerly and southerly stations we can confirm that the monthly mean temperatures in 2010 were mostly higher than those of previous years (Fig. 3).

Record-setting 2010 in southern Greenland

The longest running GEUS measurement series on ice started in 2001 on the Qassimiut lobe in southern Greenland. This locality was incorporated in the PROMICE network by establishing station QAS_L in 2007. The nearly 10 years

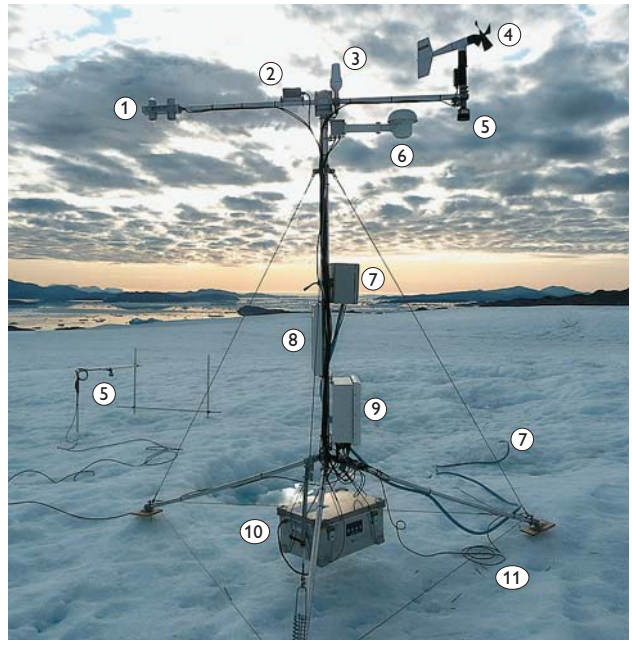

Fig. 2. PROMICE automatic weather station UPE_L photographed on 17 August 2009. **1**: radiometer. **2**: inclinometer. **3**: satellite antenna. **4**: anemometer. **5**: sonic height rangers. **6**: thermometer and hygrometer. **7**: pressure transducer. **8**: solar panel. **9**: data logger, barometer and GPS. **10**: battery box with 4 × 28 Ah batteries. **11**: 8-level thermistor string.

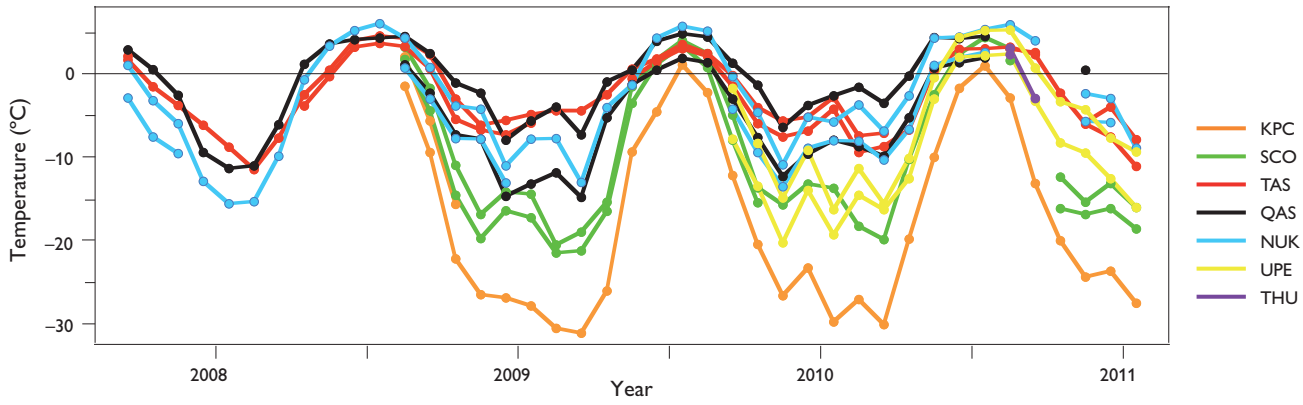

Fig. 3. Monthly mean temperatures measured at seven weather station pairs. The upper stations of each pair record the lower temperatures, and vice versa. For locations see Fig. 1.

of data from this locality provide an opportunity to put 2010 into a longer temporal perspective and assess how extraordinary 2010 was at this place. Figure 4A shows all available monthly mean temperatures measured at the QAS_L site. The Qaqortoq temperature record from 56 km southeast of QAS_L are included to help interpret the months in 2010 with data gaps due to logger failure (values are reduced by 3°C to facilitate comparison).

The climate at QAS_L is mild in terms of temperature compared to most other regions on the ice sheet (Fig. 3). The lowest winter values do not drop much below −10°C; typical monthly mean winter temperatures during the past decade were in the −10 to −3°C range. Summer (June–August) temperatures are predictable in that their mean value is within 2°C of all other years. The presence of ice limits the near-surface air temperature to about 5°C even during warm summers such as 2003. We therefore assume that the August 2010 temperature did not greatly exceed this value, even though the Qaqortoq value for this month is the highest ever recorded value (10.6°C). In our records (supported by Qaqortoq data), we see that 2010 had the highest on-ice mean temperatures for all months of the year compared to earlier values, with the exception of April (warmer in 2008), July (warmer in 2003, 2005 and 2009) and October (warmer in 2003). This is in full agreement with the values from Qaqortoq, which show above-decade average temperatures for all months except July. The most extreme values (in order of excess) were November, May, August, December and September, which exceeded the two standard deviation ranges for the 2000–2009 averages. Qaqortoq was on average an astonishing 2.0°C warmer in 2010 than in the second (2003) and third (2005) warmest years on record, 4.5 standard deviations above the 2000–2009 average (which is the warmest decade on record).

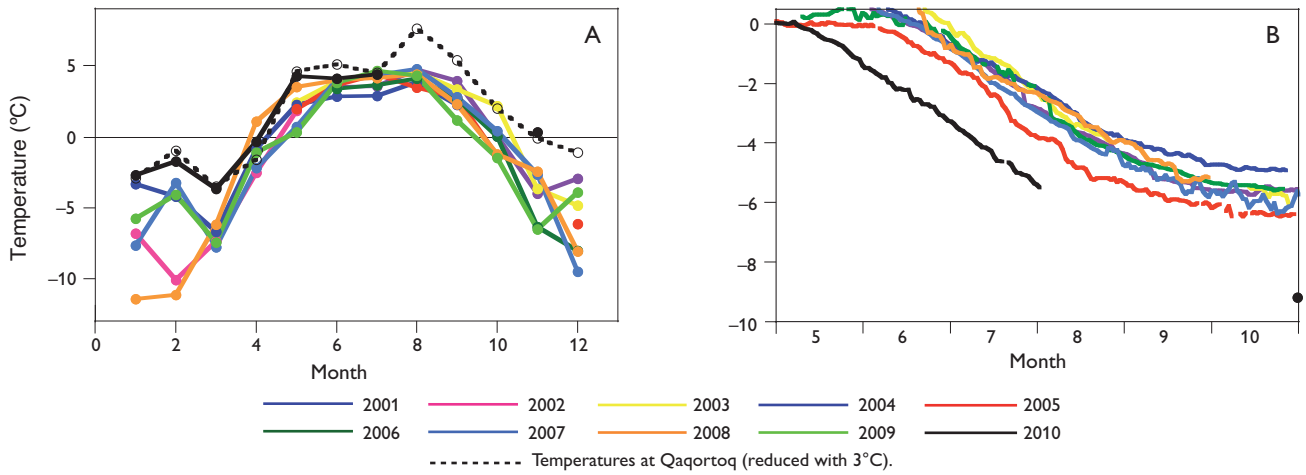

Fig. 4. **A:** Monthly mean temperatures and **B**: cumulative net ablation at lower Qassimiut station (QAS_L). The ablation measurements are by pressure transducer; supported and validated by sonic ranger where available. The black dot in **B** shows the total ablation by November 2010. Variability in the pressure transducer output is caused by atmospheric pressure.

Even though QAS_L summer temperatures are dampened by the ice surface and on average do not exceed 5°C, this does not imply that melt rates are similar between years. The energy consumed by the ice surface to cool the near-surface atmosphere (sensible heat flux) will be larger during warmer periods, as will the down-welling longwave radiation, thus enhancing melting. However, there is only a relatively small amount of year-to-year variability in melt rates (given the slopes of the ablation curves from the pressure transducer in Fig. 4B) since solar radiation is the main contributor to melt energy (Van As *et al.* 2009). More important to net ablation is the length of the ice-melt season, which largely depends on the duration of the period with positive temperatures and the amount of snow accumulation in the preceding winter. For instance, even though the melt rate in 2003 was above average due to high temperatures, the total ablation was near average because of the time it took to melt the relatively large amount of snow that had accumulated during the preceding winter. The year 2005 had lower summer temperatures, but a larger ablation total as there was very little snow accumulation the previous winter. The net ice ablation observations for the period 2001–2009 range from 5 m to 6.5 m of ice per year, which are the largest ablation totals measured anywhere on the Greenland ice sheet. For 2010 the extreme months of August and September are lacking from our data series, but spring values show that hardly any snow had accumulated in winter, and that the melt of the bare ice surface began in early May, 1–2 months earlier than in previous years. Melt rates were high in late summer and autumn, setting a new ablation record with a measured end-of-year total of about 9 m of ice (Fig. 4B, black dot). Similar record setting ablation is expected to have taken place in all of southern Greenland, as well as along the western margin of the Greenland ice sheet (Tedesco *et al.* 2011).

Conclusions

PROMICE has been successful in acquiring near-surface meteorological data over the Greenland ice sheet since 2007. Temperature measurements display distinct differences between the locations due to solar influences, elevation and regional climate. The PROMICE temperature record confirms that 2010 was an exceptionally warm year in the southern and western regions of Greenland, although a longer time series is needed to quantify the 2010 anomaly over the ice sheet. A record-setting net ablation of 9 m of ice in Greenland was measured on the southernmost part of the ice sheet in 2010. The enhanced down-welling longwave radiation and sensible heat flux due to the high atmospheric temperatures are not the main reason for the large ablation; low snow accumulation in the previous winter and a long melt season are.

Acknowledgements

The Programme for Monitoring of the Greenland Ice Sheet (PROMICE) is funded by the Danish Ministry of Climate and Energy, and is conducted in collaboration with the National Space Institute (DTU Space) and Asiaq (Greenland Survey). The Greenland Climate Research Centre (GCRC) co-finances the NUK stations through the FreshLink and ImGlaCo projects.

References

Ahlstrøm, A.P. & PROMICE project team 2008: A new programme for monitoring the mass loss of the Greenland ice sheet. Geological Survey of Denmark and Greenland Bulletin **15**, 61–64.

Box, J.E. 2002: Survey of Greenland instrumental temperature records: 1873–2001. International Journal of Climatology **22**, 1829–1847.

IPCC 2007: Intergovernmental Panel on Climate Change (IPCC) Fourth Assessment Report (AR4), Climate Change 2007. 4 volumes. Cambridge: Cambridge University Press.

Khan, S.A., Wahr, J., Bevis, M., Velicogna, I. & Kendrick, E. 2010: Spread of ice mass loss into northwest Greenland observed by GRACE and GPS. Geophysical Research Letters **37**, L06501. Doi: 10.1029/2010GL042460.

Rignot, E., Velicogna, I., Van den Broeke, M.R., Monaghan, A. & Lenaerts, J. 2011: Acceleration of the contribution of the Greenland and Antarctic ice sheets to sea level rise. Geophysical Research Letters **38**, L05503. Doi:10.1029/2011GL046583.

Tedesco, M., Fettweis, X., Van den Broeke, M.R., Van de Wal, R.S.W., Smeets, C.J.P.P., Van de Berg, W.J., Serreze, M.C. & Box, J.E. 2011: The role of albedo and accumulation in the 2010 melting record in Greenland. Environmental Research Letters **6**, 014005. Doi: 10.1088/1748-9326/6/1/014005.

Van As, D., Bøggild, C.E., Nielsen, S., Ahlstrøm, A.P., Fausto, R.S., Podlech, S. & Andersen, M.L. 2009: Climatology and ablation at the South Greenland ice sheet margin from automatic weather station observations. The Cryosphere Discussions **3**, 117–158.

Van den Broeke, M., Bamber, J., Ettema, J., Rignot, E., Schrama, E., Van de Berg, W.J., Van Meijgaard, E., Velicogna, I. & Wouters, B. 2009: Partitioning recent Greenland mass loss. Science **326**, 984–986.

Velicogna, I. 2009: Increasing rates of ice mass loss from the Greenland and Antarctic ice sheets revealed by GRACE. Geophysical Research Letters **36**, L19503. Doi: 10.1029/2009GL040222.

Authors' address

Geological Survey of Denmark and Greenland, Øster Voldgade 10, DK-1350 Copenhagen K, Denmark. E-mail: *dva@geus.dk*

DODEX – Geoscience Documents and Data for Exploration in Greenland

Peter Riisager, Mikael Pedersen, Mette Svane Jørgensen, Frands Schjøth and Leif Thorning

In the following we describe the project Geoscience Documents and Data for Exploration in Greenland, in short DODEX. A central part of DODEX is an interactive web application (http://www.geus.dk/dodex/) that provides easy access to all non-confidential company geoscience reports received by the authorities in Greenland and Denmark in accordance with the Mineral Resources Act of Greenland (1 January 2010) and associated regulations. From the web application it is possible to search in the DODEX report database using alphanumeric and geographic search criteria and to access report metadata. It is also possible to download the actual report as a PDF file. In addition to the open DODEX web application, the project also includes the development of a closed web application where authorised users can access confidential reports. The DODEX project was carried out at the Geological Survey of Denmark and Greenland (GEUS) in cooperation with the Bureau of Minerals and Petroleum (BMP) under the Government of Greenland as part of the promotion of the mineral resources of Greenland.

Data handling and database

The Mineral Resources Act of Greenland stipulates that companies holding licences for exploration or exploitation must submit reports on and data from their activities in Greenland to BMP. These reports are forwarded to GEUS where they are scanned and entered into the database. Most new reports are confidential for a specific period of time. In

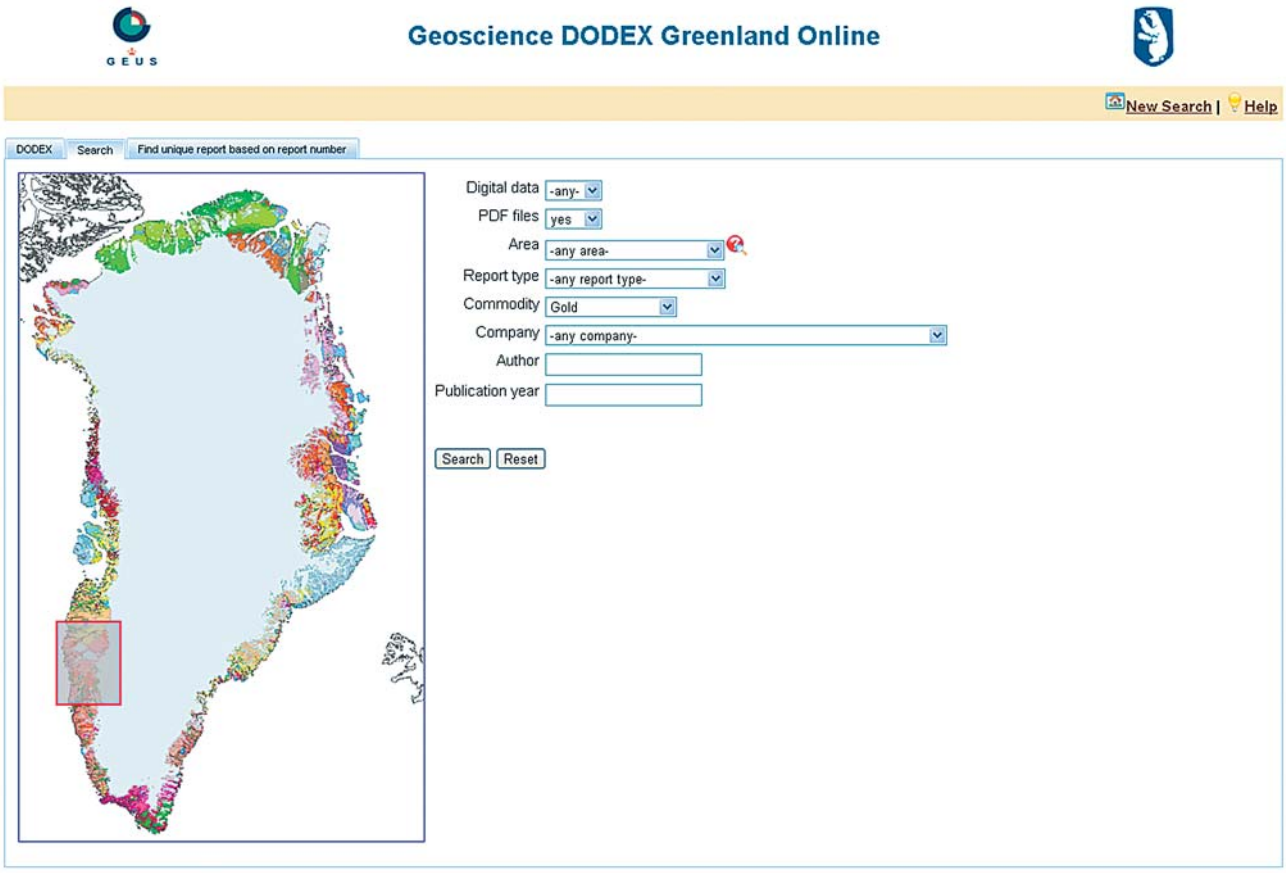

Fig. 1. The DODEX web application allows users to search the database using alphanumeric or geographical search criteria. Here the user searches for reports on gold in PDF files. The research result will include all reports with geo-references located in the marked red rectangle.

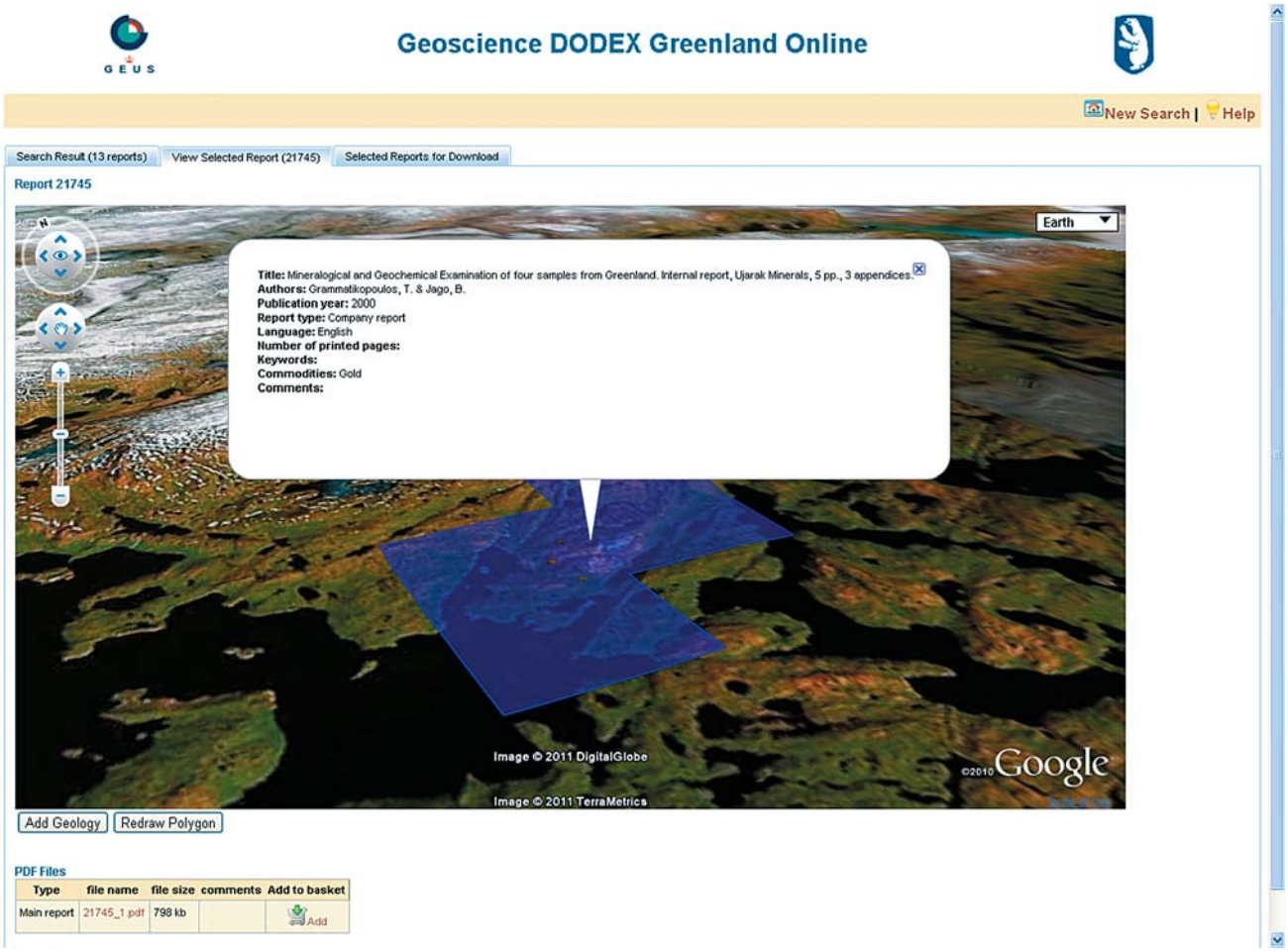

Fig. 2. The report geo-reference is marked by a blue polygon, while other metadata are listed in the information window.

the case of exploration licences, after a five-year confidentiality period, or two years after the relinquishment of an exploration licence, the geoscience reports and submitted data will be considered to be in the public domain and become available to all.

Besides entering new reports as they are received at GEUS, we also continuously update the database by scanning and geo-referencing existing reports. The geo-references are polygons that represent areas that are treated in the report. Many of the reports were loaded into the database from older databases, and for most of those the area of interest was automatically defined as the area covered by the licence. Many of these geo-references have later been edited to represent more accurately the locality or localities treated in the report, and this process of narrowing the areas of interest will continue. New reports entered into the database will be geo-referenced at the time of registration as accurately as practically possible.

The reports and report metadata are stored in a relational database housed and maintained by GEUS (Tulstrup 2004). The DODEX database model is designed to hold quite a long list of report metadata including obvious parameters such as authors, company, year of publication and commodities described, but also more complex parameters such as geographic reference, confidentiality, and status with respect to quality assurance. At the time of writing the DODEX database contains 2151 reports, of which 1197 are non-confidential. Of the 1197 released reports 784 have an associated PDF file, and 731 are geo-referenced.

User and quality control

User control is implemented by database roles that define five different user types, listed with increasing privileges:

1. The public users are only allowed to access non-confidential reports that have been quality assured, and are released. Public users correspond to users of the publicly available DODEX search web application (Figs 1, 2) described in the next section.
2. The trusted users are given a username and password that allow them to log into a restricted web applica-

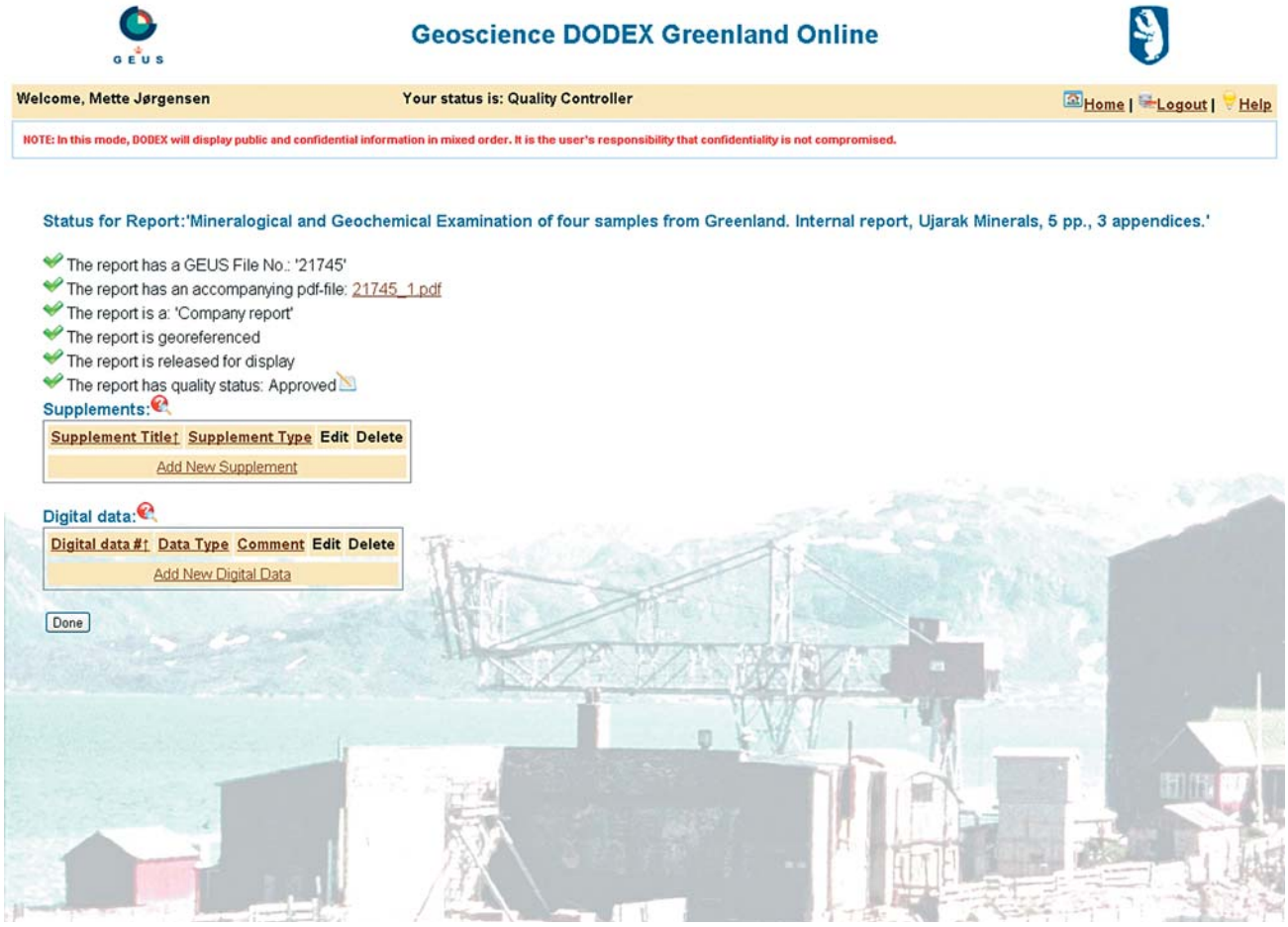

Fig. 3. The DODEX administration is handled in a separate web application, where authorised users, depending on their type can view, update, edit, and delete reports. A screen view of the application for a quality controller to check the status of a report is shown.

tion (Fig. 3), where they can view confidential and unreleased reports. Trusted users can only view reports and are not allowed to change the database content.

3. The compilers are also allowed to login to a restricted web application where they can upload and edit reports, however, they are not allowed to change the confidentiality status of reports or release the report for public users.
4. The quality controllers have all the compiler's privileges and in addition the quality controllers can change report confidentiality status and release reports for public users. The main function of the quality controllers is to review the database work performed by the compilers and to control the quality before reports are released.
5. The administrators develop the system, and can create, read, update and delete all DODEX reports and metadata. Overall, the setup for DODEX user management and quality assurance has proved successful, and hence has been copied in several later GEUS database projects.

The DODEX public search web application

The public search web application that is available at http://www.geus.dk/dodex/ constitutes the central part of the DODEX project. It is designed to be interactive and easy to use, providing easy access for interested parties around the world to all non-confidential company geoscience reports on Greenland. From the web application it is possible via alphanumeric and geographic search criteria to search the DODEX report database (Fig. 1). Greenland covers a large geographical area, and an important aspect of the project is that reports are geo-referenced to allow searches in the database for reports relevant for a particular part of the island. The geo-reference polygons of the reports are used for searches on a map of Greenland (Fig. 1). To minimise transmission time, a relatively simple geological map is used on screen in UTM zone 24, with search polygons calculated in decimal degrees, which are the units for the coordinates of report polygons. The search will extract from the database all reports with

an area of interest overlapping the search polygon. Alphanumeric search criteria can be combined with a geographic search (Fig. 1). For the individual reports, public users can obtain a long list of report metadata and download the actual report as a PDF file. It is also possible to add reports to a shopping cart and subsequently get several reports sent by e-mail.

Each search is logged and stored in the database. Since its start in 2008, we have registered a total of 3271 queries from 212 individual users. Most often queries are based on geographic location, with North Greenland and South-West Greenland being the two most popular regions. The two hitherto most sought after commodities are gold and niobium.

DODEX administration

The DODEX administration web application is developed for three user types: trusted users, compilers and quality controllers. The administration web application demands login username and password. Security is implemented in the web application. It also uses a dedicated one-to-one connection to the database, adding a second layer of security provided by the underlying Oracle database authentication and authorisation procedures. This means that when a DODEX user logs into the web application the user will also log into a dedicated Oracle account. At database level, the authorisation ensures that the users are able to select only data they have the privilege to see, and to create, update and delete. The administration web application is designed to make it easy for the various user types to perform their individual tasks, for example providing the quality controller with an overview of the status of a report (Fig. 3).

Concluding remarks

The joint GEUS-BMP DODEX project supports GEUS' obligations, described in the 2008–2011 ministerial contract, to make relevant geoscientific data from Denmark and Greenland accessible to the general public and private companies. The project is in line with GEUS' ambitions to embrace the ongoing development in information technology, and, in particular, the advance in web technology to develop more effective tools to make the large quantities of scientific data we hold in our databases available to a broader public (e.g. Riisager *et al.* 2010; Hansen & Pjetursson 2011 – this volume).

The DODEX project represents the first attempt at GEUS to use new open-source Java frameworks such as Hibernate, and various Java Server Faces frameworks. These steps to modernise software development at GEUS have proved successful and are now incorporated in its database and software group.

Most importantly, the DODEX project has resulted in a new database for geoscience reports on Greenland, and web tools for GEUS personnel to update and extend this database, and public users to see and download non-confidential reports. Hence, DODEX has reduced much of the work at GEUS with organising reports, and photocopying and mailing reports to interested parties, and at the same time made the reports more readily available to the outside world.

References

Hansen, M. & Pjetursson, B. 2011: Free, online Danish shallow geological data. Geological Survey of Denmark and Greenland Bulletin **23**, 53–56.

Riisager, P., Keulen, N., Larsen, U., McLimans, R.K., Knudsen, C. & Tulstrup, J. 2010: Interactive web analysis and presentation of computer-controlled scanning electron microscopy data. Geological Survey of Denmark and Greenland Bulletin **20**, 103–106.

Tulstrup, J. 2004: Environmental data and the Internet: openness and digital data management. Geological Survey of Denmark and Greenland Bulletin **4**, 45–48.

Authors' address

Geological Survey of Denmark and Greenland, Øster Voldgade 10, DK-1350 Copenhagen K, Denmark. E-mail: *pri@geus.dk*

Quality control of airborne geophysical data from the EU Mining Sector Support Programme, Ghana

Thorkild M. Rasmussen, Leif Thorning, Arne V. Olesen and Frands Schjøth

On 2 December 2002, EU Commissioner Poul Nielson on behalf of the European Development Fund signed a €40 million grant to the Ghana Government. The purpose of this grant was to finance a Mining Sector Support Programme (MSSP) that covered a broad spectrum of geoscientific projects and other projects aimed at an overall strengthening and modernisation of Ghana's mining sector. One of the major components was collection and interpretation of airborne geophysical data contracted to the two commercial geophysical companies Fugro Airborne Surveys and Geotech Airborne Ltd. The Geological Survey of Denmark and Greenland (GEUS) was contracted to perform the quality control (QC) of the airborne geophysical data collection and processing in a separate MSSP project (No 8 ACP GH 027/37). The initial Provision of quality-control services to the Airborne Geophysical Survey required GEUS to be on site in Ghana for 22 man-months; an expansion of the programme and various circumstances (see below) resulted in a total of 37.25 man-months before the project was completed in January 2010. The Danish National Space Center was subcontracted by GEUS to perform part of the QC of gravity data acquisition and processing. The QC project was reported by Thorning *et al.* (2010).

Results from some of the geoscientific projects of the MSSP were presented at a workshop in 2008 and a series of small articles from the presentations were published (Kalsbeek 2008).

Organisational setup for the airborne geophysics projects within the MSSP

Interactions between GEUS and several organisations were required in order to carry out the project. The Geological Survey Department (GSD) within the Ministry of Lands and National Resources of Ghana was the main beneficiary institution of the airborne geophysical surveying. A GSD employee acted as supervisor of the projects to collect airborne geophysical data as well as of the QC project. In reality three persons were appointed during the four-year course of the project. Other organisations involved were the MSSP Programme Management Unit established under a separate contract and supervised by the Minerals Commission. This is the main promotional and regulatory body for the minerals sector in Ghana, which acted as executing organisation for the MSSP. In addition, the European Delegation in Ghana and the National Authorising Officer of the Ministry of Finance of Ghana took part in the administration.

Contributions to the projects came from several of the two geophysical companies' offices; Fugro's offices in Accra, Johannesburg, Ottawa, Perth and London and Geotech's offices in Accra, Toronto and Johannesburg were involved.

The EU delegation and the National Authorising Officer undertook the contracting for the various MSSP projects. GEUS did not have formal obligations with respect to the technical specifications in the contract with Fugro Airborne Surveys, but a considerable amount of assistance from GEUS was required in order to clarify various technical issues. The contract with Fugro was signed before GEUS was awarded the QC project. GEUS assisted in setting up the tender documents for the airborne data collection project that was later awarded to Geotech Airborne Ltd. in 2008.

One of the lessons learned with respect to organising airborne geophysical survey projects similar to those performed in Ghana is that the QC team selected for the external quality control should be involved at an early stage and should be consulted concerning the setup of the tender specifications used for the contract with the geophysical consultant performing the measurements.

The geophysical survey data

The surveys performed by Fugro involved the following: (1) Remote sensing interpretation (in co-operation with British Geological Survey (BGS)), (2) acquisition and interpretation of airborne magnetic data, (3) acquisition and interpretation of airborne gamma-spectrometric data, (4) acquisition and interpretation of airborne gravity data and (5) acquisition and interpretation of airborne time-domain electromagnetic (GEOTEM) data. The surveys performed by Geotech Airborne Ltd. involved (1) Acquisition and interpretation of airborne magnetic data and (2) acquisition and interpretation of airborne time-domain electromagnetic (VTEM) data.

During all flights the surveys employed two methods simultaneously, of which magnetic data acquisition was one.

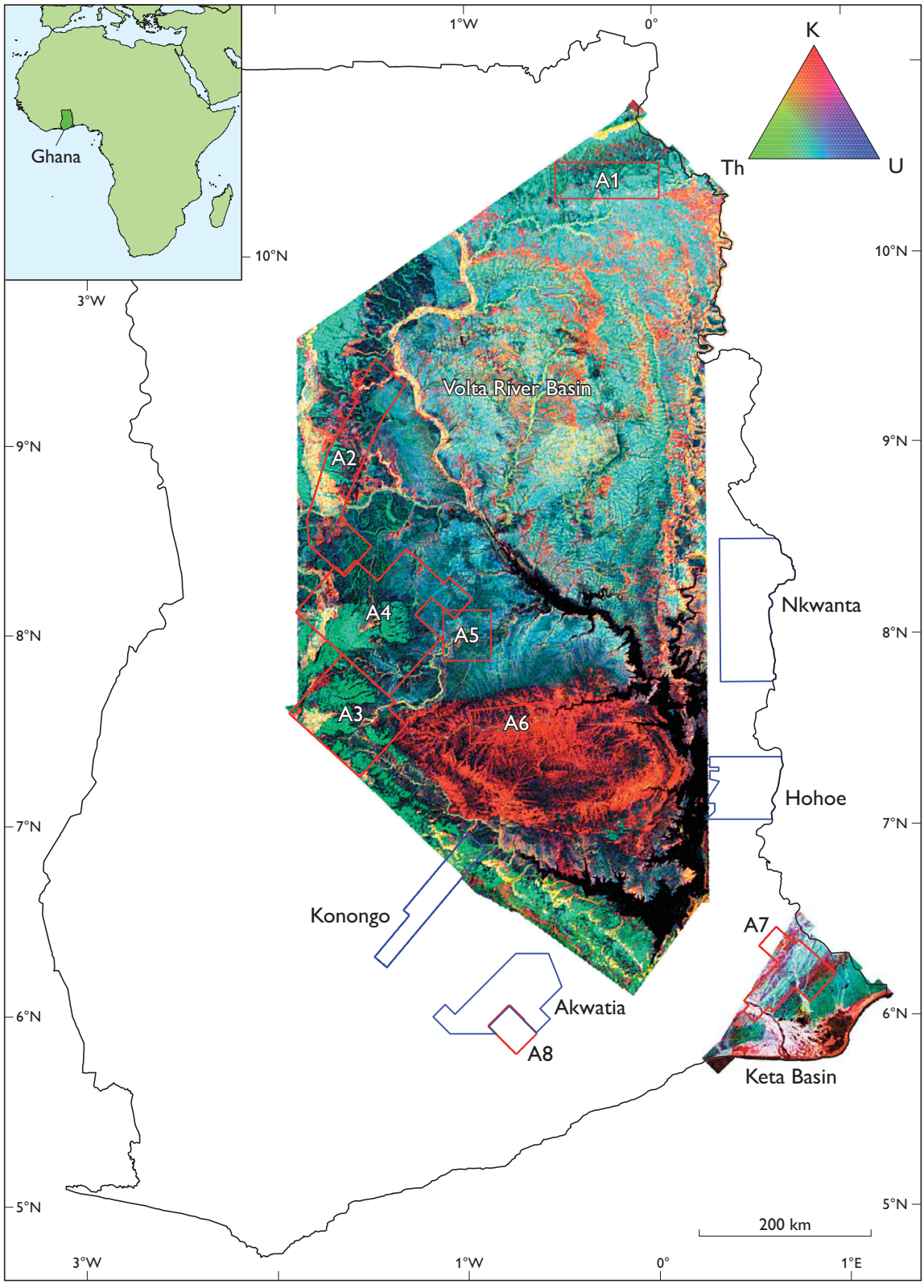

Fig. 1. Map of Ghana with ternary **U-Th-K** images of the gamma-ray spectrometry data from the Volta River and Keta basin surveys. Polygons show survey block boundaries for eight areas covered by detailed GEOTEM surveys (red colour) and for four areas covered by VTEM surveys (blue colour).

The combined gamma-spectrometry and magnetic survey by Fugro included measurements of the horizontal gradient of the magnetic total field in addition to the magnetic total field recordings. The inclusion of the horizontal gradient data improved the lateral resolution in the description of the magnetic field anomalies. The surveys performed by Fugro used different fixed-wing aircraft as survey platforms, whereas a helicopter was used for the surveys performed by Geotech.

Figure 1 outlines the areas that were covered by the airborne surveys. The Volta River and Keta basins were surveyed by Fugro. These areas had not previously been covered by detailed airborne geophysical surveys, whereas most of the surrounding 'basement' had been covered before. With the completion of the two new surveys the entire onshore area of Ghana is now covered by high-resolution magnetic and gamma-spectrometry data. This puts Ghana in a leading position with respect to providing modern airborne geophysical data to the mining industry. The Volta River and Keta basins gamma-spectrometric and magnetic surveys were flown with a 500 m line separation and a survey altitude of 120 m. Gravity data were also obtained for the two basin areas, using a mean survey altitude of 860 m above ground and a flight line separation of 5000 m.

Reconnaissance GEOTEM data were collected over the entire Volta River and Keta basins using 20 km flight-line separation. Later, the areas numbered A1–A8 in Fig. 1 were flown with the GEOTEM system using a flight-line separation of 200 m and 400 m. The survey blocks referred to as Nkwanta, Hohoe, Akwatia and Konongo were subsequently flown with the VTEM system using 400 m line separation.

Initially, the surveys planned were mainly directed towards obtaining an understanding of the geology of the two basin areas and only included those performed by Fugro.

Fig. 2. The first author (right) discusses the methods of the VTEM system during a break in the surveying of the Akwatia block with the Geotech operators. The outer transmitter coil has a diameter of *c.* 26 m and carries a current of *c.* 200 A before turn-off of the transient signal.

The VTEM survey performed by Geotech was added to the MSSP at a late stage and focused on areas outside the basins. Fugro, BGS and Geotech performed geological field work as part of a follow-up of the airborne surveying. Other MSSP geoscientific projects had activities in the areas covered by the geophysical surveys, but the timing of the projects did not allow full integration of data from the various projects. The QC was expanded to include storing of the geophysical data on a server on the Geological Survey Department's computer system (Schjøth *et al.* 2010).

The quality control process carried out by GEUS was complex and sometimes very difficult, but mostly performed on good terms with the geophysical contractors. The quality of the final data now available in Ghana for the mining sector and the scientific community was often significantly improved by the process.

QC and training of Geological Survey Department personnel

The quality control performed by GEUS may be viewed as a data assessment independent of the geophysical contractors' own data quality control. Although independent, the quality control by the QC team builds on a high degree of interaction with the geophysical contractors (Fig. 2). Even though the QC team, the client and the geophysical contractors basically have the same goal of obtaining high-quality data, different views and interests may often exist in terms of defining a proper balance between data quality and project delays.

Analyses of data with respect to quality from a technical point of view are clearly a major concern of the QC team. Some of these analyses follow fairly standardised methodologies and checking procedures, whereas others require an in-depth understanding of data acquisition and processing techniques. In some cases, the acquired field data may be in accordance with the specifications and pass the first routine check, but subsequent application of more advanced checking procedures after the contractor's processing of the data may reveal problems that were not initially identified.

An important part of the obligations by GEUS was the inclusion of a training component involving two GSD employees and the production of a QC manual (Rasmussen *et al.* 2010) including examples of data issues dealt with during the project. The airborne geophysical contractors also trained GSD personnel. The contracts with GEUS and the two geophysical contractors were very ambitious with respect to involvement of GSD personnel in the projects. Significant knowledge transfer and interaction related to QC took place throughout the entire project period, through regular courses and especially intensive hands-on training provided by GEUS as part of the actual work with QC.

Conclusions

For obvious reasons the authors are somewhat subjective in assessing the impact of the work performed. Nevertheless, we conclude that the GEUS contribution did have significant influence on the quality of the data released from the project – a conclusion that is supported by statements of GSD personnel, the geophysical contractors and an independent evaluation committee. Furthermore, during the course of the project, a constructive working relationship between GSD and GEUS personnel was established that would be beneficial to both parties in future cooperation.

References

Kalsbeek, F. (ed.) 2008: The Voltaian Basin, Ghana. Workshop and excursion, March 10–17, 2008, 136 pp. Copenhagen: Geological Survey of Denmark and Greenland. http://www.geus.dk/program-areas/common/voltaian_workshop_report.pdf .

Rasmussen, T.M., Thorning, L. & Olesen, A.V. 2010: Quality control manual for airborne geophysics. The European Development Fund. Project no. 8 ACP GH 027/37. Mining Sector Support Programme. Geophysical investigation. Danmarks og Grønlands Geologiske Undersøgelse Rapport **2010/42**, 207 pp.

Schjøth, F., Rasmussen, T.M. & Thorning. L., 2010: Guide to the GSD DAP-server depository for airborne geophysical data. Danmarks og Grønlands Geologiske Undersøgelse Rapport **2010/43**, 69 pp.

Thorning, L., Rasmussen, T.M. & Schjøth, F. 2010: Final report. Provision of quality control services to the airborne geophysical survey. The European Development Fund. Project no. 8 ACP GH 027/37. Mining Sector Support Programme. Danmarks og Grønlands Geologiske Undersøgelse Rapport **2010/44**, 35 pp.

Authors' addresses

T.M.R., L.T.H. & F.S.C., *Geological Survey of Denmark and Greenland, Øster Voldgade 10, DK-1350 Copenhagen K, Denmark*. E-mail: *tmr@geus.dk.*

A.V.O., *DTU Space, National Space Institute, Technical University of Denmark, Juliane Maries Vej 30, DK-2100 Copenhagen Ø, Denmark.*

De Nationale Geologiske Undersøgelser for Danmark og Grønland (GEUS)

Geological Survey of Denmark and Greenland
Øster Voldgade 10, DK-1350 Copenhagen K
Denmark

The series *Geological Survey of Denmark and Greenland Bulletin* started in 2003 and replaced the two former bulletin series of the Survey, viz. *Geology of Greenland Survey Bulletin* and *Geology of Denmark Survey Bulletin*. Some of the twenty-one volumes published since 1997 in those two series are listed on the facing page. The present series, together with *Geological Survey of Denmark and Greenland Map Series*, now form the peer-reviewed scientific series of the Survey.

Geological Survey of Denmark and Greenland Bulletin

1	The Jurassic of Denmark and Greenland, 948 pp. (28 articles), 2003. *Edited by* J.R. Ineson & F. Surlyk.	500.00
2	Fish otoliths from the Paleocene of Denmark, 94 pp., 2003. *By* W. Schwarzhans.	100.00
3	Late Quaternary environmental changes recorded in the Danish marine molluscan faunas, 268 pp., 2004. *By* K.S. Petersen.	200.00
4	Review of Survey activities 2003, 100 pp. (24 articles), 2004. *Edited by* M. Sønderholm & A.K. Higgins.	180.00
5	The Jurassic of North-East Greenland, 112 pp. (7 articles), 2004. *Edited by* L. Stemmerik & S. Stouge.	160.00
6	East Greenland Caledonides: stratigraphy, structure and geochronology, 93 pp. (6 articles), 2004. *Edited by* A.K. Higgins & F. Kalsbeek.	160.00
7	Review of Survey activities 2004, 80 pp. (19 articles), 2005. Edited by M. Sønderholm & A.K. Higgins.	180.00
8	Structural analysis of the Rubjerg Knude Glaciotectonic Complex, Vendsyssel, northern Denmark, 192 pp., 2005. *By* S.A.S. Pedersen.	300.00
9	Scientific results from the deepened Lopra-1 borehole, Faroe Islands, 156 pp. (11 articles), 2006. *Edited by* J.A. Chalmers & R. Waagstein.	240.00
10	Review of Survey activities 2005, 68 pp. (15 articles), 2006. *Edited by* M. Sønderholm & A.K. Higgins.	180.00
11	Precambrian crustal evolution and Cretaceous–Palaeogene faulting in West Greenland, 204 pp. (12 articles), 2006. *Edited by* A.A. Garde & F. Kalsbeek..	240.00
12	Lithostratigraphy of the Palaeogene – Lower Neogene succession of the Danish North Sea, 77 pp., 2007. *By* P. Schiøler, J. Andsbjerg, O.R. Clausen, G. Dam, K. Dybkjær, L. Hamberg, C. Heilmann-Clausen, E.P. Johannessen, L.E. Kristensen, I. Prince & J.A. Rasmussen.	240.00
13	Review of Survey activities 2006, 76 pp. (17 articles), 2007. *Edited by* M. Sønderholm & A.K. Higgins.	180.00
14	Quaternary glaciation history and glaciology of Jakobshavn Isbræ and the Disko Bugt region, West Greenland: a review, 78 pp., 2007. *By* A. Weidick & O. Bennike.	200.00
15	Review of Survey activities 2007, 96 pp. (22 articles), 2008. *Edited by* O. Bennike & A.K. Higgins.	200.00
16	Evaluation of the quality, thermal maturity and distribution of potential source rocks in the Danish part of the Norwegian–Danish Basin, 66 pp., 2008. *By* H.I. Petersen, L.H. Nielsen, J.A. Bojesen-Koefoed, A. Mathiesen, L. Kristensen & F. Dalhoff.	200.00
17	Review of Survey activities 2008, 84 pp. (19 articles), 2009. *Edited by* O. Bennike, A.A. Garde & W.S. Watt.	200.00
18	Greenland from Archaean to Quaternary. Descriptive text to the 1995 Geological map of Greenland, 1:2 500 000. 2nd edition, 126 pp., 2009. *By* N. Henriksen, A.K. Higgins, F. Kalsbeek & T.C.R. Pulvertaft.	280.00
19	Lithostratigraphy of the Cretaceous–Paleocene Nuussuaq Group, Nuussuaq Basin, West Greenland, 2009. *By* G. Dam, G.K. Pedersen, M. Sønderholm, H.H. Midtgaard, L.M. Larsen, H. Nøhr-Hansen & A.K. Pedersen.	300.00
20	Review of Survey activities 2009, 106 pp. (23 articles), 2010. *Edited by* O. Bennike, A.A. Garde & W.S. Watt.	220.00
21	Exploration history and place names of northern East Greenland, 368 pp., 2010. *By* A.K. Higgins.	200.00
22	Lithostratigraphy of the Upper Oligocene – Miocene succession of Denmark, 92 pp., 2010. *By* E.S. Rasmussen, K. Dybkjær & S. Piasecki.	240.00
23	Review of Survey activities 2010, 84 pp. (19 articles), 2011. *Edited by* O. Bennike, A.A. Garde & W.S. Watt.	

Geological Survey of Denmark and Greenland Map Series

1	Explanatory notes to the Geological map of Greenland, 1:500 000, Humboldt Gletscher, Sheet 6, 48 pp. + map, 2004. *By* P.R. Dawes.	280.00
2	Explanatory notes to the Geological map of Greenland, 1:500 000, Thule, Sheet 5 (1991), 97 pp. + map, 2006. *By* P.R. Dawes.	300.00
3	Explanatory notes to the Geological map of Greenland, 1:100 000, Ussuit 67 V.2 Nord, 40 pp. + map, 2007. *By* J.A.M. van Gool & M. Marker.	280.00
4	Descriptive text to the Geological map of Greenland, 1:500 000, Dove Bugt, Sheet 10, 32 pp. + map, 2009. *By* N. Henriksen & A.K. Higgins.	240.00
5	Descriptive text to the Geological map of Greenland, 1:100 000, Kangaatsiaq 68 V.1 Syd and Ikamiut 68 V.1 Nord, 41 pp. + 2 maps, 2010. *By* A.A. Garde & J.A. Hollis.	280.00

Geology of Greenland Survey Bulletin (173–191; discontinued)

177	Accretion and evolution of an Archaean high-grade grey gneiss – amphibolite complex: the Fiskefjord area, southern West Greenland, 115 pp., 1997. *By* A.A. Garde.	200.00
178	Lithostratigraphy, sedimentary evolution and sequence stratigraphy of the Upper Proterozoic Lyell Land Group (Eleonore Bay Supergroup) of East and North-East Greenland, 60 pp., 1997. *By* H. Tirsgaard & M. Sønderholm.	200.00
179	The Citronen Fjord massive sulphide deposit, Peary Land, North Greenland: discovery, stratigraphy, mineralization and structural setting, 40 pp., 1998. *By* F.W. van der Stijl & G.Z. Mosher.	200.00
180	Review of Greenland activities 1997, 176 pp. (26 articles), 1998. *Edited by* A.K. Higgins & W.S. Watt.	200.00
181	Precambrian geology of the Disko Bugt region, West Greenland, 179 pp. (15 articles), 1999. *Edited by* F. Kalsbeek.	240.00
182	Vertebrate remains from Upper Silurian – Lower Devonian beds of Hall Land, North Greenland, 80 pp., 1999. *By* H. Blom.	120.00
183	Review of Greenland activities 1998, 81 pp. (10 articles), 1999. *Edited by* A.K. Higgins & W.S. Watt.	200.00
184	Collected research papers: palaeontology, geochronology, geochemistry, 62 pp. (6 articles), 1999.	150.00
185	Greenland from Archaean to Quaternary. Descriptive text to the Geological map of Greenland, 1:2 500 000, 93 pp., 2000. *By* N. Henriksen, A.K. Higgins, F. Kalsbeek & T.C.R. Pulvertaft.	225.00
186	Review of Greenland activities 1999, 105 pp. (13 articles), 2000. *Edited by* P.R. Dawes & A.K. Higgins.	225.00
187	Palynology and deposition in the Wandel Sea Basin, eastern North Greenland, 101 pp. (6 articles), 2000. *Edited by* L. Stemmerik.	160.00
188	The structure of the Cretaceous–Palaeogene sedimentary-volcanic area of Svartenhuk Halvø, central West Greenland, 40 pp., 2000. *By* J. Gutzon Larsen & T.C.R. Pulvertaft.	130.00
189	Review of Greenland activities 2000, 131 pp. (17 articles), 2001. *Edited by* A.K. Higgins & K. Secher.	160.00
190	The Ilímaussaq alkaline complex, South Greenland: status of mineralogical research with new results, 167 pp. (19 articles), 2001. *Edited by* H. Sørensen.	160.00
191	Review of Greenland activities 2001, 161 pp. (20 articles), 2002. *Edited by* A.K. Higgins, K. Secher & M. Sønderholm.	200.00

Geology of Denmark Survey Bulletin (36–37; discontinued)

36	Petroleum potential and depositional environments of Middle Jurassic coals and non-marine deposits, Danish Central Graben, with special reference to the Søgne Basin, 78 pp., 1998. *By* H.I. Petersen, J. Andsbjerg, J.A. Bojesen-Koefoed, H.P. Nytoft & P. Rosenberg.	250.00
37	The Selandian (Paleocene) mollusc fauna from Copenhagen, Denmark: the Poul Harder 1920 collection, 85 pp., 2001. *By* K.I. Schnetler.	150.00

Prices are in Danish kroner exclusive of local taxes, postage and handling

Note that information on the publications of the former Geological Survey of Denmark and the former Geological Survey of Greenland (amalgamated in 1995 to form the present Geological Survey of Denmark and Greenland) can be found on *www.geus.dk*